



Università degli Studi di Cagliari

Molecular and Translational Medicine PhD

Cycle XXXIII

**Study of deferiprone-induced agranulocytosis
in β -thalassemic patients through a
metabolomics approach**

Scientific Disciplinary Sector

MED/05

PhD Student

Dott.ssa Antonina Balsamo

Coordinator of the PhD Programme

Prof. Sebastiano Banni

Supervisor

Prof. Luigi Atzori

Final exam. Academic Year 2019 – 2020

Thesis defence: July 2021 Session

INDEX

ABSTRACT	4
LIST OF FIGURES	6
LIST OF TABLES	8
LIST OF ABBREVIATIONS	9
I. INTRODUCTION	12
METABOLOMICS	15
BETA-THALASSEMIA	18
PATHOPHYSIOLOGY	19
B-THALASSEMIA MAJOR	21
CHELATION THERAPY	22
DEFERIPRONE-INDUCED AGRANULOCYTOSIS	25
II. AIM OF THE STUDY	28
III. METHODS	30
STUDY DESIGN	30
SPECIMEN COLLECTION	30
PATIENTS	33
COMPARISON OF TWO COMMONLY USED ISOLATION PROTOCOLS FOR PURITY OF ENRICHED GRANULOCYTES	35
LYMPHOLYTE-H DENSITY GRADIENT FOR ISOLATION OF PMNs PROCEDURE	35
LYMPHOLYTE-POLY DENSITY GRADIENT FOR ISOLATION OF PMNs PROCEDURE.....	36
ANALYSIS OF PURITY AND VIABILITY	36
MORPHOLOGICAL EVALUATION OF THE CELLS	36
FACS ANALYSIS	37
TRYPAN BLUE EXCLUSION TEST OF CELL VIABILITY	37
SAMPLE PREPARATION FOR INTRACELLULAR METABOLITE EXTRACTION	38
CELL NUMBER OPTIMIZATION	38
PMNs SAMPLE PREPARATION FOR METABOLOMICS ANALYSIS	39
GAS CHROMATOGRAPHY-MASS SPECTROMETRY ANALYSIS	40
¹H-NMR MEASUREMENTS	40
PLASMA SAMPLES PREPARATION FOR GC-MS and ¹H-NMR ANALYSIS	42
CELLULAR ROS DETECTION	43
DETERMINATION OF REDUCED (GSH) AND OXIDIZED (GSSG) GLUTATHIONE	44
STATISTICAL ANALYSIS	45
MULTIVARIATE STATISTICAL ANALYSIS	45

UNIVARIATE STATISTICAL ANALYSIS.....	46
IV. RESULTS	47
OPTIMISING PROTOCOLS FOR GC-MS and ¹H-NMR METABOLOMICS ANALYSES OF HUMAN NEUTROPHILS.....	47
COMPARISON OF TWO COMMERCIAL USED ISOLATION PROTOCOLS FOR PURITY OF ENRICHED GRANULOCYTES	47
METABOLITE EXTRACTION	49
PMNs METABOLOMICS ANALYSIS.....	51
REDOX STATUS IN POLYMORPHONUCLEAR NEUTROPHIL	67
PLASMA METABOLOMICS ANALYSIS	69
¹ H-NMR METABOLOMICS ANALYSIS	69
GC-MS METABOLOMICS ANALYSIS	75
V. DISCUSSION.....	84
VI. CONCLUSIONS	92
VII. BIBLYOGRAPHY	93

ABSTRACT

β -Thalassemia is one of the most prevalent forms of congenital blood disorders, characterised by a reduced or absent ability to produce haemoglobin. The mainstay of treatment consists of blood transfusion to maintain the patient's haemoglobin above 9-10 g/dL. Repeated transfusions result in an excessive accumulation of iron in the body, removal of which is achieved through iron chelating agents. Deferiprone is the first orally bioavailable iron chelator, approved for clinical use in 1997. Considering its potential toxicity, the use of Deferiprone is allowed in Europe only for the treatment of thalassemia major, when Deferoxamine therapy is contraindicated or unappropriated. The main Deferiprone adverse effect is the development of agranulocytosis (in 1–2% of patients). The mechanisms behind this negative effect remain largely unresolved. Currently, only a few metabolomics studies have been performed on neutrophils. Neutrophils are the immune cells forming the major arm of innate immunity. Due to their physiological characteristic, the study of these cells in vitro presents several difficulties meaning that standard protocols for most assays must be optimised. This thesis aimed to establish protocols for the study of the metabolomic profile of human neutrophils in healthy and pathological conditions. In particular, this study aimed to investigate the PMNs (polymorphonuclear leukocytes) metabolic profile of beta thalassaemic patients treated with iron chelator Deferiprone, to explore its potential relationship with the onset of agranulocytosis, using a metabolomics approach. Our data demonstrated that analysis of the metabolomic profiles in PMNs with GC-MS, allowed us to identify different metabolites including organic acids, amino acids, fatty acids, and sugars. The results showed a different metabolomic profile between PMNs obtained from patients with Deferiprone-induced agranulocytosis and PMNs of patients without Deferiprone-induced agranulocytosis. Multivariate statistical analysis of GC-MS data revealed that the PMNs of patients with Deferiprone-induced agranulocytosis have a metabolic profile characterized by an increase of metabolites directly involved in the metabolic pathways of glutathione synthesis and by a decrease of arachidonic acid stearic acid and inosine.

Considering the important physiological roles of these metabolites, our results could shed light on the physiopathological mechanisms of this harmful side effect of DFP treatment. This work is a pilot study that has been only validated in a small independent cohort and, therefore, further confirmation in larger studies is required.

LIST OF FIGURES

Figure 1. A typical workflow of metabolomic studies.

Figure 2. Hemoglobin structure.

Figure 3. Flow chart on sample collection and analysis.

Figure 4. Purities of enriched granulocyte.

Figure 5. Comparison of different metabolite extraction mixture.

Figure 6. PCA scores plot of PMN samples from patients and control subjects.

Figure 7. PLS-DA scores plot of PMN samples from patients and control subjects,

Figure 8. OPLS-DA analysis of PMN samples A vs C.

Figure 9. OPLS-DA analysis of PMN samples NA vs C.

Figure 10. OPLS-DA analysis of PMN samples NA vs A.

Figure 11. Discriminant metabolites in A patients vs healthy subjects.

Figure 12. Discriminant metabolites in NA patients vs healthy subjects.

Figure 13. Discriminant metabolites in A patients vs NA patients.

Figure 14. ROS production DFP induct in PMNs.

Figure 15. GSH/GSSG ratio in PMNs treated with different doses of DFP.

Figure 16. PLS-DA analysis of plasma samples.

Figure 17. OPLS-DA analysis of plasma samples A vs C.

Figure 18. OPLS-DA analysis of plasma samples NA vs C.

Figure 19. Discriminant metabolites in A patients vs healthy subjects.

Figure 20. Discriminant metabolites in NA patients vs healthy subjects.

Figure 21. PLS-DA analysis of plasma samples of patients and healthy controls.

Figure 22. OPLS-DA analysis of plasma samples A vs C.

Figure 23. OPLS-DA analysis of plasma NA vs C.

Figure 24. Discriminant metabolites in A patients vs healthy subjects.

Figure 25. Discriminant metabolites in NA patients vs healthy subjects.

LIST OF TABLES

Table 1. Summary of clinical and pathological data of the studied subjects.

Table 2. Optimisation of blood sample volume and neutrophil number required for the acquisition of ¹H-NMR and GC-MS spectra with a good signal-to-noise ratio.

Table 3. Comparison of yields and purities of granulocytes, time consumption, of the two different isolation procedures used in the study: (i) Lympholyte-H (ii) Lympholyte-poly.

Table 4. PMNs samples MVA parameters.

Table 5. Statistical differences of metabolites characterized by Variable Importance for the Projection (VIP) > 1.

Table 6. Statistical differences of metabolites characterized by Variable Importance for the Projection (VIP) > 1.

Table 7. Statistical differences of metabolites characterized by Variable Importance for the Projection (VIP) > 1.

Table 8. Summary table of significantly increase and decrease metabolites with GC-MS Method in the three different groups.

Table 9. PMNs samples MVA parameters.

Table 10. PMNs samples MVA parameters.

Table 11. Summary table of significantly increase and decrease plasma metabolites in two different methods (H-NMR/GC-MS) and two different groups

LIST OF ABBREVIATIONS

A	β-Thalassemic Patients with Deferiprone-induced agranulocytosis
AA	Arachidonic Acid
ANC	Absolute Neutrophil Count
APC	Allophycocyanin
BSA	Bovine Serum Albumin
C	Control Group
CE-MS	Capillary Electrophoresis-Mass Spectrometry
CV-ANOVA	Cross-Validation- ANalysis Of VAriance
DCFH-DA	Dichlorofluorescein Diacetate
DFO	Deferoxamine
DFP	Deferiprone
DFX	Deferasirox
DNA	DeoxyriboNucleic Acid
EDTA	Ethylenediamine-Tetraacetic Acid
EI	Electron Ionisation
FACS	Fluorescent-Activated Cell Sorter
FITC	Fluorescein Isothiocyanate
GC-MS	Gas Chromatography Mass Spectrometry
G-CSF	Granulocyte Colony-Stimulating Factor

GM-CSF	Granulocyte-Macrophage Colony-Stimulating Factor
GSH	Reduced Glutathione
GSSG	Oxidised Glutathione
HBSS	Hanks' Balanced Salt Solution
HCV	Hepatitis C Virus
HPLC	High-Performance Liquid Chromatography
LC-MS	Liquid Chromatography-Mass Spectrometry
MS	Mass Spectrometry
MSTFA	N-Methyl-N-(trimethylsilyl)Trifluoroacetamide
MVA	Multivariate Analysis
NA	β-Thalassemic patients without Deferiprone-induced-agranulocytosis
NMR	Nuclear Magnetic Resonance
OPLS-DA	Orthogonal Partial Least Square-Discriminant Analysis
PBS	Phosphate-Buffered Saline
PCA	Principal Component Analysis
PBMC	Peripheral Blood Mononuclear Cells
PMNs	Polymorphonuclear Neutrophils
PLS-DA	Partial Least Square-Discriminant Analysis
PGE₂	Prostaglandin E₂
PGI₂	Prostacyclin I₂

QC	Quality Control
RBC	Red Blood Cells
RNA	Ribonucleic Acid
ROS	Reactive Oxygen Species
TBH	Ter-Butyl Hydroperoxide
TCA	Trichloroacetic AcidTM
TM	Thalassemia Major
TIC	Total Ion Chromatogram

I. INTRODUCTION

Human polymorphonuclear neutrophils are the most abundant nucleated cell in circulating blood (2 to 8×10^6 for ml). Neutrophils are the immune cells forming the major arm of innate immunity. They are produced in the bone marrow from hematopoietic stem cells, through a tightly regulated process of granulopoiesis. In healthy individuals, neutrophil patrols the peripheral blood and mucous membranes in an inactive or “resting state”, but upon infectious challenges can be rapidly recruited to sites of infection to engulf and kill pathogens and further direct the adaptive immune response. On the other hand, aberrant neutrophil responses lead to tissue damage and are associated with pathological conditions like sepsis, asthma, ischemia-reperfusion injury, and rheumatoid arthritis (1,2). Neutrophils are generated in the bone marrow at a rate of 10^{11} cells/day but during stress conditions, their maturation time in the bone marrow may be shortened and their production increased to 10^{12} cells per day (3). Neutrophils can adhere to the endothelium of blood vessels by adhesion receptor-ligand interactions. These cells form the margined pool which constitutes about half of total blood neutrophils. When activated, neutrophils can undergo selectin-dependent capture and roll along the vascular endothelium, followed by integrin-dependent adhesion and migration into tissues where they can survive for 1-2 days. Here neutrophils are capable of ingesting microorganisms or particles by phagocytosis. Upon phagocytosis of foreign material, neutrophils undergo an oxidative (respiratory) burst. In this process, reactive oxygen species are quickly released to facilitate bacteria-killing (1,4,5). Neutrophil disorders can result from a reduced number of cells or defective cell function. When the neutrophil count drops to 0.5×10^9 cells/L or lower, it is termed agranulocytosis. Low neutrophil counts can be the result of congenital disorders such as severe congenital neutropenia, cyclic neutropenia, myelokathexis, and the Shwachman-Diamond syndrome. In these cases, neutrophil progenitor cells fail to complete the process of proliferation, differentiation, and maturation in the bone marrow and fail to enter the circulation. Some of these disorders may be associated with accelerated apoptotic cell death of the myeloid precursors.

Alternatively, low neutrophil counts can also be induced by drugs. Drug-induced hematological disorders constitute up to 30% of all blood dyscrasias seen in the clinic and predicting them is often difficult, and this makes clinical decision-making challenging (6). Neutropenic patients exhibit a higher susceptibility to recurrent infections, while agranulocytosis is a potentially life-threatening condition. A recent resurgence in the interest of the cellular metabolism in the context of immunity and inflammation (immunometabolism) has led to an increased understanding of the complex changes in metabolic regulation that take place in cells of the immune system during activation in different pathologies (7). Currently, only a few metabolomics studies have been performed on these immune cells. The metabolome, defined as the total repertoire of small molecules characterizing a biological system (8), is the downstream result of genomic and proteomic activity and therefore provides important insight into multiple levels of physiological regulation (9). Therefore, metabolomics is a promising tool for identifying biomarkers and elucidating mechanisms in diverse physiological and pathophysiological states by allowing the exploration and integration of multiple pathways and networks (9). Neutrophils are the most abundant of all white blood cells and are the first responder in case of infections and inflammation. As such, they are highly sensitive to external cues and are easily activated. Besides, neutrophils have a very short half-life and a rapid turnover. All together these characteristics raise issues. Making the study of human neutrophils in vitro technically challenging without the development of specific optimized protocols. The first step to study PMNs in vitro is to isolate them from peripheral venous blood. There are several neutrophil purification strategies, each with its pros and cons. Isolation requires an efficient, aseptic, and reproducible method to obtain pure and viable cells, and ex vivo handling should not influence neutrophil behaviour. The neutrophils are considerably more sensitive to manipulation than other cell types. A critical step in working with neutrophils is their purification from whole blood: excessive centrifugation, agitation, or rough handling can lead to unwanted activation. Preparation protocols must take into account final cell purity, which should be free of contaminating peripheral blood mononuclear cells (PBMC) (10,11). Neutrophils are terminally differentiated cells and as

such are short-lived particularly in cultures with a lifespan shorter than 8 hours *in vitro* (12). For these reasons, neutrophils must be isolated from whole blood within one hour of venepuncture to preserve the functional integrity of the cells and prevent cell death. Therefore experimental time points are an important consideration when planning metabolomics experiments to detect neutrophils' function. Also, optimisation of neutrophils cells number is necessary, as the total numbers of neutrophils routinely obtained from the blood of patients and healthy donors can be low, particularly from paediatric patients. The total number of neutrophils obtained from a single blood sample may be as low as 2×10^6 cells. Furthermore, the level of metabolic activity in neutrophils compared to other primary human cells is unknown, but presumed lower, particularly in healthy, non-activated neutrophils. Therefore, it was critical to determine the minimum volume of peripheral blood to obtain the optimal number of neutrophils required to detect the highest number of metabolites with the two major platforms for metabolomics analysis: Nuclear Magnetic Resonance (NMR) spectroscopy and Mass Spectrometry (MS) and to generate optimal signal-to-noise ratio. In particular, this study aimed to investigate metabolic profiles able to predict the onset of agranulocytosis in beta thalassaemic patients treated with the iron chelator Deferiprone (DFP) with a metabolomic approach. To do this it was necessary to establish protocols to optimise sample preparation, metabolite extraction, and analysis that minimised the chemical and physical degradation of metabolites in PMNs (polymorphonuclear) leukocytes of the patients enrolled in the study: patients with Deferiprone-induced agranulocytosis vs patients without Deferiprone-induced agranulocytosis. Agranulocytosis, (defined as a confirmed absolute neutrophil count less than $0.5 \times 10^9/L$), is the most serious side effect associated with the use of DFP, occurring in about 1% of the patients (13). The study was designed in consideration of the high number of beta-thalassaemic patients in Sardinia requiring deferiprone treatment. At the Microcitemico Hospital in Cagliari, where the study was conducted, approximately 500 beta thalassaemic patients undergo transfusions every 2-3 weeks. Among them, there is a small but significant cohort of beta thalassaemic patients who developed agranulocytosis during iron chelation therapy with the drug DFP. In thalassaemia

major (TM) patients, iron accumulation occurs rapidly as a result of repeated transfusion from an early age. If inadequately chelated, these patients will develop endocrinopathies and cardiac failure from iron deposition in these organs. With the early introduction of chelation therapy, these consequences are now less commonly seen in TM than previously, although patients may still suffer serious complications from iron overload such as endocrinopathies and cardiac decompensation if inadequately treated (14). Before addressing the specific aims of this thesis, a brief description of the methodologic approach, thalassemia syndrome, and iron chelation therapy is needed.

METABOLOMICS

Metabolome is defined as the complete set of metabolites of a given cell, tissue, organ, or organism and comprises a large number of small molecular weight compounds (generally with a molecular mass <1500 Da), such as lipids, amino acids, nucleotides, organic acids, etc. Metabolome components span a diverse range of compounds with different properties. For example, within lipids alone, there are high abundance compounds, such as fatty acids, triglycerides, or phospholipids, but other compounds with lower abundance, such as eicosanoid derived from arachidonic acid, also have significant regulatory effects (15,16). Considering that metabolites are the final product of the gene expression and the protein activity, among the other “omics” technologies, metabolomics is the research platform most closely related to the phenotype (17). In particular, metabolomics allows to study of the metabolic fingerprint and provides an integrated view of metabolic networks at all levels of biological complexity: organism, tissues, cells, or cell compartments (18, 19). The metabolic profile is deeply influenced by genetic and environmental factors (diet, lifestyle, gut microbiota activity) or exogenous compounds (drugs) under physiological or pathological conditions (20). The identification of these metabolic signatures in different conditions can provide useful information for the diagnosis, prognosis, and for predicting

pharmacological response to therapy (21). In this context, metabolomics can represent a powerful tool in “Precision Medicine” to identify disease prevention strategies and clinical care protocols tailored for each patient (22). Furthermore, the emerging “Pharmacometabolomics” approach aims to identify individual metabolomic characteristics able to predict drug effectiveness and/or toxicity and to provide new insights into drug mechanism of action (23).

After the design of the study, each metabolomics study requires an evaluation of the sample preparation, the extraction procedure, and a combination of different analytical techniques to achieve as much information as possible. The metabolomics analytical workflow can be divided into different crucial steps, from the sample collection to the metabolomics profile and data analysis (Fig. 1).

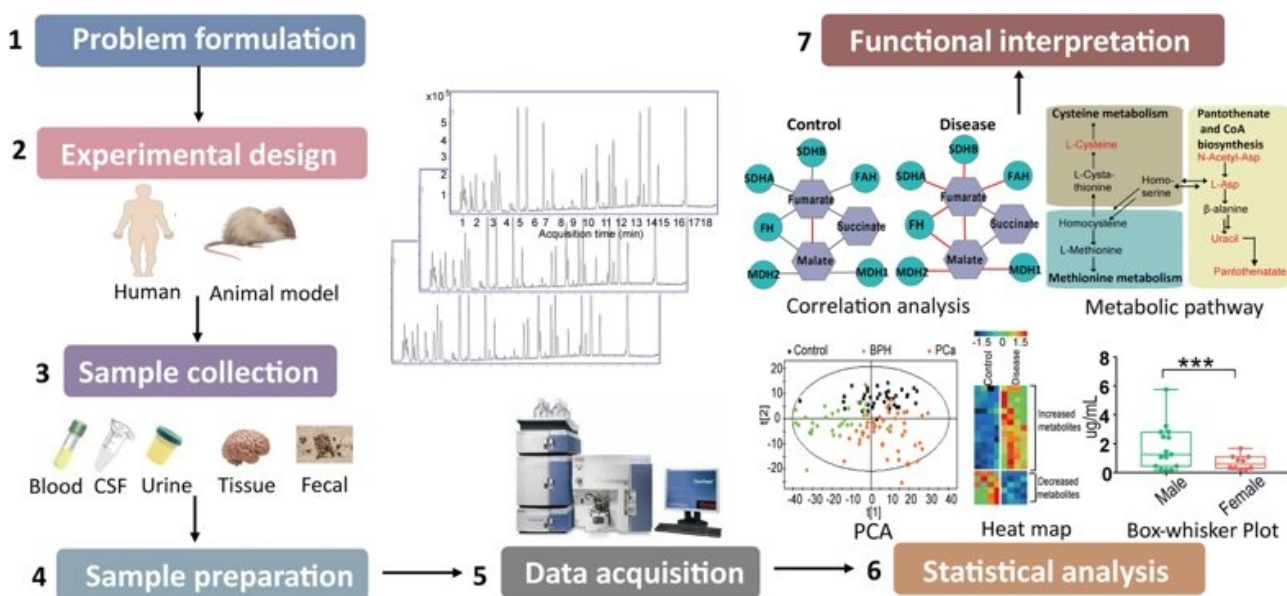


Figure 1. A typical workflow of metabolomic studies.

Sample collection is the first step, which may determine the success of the metabolomics experiment. There is a wide variety of biological samples that can be used for metabolomics studies, and the sample characteristics (in terms of different biospecimens, collection techniques, or

genetic and environmental condition such as gender, age, or diet) may affect the analysis, introducing potential sources of variability or bias into the experiment. Furthermore, the sample preparation steps before metabolite detection are one of the major causes of analytical errors and include quenching methods to stop any metabolic process and metabolite extraction protocols to increase the abundance of molecular compounds and to remove potential interferents. The development of the appropriate sample preparation protocol can increase the specificity and sensitivity of the method (24). In general, the metabolomic experiments can be designed with either a targeted or untargeted approach. Untargeted metabolomics, or global metabolome analysis, is a powerful approach that aims to discover and identify a wide range of both unknown and known metabolites in a biological sample. This approach is ideal for biomarkers discovery and hypothesis-generating studies (25). On the contrary, the targeted approach aims to identify and quantify a specific set of metabolites of interest or a defined chemical class of small molecules, maximizing the sensitivity. Targeted metabolomics are very useful for hypothesis-driven studies and molecular pathways validation (26). Considering this, there is no single analytical method for the analysis of the metabolome, and the choice depends both on the type of the sample and on the type of required information (27). The two main analytical platforms in metabolomic studies are Nuclear Magnetic Resonance Spectroscopy (NMR) and Mass Spectrometry (MS), which usually is coupled with different separation technologies, such as gas-chromatography (GC-MS), liquid chromatography (LC-MS), and capillary electrophoresis (CE-MS) (28). NMR has an important role in metabolomics owing to its easy and rapid sample preparation, non-destructive analysis, no need for chromatographic separation, and a high degree of reproducibility. However, it has lower sensitivity and resolution compared to MS-based techniques (29). Mass spectrometry employs a range of different mass analyser depending on the type of experiments, such as single quadrupole, triple quadrupole, time-of-flight mass spectrometry, and ion traps. Among all the separation techniques, GC-MS and LC-MS are the most widely used in metabolomics approach, while recently CE-MS is getting more attention in this field (30, 31). LC-MS has several advantages over GC-MS, requiring

minimal sample preparation, no need for sample derivatization, and capabilities for analysing more polar and higher molecular weight compounds. One of the disadvantages of LC-MS is the ion suppression, as the ionization processes may depend on the presence of matrix compounds, and this effect is closely dependent on the type of ionization (Electrospray Ionisation or Atmospheric Pressure Chemical Ionization). On other hand, GC-MS presents several advantages, such as high separation efficiency and highly reproducible performance. Electron impact ionization (EI) is the method of choice for GC-MS experiments; this hard ionization method induces significant metabolite fragmentation and leads to complex and specific fragmentation patterns (32). One of the disadvantages is that metabolites, after the required derivatization, are not very stable and they can be degraded during injection and separation (33, 34). In terms of mass analysers, a single quadrupole or a time-of-flight (TOF) are the most used in GC-MS analysis. Metabolite detection employs several options including single (MS) or tandem (MS/MS) mass analysers, which show different sensitivity and resolution performances. The MS/MS mode, which is characterized by an additional MS/MS fragmentation, provides important information about the identification and the structure of the metabolites and is employed in targeted metabolomic approaches (31).

BETA-THALASSEMIA

Beta-thalassemia is one of the most common autosomal recessive disorders worldwide characterized by anomalies in the synthesis of the haemoglobin subunit beta resulting in variable phenotypes ranging from severe anaemia to clinically asymptomatic individuals. The annual incidence of symptomatic people is estimated at 1/100.000 worldwide and 1/10.000 in the UE. Approximately 68.000 children are born with various thalassemia syndromes each year (35). β -thalassemia is a highly prevalent disease, with 80 to 90 million people reported to be carriers (1,5% of the global population). Three main forms have been described β -thalassemia major, also referred to as Mediterranean anaemia or Cooley's anaemia, β -thalassemia intermedia and thalassemia minor,

also called β -thalassemia trait, β -thalassemia carrier or heterozygous β -thalassemia. Beta-thalassemia is prevalent in Mediterranean countries, Central Asia, India, Southern China the Middle East, and the Far East, Africa, and South America. The highest carrier frequency is reported in Southeast Asia, Cyprus (14%), Sardinia (10,3%). The reason for the highest carrier frequency of Beta-thalassemia in these regions is most likely related to the selective pressure from Plasmodium falciparum malaria (36). Inter-marriage between different ethnic groups and population migration has introduced thalassemia in almost every country of the world.

PATHOPHYSIOLOGY

Human hemoglobin is a heterotetramer protein, composed of two alpha and two beta subunits as shown in Figure 2. Each subunit contains a heme group, an iron-containing compound that binds to oxygen. The synthesis of hemoglobin is controlled by two developmentally regulated multigene clusters: the alpha-like globin cluster on chromosome 16 and the beta-like globin cluster on chromosome 11. In a healthy person, the synthesis of alpha and beta-globin chains is finely balanced during terminal erythroid differentiation. Beta-thalassemia is caused by a reduced (β^+) or absence (β^0) synthesis of β globin chains. The altered production of β chains is due to the presence of point mutations or small deletions at the level of the globin β cluster (37, 38). Genotypically the β -thalassemia are very heterogeneous; to date, over 200 beta-globin gene mutations are known to cause a partial or total deficit of chain synthesis globin beta. Most of these mutations regard single nucleotide variations or small deletions or insertions of nucleotides leading to frameshift alterations that determine defective gene transcription or mRNA maturation and translation defects. Beta globin gene deletion defects are rare and limited to sporadic families. These mutations result in excess production of unbound alpha globin chains, which cannot form tetramers and therefore precipitate erythroid precursors in the bone marrow, forming large intracellular inclusion bodies (39). These excess chains are very unstable and become associated

with the red cell membrane and ultimately destroy the developing erythroid precursors with different mechanisms including oxidative damage to cell membranes and interference with cell division. The degree of globin chain reduction is determined by the nature of the mutation in the beta-globin gene. This premature death of erythroid precursors results in the development of anaemia due to ineffective erythropoiesis. The red cells that mature and enter the circulation are prematurely destroyed in the splenic microcirculation due to the presence of inclusion bodies. Therefore, the anaemia in thalassemia syndromes is caused by ineffective erythropoiesis and a shortened red cell survival.

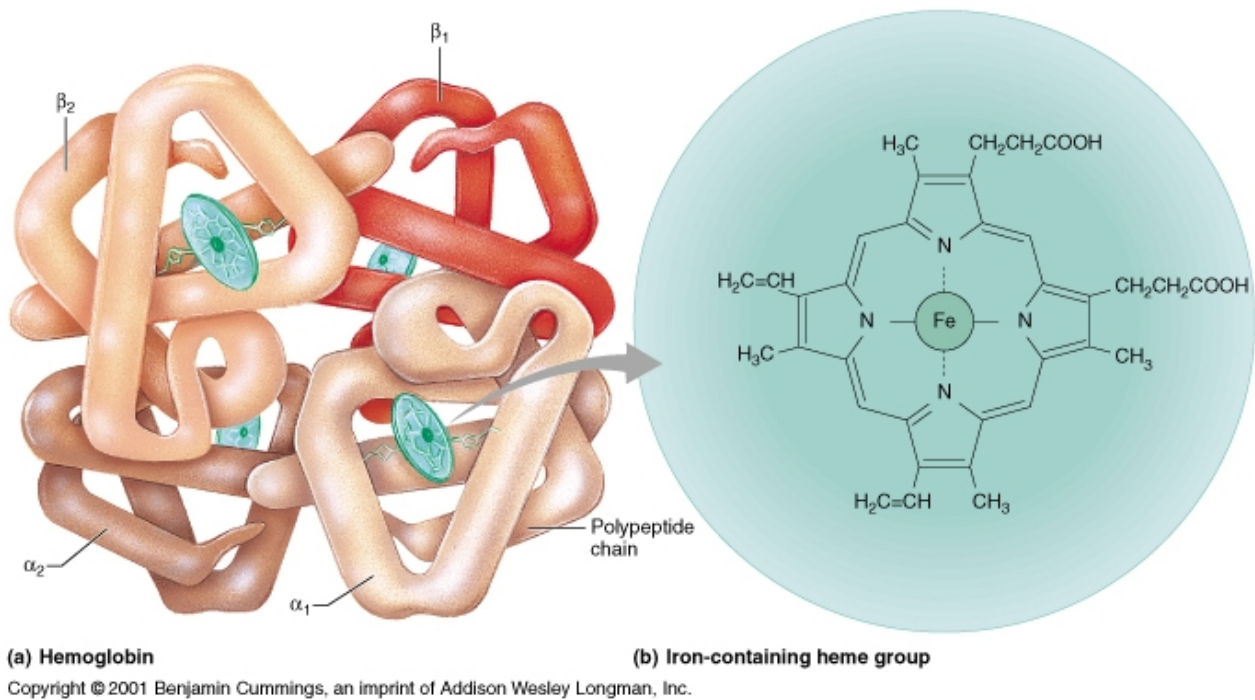


Figure 2. Hemoglobin structure.

B-THALASSEMIA MAJOR

In the β -thalassemia major patients genotype is characterized by low presence (β^0/β^+) or total absence (β^0/β^0) of beta-globin chains. Clinical presentation of thalassemia major occurs between the ages of 6 and 24 months. Affected infants fail to thrive and become progressively pale. Feeding problems, irritability, diarrhea, recurrent bouts of fever, and progressive enlargement of the abdomen caused by spleen and liver enlargement may occur. Nowadays treatment with a regular transfusion program that maintains a minimum Hb concentration of 9.5 to 10.5 g/dL allows for normal growth and development and may improve the overall prognosis (40). Repeated transfusion represents the major cause of iron overload in thalassemia major. If this excess iron is not removed, it can cause damage to important organs such as the liver and heart. Complications of iron overload in children include growth retardation and failure or delay of sexual maturation. In adults, overload-related complications include involvement of the heart, liver, and endocrine glands (41). Iron overload is an unavoidable consequence of regular transfusions because the human body lacks a mechanism to excrete excess iron. In regularly transfused patients, iron overload is due mostly to red cell breakdown. When the iron-binding capacity of transferrin is saturated, iron can appear in the serum as non-transferrin-bound iron, which is a powerful catalyst for the formation of free radicals capable of causing oxidative stress and damage to mitochondria, lipid membranes, lysosome, protein, and DNA. The cell death that occurs will result in fibrosis and loss of organ function and favours the development of iron overload complications (42,43). Oxidative damage is thought to be the key reason leading to organ impairment typical of thalassemia. However, the most common complications related to transfusion hemosiderosis can be prevented by adequate iron chelation.

CHELATION THERAPY

Iron overload is an unavoidable consequence of regular transfusion because the human body lacks a mechanism to excrete excess iron. However, the most common complications related to transfusional hemosiderosis, such as heart failure, cirrhosis, growth retardation, and multiple endocrine abnormalities, can be prevented, and to some extent, reverted by adequate iron chelation. Prevention of iron toxicity is the main objective of iron chelation therapy in transfusion dependent-patients. An iron chelator aims to minimize the risk of iron-induced toxicity. This is accomplished by the combined mechanism of inactivating current iron deposits and removing excess iron from the body through the urine and/or faeces thereby reducing tissue iron stores to levels that can be tolerated by the organs. Three iron chelation are currently available: Deferoxamine (DFO), Deferiprone (DFP), and Deferasirox (DFX) (44). Deferoxamine (DFO) is the first chelator introduced in clinical practice for the treatment of iron overload and unequivocally demonstrated the value of iron chelation therapy for removing excess iron from the body. DFO is an exadentate iron chelator that is not orally absorbed and thus needs to be administered five to seven days a week by 8-12-hour continuous subcutaneous infusion via a portable pump. In high-risk cases, continuous administration of DFO via an implanted delivery system or subcutaneously were the only options to intensify the chelation therapy before the advent of the combined treatment with DFO and DFP (45). The most frequent adverse effects of DFO are local reactions at the site of infusion. Other complications include ocular and auditory toxicity, growth restriction, and, rarely renal impairment and interstitial pneumonitis. DFO administration also increases infections by *Yersinia Enterocolitica* and other pathogens (*Klebsiella Pneumonia*). The use of DFO prevents the secondary effects of iron overload and decreases morbidity and mortality among those patients who can comply with regular prolonged infusions (46). The major problem of DFO chelation therapy is low compliance resulting from complications of administration. In fact, despite the very clear benefits of chelation therapy, it is a difficult treatment to use and adherence to therapy has been a major issue

for both clinicians and patients. These limitations lead to the search and development of oral chelator that is at least as effective as deferoxamine and has a reasonable tolerability profile. The first oral chelator to be licensed (47) was Deferiprone (DFP) (3-hydroxy-1,2-dimethylpyridin-4one) a synthetic analogue of mimosine, isolated from the legume *Mimosa peduca*. DFP has strong iron-binding properties with a high degree of relative specificity for the trivalent form of iron, binding it in a 3:1 complex (48). As a water-soluble compound with a molecular weight of only 139 Da, it would be expected to move freely through cell membranes throughout the body. DFP is rapidly and completely absorbed after oral administration, with peak plasma levels typically occurring about 1 hour after administration. The drug is rapidly eliminated from the body with a half-life of about 2 hours due to hepatic biotransformation, with glucuronidation accounting for almost all the metabolism. About 90% of the drug is excreted in the urine as glucuronide (49). Deferiprone has been approved for thalassemia-major patients for whom deferoxamine therapy is contraindicated or inadequate. The most serious side effect associated with the use of DFP is agranulocytosis, defined as a confirmed absolute neutrophil count less than $0.5 \times 10^9/L$, and occurring in about 1% of the patients (13, 50). More common but less severe side effects are arthropathy, gastrointestinal symptoms, arthralgia, fluctuating liver enzymes, and zinc deficiency. The effect of DFP on liver iron concentration may vary among the individuals treated. Independent studies have shown that DFP therapy is associated with reduced cardiac morbidity and mortality (51-53). Deferiprone is more cardioprotective than deferoxamine, studies have shown that individuals being treated with deferiprone have better myocardial MRI patterns and less probability of developing (or worsening pre-existing) cardiac disease (54, 55). In an individual with severe iron overload, DFO and DFP can be used in combination to reach levels of iron excretion that cannot be achieved by either drug alone without increasing toxicity (56, 57), Deferasirox (DFX) was developed as a once-daily oral monotherapy for the treatment of transfusional iron overload. A large program of clinical trials has shown to be effective in adults and children and has a defined safety profile that is clinically manageable with appropriate monitoring (58, 59). Adverse events occurring more frequently are

gastrointestinal disorders, skin rash, and a mild, non-progressive increase in serum creatinine concentration (59). Cases of renal failure, hepatic failure, cytopenias, and gastrointestinal hemorrhage have been reported in the post-marketing phase. If provided adequate doses are administered, there is a good response to DFX of baseline liver iron concentration values (60). The efficacy of DFX in improving myocardial functionality and maintain a normal left ventricle ejection fraction has been demonstrated in prospective studies (61). However, DFX has not been evaluated in formal trials for affected individuals with symptomatic heart failure or low left-ventricle ejection fraction. Strategies of chelation using a combination of deferoxamine and deferiprone have been effective in individuals with severe iron overload. Combined chelation offers several potential advantages. Drugs with distinct physicochemical properties have different iron-carrying capacities and may access different iron pools. It has been suggested that deferiprone, with low molecular weight, acts as an intracellular chelating shuttle and the large and hydrophilic molecule of DFO serves as an extracellular iron sink (62). In individuals with severe iron overload retrospective, prospective, and randomized clinical studies have shown that combined iron chelation with deferiprone and deferoxamine rapidly reduces myocardial siderosis, improves endocrine and cardiac function, reduces liver iron and serum ferritin concentrations, reduces cardiac mortality, and improves survival (63,64). Strategies of chelation using a combination of DFO and DFP could have an increased chelation efficacy and sometimes allow drug doses and toxicity to be reduced and the number of days of DFO infusion to be decreased, improving compliance and quality of life.

DEFERIPRONE-INDUCED AGRANULOCYTOSIS

To minimize the risk of developing agranulocytosis and its potential complications, all patients taking deferiprone are expected to have their blood absolute neutrophil count (ANC) monitored weekly to discontinue therapy at the first sign of infection or of neutropenia ($ANC < 1.5 \times 10^9/L$) and to avoid rechallenge (65, 66). However, the rationale for imposing weekly testing on both patients and health resources has been questioned (67). Thalassemia patients frequently experience transient episodes of mild or moderate neutropenia, independent of deferiprone (68, 69), and neutropenia during deferiprone therapy often does not progress to agranulocytosis, even with continued treatment (70-73). Indiscriminately stopping or interrupting deferiprone at the onset of neutropenia may appear to be a prudent safety measure, but may fail to balance benefits and risk for individuals. There is a need to identify risk factors for agranulocytosis during deferiprone therapy, the effectiveness of weekly ANC monitoring in avoiding its consequence, and the rate of its recurrence upon rechallenge. This goal requires large patient cohorts, but deferiprone is approved as an orphan drug, and the low incidence of agranulocytosis in the relatively small cohort of patients treated with this drug limits the potential database. Drug-induced idiosyncratic agranulocytosis is a serious and sometimes fatal complication, and a wide spectrum of drugs can cause agranulocytosis. Hence, attempts to identify factors that might reduce the incidence of this event and minimize its complications are warranted. Drug-induced agranulocytosis is characterized by a neutrophil count of fewer than $0.5 \times 10^9/L$ ($500 \text{ cells}/\text{mm}^3$) with no relevant decrease in haemoglobin and platelet counts in the peripheral blood. In Europe, the incidence rate is reported to range from 1.6 to 9.2 cases per million population. In the United States, reported rates are slightly higher, ranging from 2.4 to 15.4 cases per million population (74, 75). Geographic variability in incidence is related to both differences in reporting and medication usage but could also suggest a difference in susceptibility. Older patients are thought to be at greater risk for drug-induced agranulocytosis, probably because of increased medication use (75).

The pathogenesis of drug-induced agranulocytosis is not completely understood, especially those which are idiosyncratic. Two mechanisms, direct toxicity, and immune-mediated toxicity have been proposed. Direct toxicity to myeloid cells, particularly neutrophils, has been shown with medications such as chlorpromazine, procainamide, clozapine, dapsone, sulphonamides, carbamazepine, phenytoin, indomethacin, and diclofenac. The toxicity may be due to either the parent drug or a toxic metabolite or a byproduct. The severity of neutropenia associated with these drugs is often dose-dependent, but the occurrence of reactions is still idiosyncratic (76). In some cases, there is a rapid onset of the reaction upon rechallenge which is suggestive of the involvement of an adaptive immune mechanism. Drug-specific antibodies were also found to be involved in the mechanism of certain drugs associated with agranulocytosis. These include aminopyrine, amodiaquine, penicillin, propylthiouracil, sulfamethoxazole, sulfasalazine, and trimethoprim. Over the last decade, the same new concepts have emerged concerning a new understanding of the regulation of myelopoiesis and neutrophil maturation that might be a starting point for discussions of non-immune and cell-mediated immune. Among the former is the role of reactive oxygen species (ROS) that transform a drug to a compound that might serve as an antigen, a hapten, or modifier of metabolic reactions that are vital for the survival of the neutrophil. The characteristic of deferiprone-induced agranulocytosis is typical of idiosyncratic drug reactions (77-80) in that: it is an unpredictable and rare event; onset is delayed (occurrence peaks after 1-3 month and time of the first onset extends beyond one year); incidence is not dose-related within the therapeutic range. This is consistent with the lack of dependence of clozapine-associated agranulocytosis and neutropenia on dose (81) but in contrast with the dose-dependency of beta-lactam antibiotic-mediated agranulocytosis (82). Idiosyncratic drug reactions are generally inconsistent with direct cytotoxicity, and there is growing evidence that most are mediated by the adaptive immune system. The manifestations of an “allergic” reaction, such as rash, that occur in some cases have not been recorded in deferiprone-induced agranulocytosis (83). The primary treatment of drug-induced agranulocytosis is the removal of the offending drug. After discontinuation of the drug, most cases

of neutropenia resolve over time, and only symptomatic treatment (antimicrobial for infection treatment and prophylaxis) and appropriate vigilant hygiene practices are necessary. Sargramostin (granulocyte-macrophage colony-stimulating factor [GM-CSF] and filgrastim (granulocyte colony-stimulating factor [G-CSF] have been shown to shorten the duration of neutropenia, length of antibiotic therapy, and the length of hospital stay (84)

II. AIM OF THE STUDY

The study of human neutrophils in vitro presents several technical challenges meaning that standard protocols for most assays must be optimised. Previous reports have claimed that the neutrophil isolation procedure can affect neutrophil viability, contamination, and activation state. However, these few studies have not characterised the reported variability yet. Furthermore, currently, only few metabolomics studies have been performed on these immune cells. Therefore, the overall aim of this study was to optimise protocols to study neutrophil metabolomics profiles in healthy and pathological conditions. Metabolomics has the potential to provide novel insight into disease heterogeneity and could provide new information on the molecular effect of drug therapies on neutrophil function in vivo. The second purpose of this project was to identify a metabolomic profile of neutrophils in two groups of beta-thalassaemic patients (with or without deferiprone-induced agranulocytosis). Furthermore, this study could shed some light on the physiopathological mechanisms of this deferiprone-induced side effect. Deferiprone is an effective oral iron chelator able to reduce iron overload and to maintain a safe body iron level, alone or in combination with DFO. The main DFP adverse effect is the development of agranulocytosis (in 1–2% of patients). Considering its potential toxicity, the use of Deferiprone is allowed in Europe only for the treatment of thalassemia major, when Deferoxamine therapy is contraindicated or unappropriated. The mechanisms behind this negative effect remain largely unresolved. It is known that oxidative stress, which plays a crucial role in the pathophysiology of β -thalassemia, leads to excessive production of ROS that by binding to cellular components such as DNA, proteins, and membrane lipids can induce cytotoxicity suggesting a possible role of it also in the side effects in the presence of Deferiprone. Moreover, possible changes in cellular metabolism may be present.

Based on these pieces of evidence, the **aim** of this project involves:

- To optimise GC-MS metabolomic protocol to study changes in neutrophil metabolic profiles. In particular, establish protocols to optimise sample preparation, metabolite extraction that minimise the degradation of neutrophil metabolites and avoid the introduction of interfering compounds commonly used in isolation procedures.
- The analysis and comparison of the metabolomic profiles in PMNs (polymorphonuclear) leukocytes, from the patients, enrolled in the study (Patients with Deferiprone-induced agranulocytosis *vs* patients without Deferiprone-induced agranulocytosis);
- To study the PMNs cell cultures exposed to Deferiprone.
- To integrate the data obtained from the metabolomic profiles in PMNs (polymorphonuclear) leukocytes from the patients enrolled in the study (Patients with Deferiprone-induced agranulocytosis *vs* patients without Deferiprone-induced agranulocytosis) with the plasma metabolomics profile on the same cohort.

Altogether, this might help to have a better view of the pathophysiological mechanisms behind this serious and still unpredictable collateral side-effect of the Deferiprone treatment.

III. METHODS

STUDY DESIGN

The study was conducted in different phases. First, the study was designed according to the standard of Good Clinical Practise and it was approved by the Hospital Ethics committee on 31st January 2019 Prot. PG/2019/1555. Next, adequate protocols for metabolomics analysis and oxidative status analysis of PMNs were developed. Finally, the samples were collected and analysed. Due to the total number of neutrophils that can be obtained from the blood of healthy donors and particularly from beta-thalassemic patients where it can be quite low, it was necessary to ask two or three blood samples to be collected from the subjects enrolled in the study. Between February 2019 and November 2019, a volume of 20 ml of peripheral blood specimen was collected from study participants (first blood sample). Between September 2020 and November 2020, a volume of 6 ml of the peripheral blood sample was collected from study participants (second blood sample) (Fig. 3).

SPECIMEN COLLECTION

To define the best method of 1) isolation, 2) metabolite extraction and 3) the number of cells necessary for metabolomics analysis on polymorphonuclear cells, preliminary experiments were necessary. Five ml of peripheral blood was collected from healthy donors enrolled in the study to perform pilot investigations. Once the protocols and number of cells needed were defined, approximately 20 ml of peripheral blood specimen was collected from study participants for the metabolomics CG-MS method. Next, 6 ml of the peripheral blood sample was collected from study participants to determine the oxidative status in the cells after treatment with different concentrations of deferiprone. Before isolating the neutrophils for the oxidative status

determination, 1ml of whole blood was taken, the plasma was separated and stored at -80°C until $^1\text{H-NMR/GC-MS}$ analysis. A blood specimen was collected via the standard venipuncture method in a sodium-heparin vacutainer. The use of EDTA as an anticoagulant was avoided because extra resonance signals are observed in the NMR spectrum via the formation of complexes between EDTA and Ca^{2+} and Mg^{2+} present in plasma. The peripheral blood specimen from β -Thalassemic study participants was collected before blood transfusion. Neutrophils were isolated within 1 hour of blood collection. Granulocyte isolation, count, and test of cell viability were performed in the Department of Medical Science and Public Health, Clinical and Molecular Medicine Unit, University of Cagliari c/o Regional Hospital for Microcythemias laboratory. FACS analysis was conducted at Hematology and Bone Marrow Transplant Center (A. Businco Hospital, Cagliari) laboratory. Metabolite extraction and all other experiments were performed in the Clinical Metabolomics Unit, Department of Biomedical Sciences (University of Cagliari).

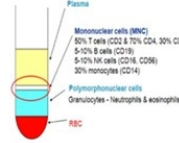
First blood sample:



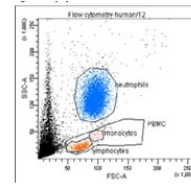
1) Twenty ml of blood sample was collected.



Gradient Centrifugation as crude Cell Separation Tool - MNC preparation



2) PMNs were carried out using a density gradient method.



3) Cell quality was checked by FACS analysis after the cell isolation



4) metabolites extracted from isolated PMNs were measured with GC- MS.



Second blood sample



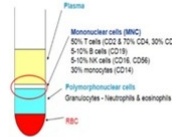
1) Six ml of blood sample was collected



2) 1ml of whole blood was taken, the plasma was separated and stored at -80°C until for H-NMR/GC-MS analysis



Gradient Centrifugation as crude Cell Separation Tool - MNC preparation



3) PMNs were carried out using a density gradient method.



4) Cell viability was tested with trypan blue tests.

5) PMNs were seeded and kept in culture for being exposed to the deferiprone in order to analyse the response to *in vitro* oxidative stress



6) ROS content was measured with DCFA and redox status by EC-HPLC analysis

Figure 3. Flow chart on sample collection and analysis.

PATIENTS

The patients and healthy subjects involved in this study were enrolled at the Microcitemico Hospital of Cagliari. Informed consent was obtained from all study participants. Twenty-three patients were enrolled in the study, eleven β -Thalassemic Patients with Deferiprone-induced agranulocytosis (A), twelve β -Thalassemic patients without Deferiprone-induced-agranulocytosis (NA). All β -Thalassemic Patients were homozygotes for β -thalassemia and receiving regular packed red cell transfusions every 2 to 3 weeks. The mean age was 42 ± 10 and 39 ± 5 for β -Thalassemic Patients with Deferiprone-induced agranulocytosis and β -Thalassemic patients without Deferiprone-induced-agranulocytosis respectively. Two β -thalassemia patients with deferiprone-induced agranulocytosis were below the average age of the patients studied (18 and 21 years old respectively). Twelve patients were positive for hepatitis C virus (HCV). The control group (C) consisted of thirteen healthy volunteers that were matched for age and sex. The clinical data of the study population are reported in Table 1. The inclusion criteria for patients groups were: patients with Beta-thalassemia major characterized by a II degree hemochromatosis undergoing iron chelation therapy; patients with deferiprone-induced agranulocytosis (granulocyte values $< 500 / \text{mm}^3$); patients on deferiprone therapy for at least 1 year. The inclusion criteria for healthy controls: subjects without β -thalassemia aged between 32 and 46 years. The exclusion criteria: neutropenic patients with granulocyte values between $500\text{-}1500 / \text{mm}^3$; patients with the reduction of other cell lines; patients treated with other drugs potentially responsible for agranulocytosis (clozapine, chloramphenicol, noramidopyrine); non beta-thalassemic subjects affected by pathologies requiring pharmacological therapies. In beta-thalassemic patients with deferiprone-induced agranulocytosis, the drug was discontinued. These patients at the time of sample collection were subjected to different chelation therapy. The clinical data of the study population are reported in Table 1.

Groups	Healthy	Agranulocytosis	No- agranulocytosis
<i>Age</i>	38±12*	42±10*	39±5*
<i>Sex (Male)</i>	7	5	7
<i>(Female)</i>	6	6	5
<i>Onset of agranulocytosis <1 anno</i>	-	8	-
<i>>1 anno</i>	-	3	-
<i>β genotype: 39/39</i>	-	8	11
<i>39/76</i>	-	1	-
<i>39/6</i>	-	-	1
<i>39/IVS-110</i>	-	1	-
<i>(-C) cd16/(-C) cd16</i>	-	1	-
<i>α genotype aa/aa</i>	-	7	9
<i>-a/aa</i>	-	3	2
<i>-a/-a</i>	-	-	1
<i>-a/aNcola</i>	-	1	-
<i>Therapy^a: monotherapy DFP</i>	-	2	8
<i>combined therapy DFO+DFP</i>	-	9	4
<i>Therapy at sample collections time^b:</i>			
<i>monotherapy DFX</i>	-	3	-
<i>monotherapy DFO</i>	-	5	-
<i>combined therapy DFO+DFX</i>	-	3	-
<i>HCV+</i>	-	4	8
<i>HCV-</i>	-	7	4

Table 1. Summary of clinical and pathological data of patients and control subjects. * Mean and standard deviation; ^a Iron chelation therapy in beta-thalassemia patients at the onset of agranulocytosis. ^b Current Iron chelation therapy after DFP discontinuation in patients with deferiprone-induced agranulocytosis

COMPARISON OF TWO COMMONLY USED ISOLATION PROTOCOLS FOR PURITY OF ENRICHED GRANULOCYTES

There are currently several materials that can be employed to produce density gradients to isolate and purify neutrophils from whole blood. The density gradient material aims to provide an appropriate separation range to isolate neutrophils at high purity from other blood cells. To establish the best protocol to isolate neutrophils for metabolite extraction, two methods were used in parallel; Lympholyte-H density gradient centrifugation and Polymorphprep density gradient centrifugation.

LYMPHOLYTE-H DENSITY GRADIENT FOR ISOLATION OF PMNs PROCEDURE

The blood was diluted with an equal volume of physiological solution. 5 ml of Lympholyte-H (Cederlane, Hornby, Ontario, Canada) were dispensed to a 15 ml centrifuge tube and 10 ml of diluted blood were carefully layered over. This was centrifuged for 40' at 200 g with the brake off. After centrifugation, mononuclear cells, remaining plasma, and Lympholyte-H were aspirated off and discarded, leaving the PMN and erythrocyte-rich pellet. The pellet was washed with 5ml of physiological solution. The tube was centrifuged for 10' to 500 g. The supernatant was again aspirated off and the cells re-suspend in 2ml of lysis buffer [ammonium chloride solution: NH_4Cl (155mM), KHCO_3 (10Mm), EDTA (0,1mM)], for the erythrocyte lysis, and incubate for 10' at room temperature. Next, the tube was centrifuged for 10' to 500 g to pellet the neutrophils. The supernatant was aspirated off, the pellet was resuspended again in 2ml of lysis buffer, to reduce residual erythrocytes, and incubate for 5', before centrifugation for 10' at 500 g. The supernatant was again aspirated off and the neutrophil pellet washed in 2ml of physiological solution, followed by re-centrifugation. The supernatant was discarded and the cells re-suspend in 2ml of physiological solution and counted with a Burker chamber. Once establishing the number of cells needed, aliquots were used for the cytocentrifuge and the FACS analysis and metabolites extraction and analysis.

LYMPHOLYTE-POLY DENSITY GRADIENT FOR ISOLATION OF PMNs PROCEDURE

Five ml of peripheral blood, anticoagulated with heparin, were obtained from patients enrolled in the study. The blood was diluted with an equal volume of physiological solution. Five ml of Lympholyte-poly (Cedarlane, Hornby, Ontario, Canada) were dispensed to a 15 ml centrifuge tube and 10 ml of diluted blood were carefully layered over. This was centrifuged for 40' at 200 g with brake off. After centrifugation, two leukocyte bands were visible. The top band at the sample/medium interface consisted of mononuclear cells and the lower band of PMNs; the erythrocytes were pelleted in the bottom of the tube. The PMNs layer was removed with a Pasteur pipette and transferred into a clean centrifuge tube and washed in 2 ml of physiological solution. Next, the tube was centrifuged for 10' to 500 g. The supernatant was discarded and the cells were resuspended in 2 ml of lysis buffer, for the residual erythrocyte lysis, and incubate for 5', before centrifugation for 10' at 500 g. The cells were washed with 2 ml of physiological solution, re-centrifuged, and resuspend in 2 ml of physiological solution. After establishing the number, the cells were used for the cytocentrifuge and the FACS analysis and metabolites extraction and analysis.

ANALYSIS OF PURITY AND VIABILITY

MORPHOLOGICAL EVALUATION OF THE CELLS

The cell suspension was diluted between $5-10 \times 10^5$ /ml in HBSS(-) and 100 μ l were loaded in a cytocentrifuge funnel and centrifugated using a cytopsin 2 Shandon centrifuge for ten minutes at 200 g to deposit a uniform layer of cells on the microscope slide. Cytocentrifuge preparations were air-dried for two hours, stained by May-Grünwald-Giemsa (five minutes with May-Grünwald, Merck No 1.01424; 20 minutes with Giemsa, Merck No 9204, diluted 1:10 with phosphate buffer, pH 7.2) and observed by using a microscope.

FACS ANALYSIS

To assess the purity, isolated PMNs were stained and analysed by flow cytometry. Before the analysis, the cell pellet was diluted to have 1.10^6 cells for ml. Then 100 μ l of Fc receptor (FcR) blocking reagent from Miltenyi Biotech (Amsterdam, the Netherlands) was added to 100 μ l diluted sample followed by incubation on ice for 15'. After this time the cells were labeled with CD 14 FITC and CD 15 APC antibodies for 30' at 4°C in the dark. The cells were centrifuged for 10' at 600 g and washed twice in PBS-0,1% bovine serum albumin (BSA) before FACS analysis. At least 10.000 stained cells were acquired using a three-laser, 8-color, BD FACSCANTO II Becton Dickinson flow cytometer (BD Biosciences, San José, CA, USA) and analysed using BD FACSDiva software. Neutrophils, monocytes, and lymphocytes were identified on forward/side scatter dot plot profile and gated. The intensity of expression was measured as mean fluorescence intensity and the positive cells were expressed as a percentage.

TRYPAN BLUE EXCLUSION TEST OF CELL VIABILITY

An aliquot of cell suspension was centrifuged at 500 g for 10', the supernatant was discarded and the cells were resuspended in a 1 ml serum-free complete medium. One aliquot of cell suspension was mixed with a part of Trypan Blue 0,4% (Gibco) and was incubated for 2'-5' at room temperature. A drop of Trypan Blue/cell mixture was applied to the Burker chamber and the cells were counted with a binocular microscope. The unstained (viable) and stained (nonviable) cells were counted. To obtain the total number of viable cells for ml of aliquot, the total number of viable cells was multiplied by 2. To obtain the total number of cells for ml of aliquot the total number of viable and nonviable cells were added and multiplied by 2. The percentage of viable cells was calculated as follows: $\text{viable cells \%} = (\text{total number of viable cells} / \text{total number cells}) \times 100$.

SAMPLE PREPARATION FOR INTRACELLULAR METABOLITE EXTRACTION

The protocol for metabolite neutrophils extraction was determined after a series of pilot studies. To perform metabolomics analysis, the cell sample, obtained with Lympholyte-H density gradient procedure, was centrifuged for 10 minutes at 3000 g, the supernatant was discarded and the cells were resuspended with a mixture of 1.2 mL of methanol/chloroform (methanol/chloroform 2:1, methanol/chloroform 1:2, methanol/chloroform 1:1) or 1.0 mL of methanol/water (80:20). To ensure the complete lysis of the cells, the extraction was combined with 20 minutes of ultrasonic treatment at a controlled temperature (4°C). After 20 minutes of sonication, samples were kept at -20°C for 20 minutes and then centrifuged at 3000 g for 30 minutes at 4°C. For GC-MS analysis, 400 µl of supernatant were aliquoted and dried with a vacuum concentrator overnight (Eppendorf concentrator plus, Eppendorf AG, Hamburg, Germany). For ¹H-NMR analysis, 700 µL of supernatant were aliquoted and dried with a vacuum concentrator overnight (Eppendorf concentrator plus, Eppendorf AG, Hamburg, Germany).

CELL NUMBER OPTIMIZATION

To define what was the minimum volume of blood necessary to obtain an optimal number of neutrophils for the acquisition of ¹H-NMR and GC-MS spectra with a good signal-to-noise ratio, three different concentrations of total neutrophils were analysed (1.4×10^6 , 2.6×10^6 , 6.9×10^6). Samples were acquired in replicate to test the reproducibility of the experiments (Table 2). Unfortunately for the NMR analyzes none of the concentrations studied satisfied the sensitivity characteristics of the instrument.

	GC-MS good signal-to-noise ratio	¹ H-NMR good signal-to-noise ratio
Blood sample Volume = 3 ml Cells n° = 1.4×10 ⁶ ±0.7×10 ⁶ *	no	no
Blood sample Volume = 6 ml Cells n° = 2.6×10 ⁶ ±0.4×10 ⁶ *	no	no
Blood sample Volume = 15 ml Cells n° = 6.9×10 ⁶ ±2.6×10 ⁶ *	yes	no

Table 2. Optimisation of blood sample volume and neutrophil number required for the acquisition of ¹H-NMR and GC-MS spectra with a good signal-to-noise ratio. * Mean and standard deviation;

PMNs SAMPLE PREPARATION FOR METABOLOMICS ANALYSIS

For GC-MS analysis the dried pellets were derivatised with 50 µl of methoxyamine dissolved in pyridine (10mg/ml) and incubate 1h a 70°C. After that time, 50 µl of N-Methyl-N(trimethylsilyl)-trifluoroacetamide (MSTFA, Sigma-Aldrich, St. Louis, MO, USA) were added and left at room temperature for 1 hour. Successively, 50µl of hexane (Sigma-Aldrich, St. Louis, MO, USA) were added and the sample was transferred in a vial for the GC-MS analysis. A pool of all the samples was created and used for quality control (QC). For ¹H-NMR analysis cells were redissolved in 690µL of potassium phosphate buffer in D₂O (100mM, pH 7.4) and 10µL of TSP (sodium 3-trimethylsilylpropionate-2,2,3,3,-d₄) as chemical shift reference (δ 0.0) (98 atom % D, Sigma-Aldrich, Milan). An aliquot of 650µL was analysed by ¹H-NMR (85).

GAS CHROMATOGRAPHY-MASS SPECTROMETRY ANALYSIS

One μl of the derivatized sample was injected splitless into a 7890A gas chromatograph coupled with a 5975C Network mass spectrometer (Agilent Technologie, Santa Clara, CA, USA) equipped with a $30\text{ m} \times 0.25\text{ mm}$ internal diameter ID fused silica capillary column with a $0.25\ \mu\text{M}$ TG-5MS stationary phase (Thermo Fisher Scientific Waltham, MA, USA). The injector and transfer line temperatures were at 250°C and 280°C , respectively. The flow rate of the gas helium (He) through the column was 1 ml/min . The column's initial temperature was kept at 60°C for 3 min increased to 140°C at 7°C/min , held at 140°C for 4 min, increased to 300°C at 5°C/min , and kept for 1 min. The identification of metabolites was performed using the standard NIST 08 and Golm Metabolome Database (GMD) mass spectra libraries, as well as by comparison with an authentic standard, when available. The R library XCMS (86, 87) was used for peak detection and retention time correction. Parameters utilized for peak deconvolution of GC-MS matrices were optimized. The resulting matrices were processed using an in-house Python script to eliminate signals present in the blanks, keeping only the most abundant feature per molecule and modifying all zeros present in the matrix by inserting half of the minimum value found for a feature. After manual correction of the filtered matrix to eliminate the internal standard and any possible remaining noise signal, median fold change normalization was performed using an in-house Python script to compensate for sample dilution biases (88).

$^1\text{H-NMR}$ MEASUREMENTS

$^1\text{H-NMR}$ measurements of samples were carried out using a Varian UNITY INOVA 500 spectrometer operating at 499.839 MHz for proton and equipped with a 5 mm double resonance probe (Agilent Technologies, CA, USA). $^1\text{H-NMR}$ spectra were acquired at 300 K with a spectral width of 6000 Hz , a 90° pulse. The acquisition time was 1.5 s , the relaxation delay was 2 s and for each sample, 512 FID were collected into 64K data points. The residual water signal was

suppressed by applying a presaturation technique with low-power radiofrequency irradiation for 2s. After Fourier transformation with 0.3 Hz line broadening and a zero-filling to 64 K, ¹H-NMR spectra were manually phased and baseline corrected using ACD Lab Processor Academic Edition (Advanced Chemistry Development, 12.01, 2010). Spectral chemical shift referencing on the TSP CH₃ at 0.00 ppm was performed on all spectra. The ACD Labs intelligent bucketing method was used for spectral integration between 0.80–8.50 ppm (89). A 0.04 ppm bucket width was defined with an allowed 50% looseness, resulting in buckets that ranged between 0.02 and 0.06 ppm in width. The degree of looseness allows the bucket width to vary over a particular value from the set bucket value. The intelligent bucket method contains an algorithm, which identifies local minima in the spectra and sets the buckets accordingly. In this manner, a peak is integrated in one bucket, although it may be differently shifted in the spectra because of pH effect, for instance. The spectral region between 4.70 and 5.20 ppm was excluded from the analysis to remove the effect of variations in the presaturation of the residual water resonance. Metabolites were identified and quantify of each NMR spectra using the Chenomx NMR Suite 7.1 (Chenomx Inc., Edmonton, Alberta, Canada). Chenomx NMR Suite is an integrated set of tools for identifying and quantifying metabolites in NMR spectra. It is equipped with reference libraries that contain numerous pH-sensitive compound models that are identical to the spectra of pure compounds obtained under similar experimental conditions (five seconds of recycle delay). Essentially, a Lorentzian peak shape model of each reference compound is generated from the database information and superimposed upon the actual spectrum. The linear combination of all modeled metabolites gives rise to the total spectral fit, which can be evaluated with a summation line.

PLASMA SAMPLES PREPARATION FOR GC-MS and ¹H-NMR ANALYSIS

The whole blood samples were collected in tubes with Na-heparin and subsequently centrifuged at 2300 g for 15 minutes. The plasma was recovered and stored at -80°C. Plasma samples were centrifuged at 3000 g for 10 minutes at 4°C and 400µL of supernatant were extracted with a modified Folch method (90). Briefly, 600µL of methanol, 600µL of chloroform and 175 µL of Milli-Q water were added to 400µL of each plasma sample. After centrifugation at 3000 g for 30 minutes at 4°C, 1 ml of hydrophilic phase, containing the low-molecular-weight water-soluble components, was separated from the lipophilic phase. For ¹H-NMR analysis, 700 µl hydrophilic phases were aliquoted and dried using a speed vacuum concentrator (Eppendorf concentrator plus, Eppendorf AG, Hamburg, Germany). Dried hydrophilic plasma extract was redissolved in 630 µl of potassium phosphate buffer in D₂O (0.1 M, pH 7) and has been added 70 µl of sodium 3-methylsilylpropionate 2,2,3,3-d₄ (TSP) as internal standard (98 atom % D, Sigma-Aldrich, Milan). Aliquots of 650 µl of plasma extract were transferred to 5mm NMR glass tubes. For GC-MS analysis, 150 µL of hydrophilic phase was dried in an Eppendorf Concentrator Plus overnight. For analysis, the samples were derivatised with 50 µL of a solution of methoxamine in pyridine (10 mg/mL) (Sigma-Aldrich, 37 St. Louis, MO, USA). After 1h at 70°C, 50µL of MSTFA (Sigma-Aldrich, St. Louis, MO, USA) were added and left at room temperature for one hour. Successively, 150µL of hexane were added and samples were transferred in a vial for the GC-MS analysis. A pool of all samples was created and used as QC.

CELLULAR ROS DETECTION

The intracellular reactive oxygen species (ROS) levels in non-treated and treated deferiprone neutrophils from patients enrolled in the study were evaluated by using the cells permeant reagent 2',7' dichlorofluorescein diacetate (DCFH-DA, Sigma, St. Louis, MO, USA), a fluorescein dye that measures hydroxyl, peroxy and other ROS activity within the cell. After diffusion into the cell, DCFH-DA is deacetylated by cellular esterases to a non-fluorescent compound, which is later oxidized by ROS into 2',7'-dichlorofluorescein (DCFH) probe. Before starting this experiment, a series of preliminary studies were conducted. It was important to check the natural fluorescence of deferiprone and the concentration of DCFH-DA required to detect ROS. Indeed, the concentration of the DCFH-DA required to detect ROS can change depending on the cell type and their activation status. Also, the ideal number of cells per well was established in the preliminary experiments. After establishing the right conditions, 6ml of peripheral blood specimen was collected from study participants. The cells isolated, as previously described, were suspended in 1ml RPMI-1640 (GIBCO Laboratories, Grand Island, NY, USA) medium supplemented with 10% of fetal bovine serum. A small aliquot was taken to count the cells and confirm cell viability with trypan blue exclusion in a 1: 1 dilution. The rest of the cells were seeded in a 25 cm flask with 2ml RPMI-1640 medium supplemented with 10% of fetal bovine serum and exposed to 20 μ M, 50 μ M, 100 μ M DFP for 2,5 hour. The control cells without DFP were processed in parallel. The cells were incubated at 37°C in a humidified atmosphere of 5% CO₂. Afterward, a small aliquot was taken to count the cells and confirm cell viability with trypan blue exclusion in a 1: 1 dilution, the rest of the cells were harvested in 15 ml tube and centrifuged for 10' at 500 g. The supernatant was discarded and the pellet was re-suspended in 1 ml of 20 μ M DCFH-DA solution. The controls cells (no DFP exposed) were divided in two 15 ml tube, after centrifugation one part were resuspended in 1ml PBS without DCFH-DA and one part in 20 μ M DCFH-DA solution. The cells were incubated in dark conditions at 37°C in a humidified atmosphere of 5% CO₂ for 30' so that the DCFH-DA could

penetrate the cells. Then the 15 ml tube was centrifuged for 10' at 500 g. The supernatant was discarded and the cells re-suspend with 1ml of PBS and seeded in 96-well plate (2×10^5 cells for well). The samples were measured in triplicate. Control cells incubated with PBS were used for basal fluorescence determination. An aliquot of control cells DCFH-DA treated was resuspended with a 5nM TBH (ter-butyl hydroperoxide) solution to induced ROS produced. The fluorescence of the cells was determined using an Infinite F200 (Tecan Salzburg, Austria) auto microplate reader at 485 and 528 nm excitation and emission wavelengths, respectively.

DETERMINATION OF REDUCED (GSH) AND OXIDIZED (GSSG) GLUTATHIONE

When the recovery of the cells was sufficient, they were used for ROS measurement by high-performance liquid chromatography linked with an electrochemical detector (HPLC– ECD). The method described by Khan et al for the determination of reduced [GSH] and oxidized glutathione [GSSG]) was used (91). An aliquot of cells (1×10^6 cells/sample) cultured in RPMI-1640 medium supplemented with 10% of fetal bovine serum and exposed to 20 μ M, 50 μ M, 100 μ M DFP for 2,5 hour were centrifuged at 500 g for 10 minutes and the supernatant was discarded. Cells seemed in RPMI-1640 medium alone DFO were used as controls. The cell pellet was suspended with 1 ml of MPA (metaphosphoric acid) 10% plus 1 ml of 0,05% TCA (trichloroacetic acid) solution (Sigma-Aldrich, Milan, Italy). After centrifugation, the clear supernatant was injected into the HPLC system. GSH/GSSG levels were determined by electrochemical detection, using an HPLC (Agilent 1260 infinity, Agilent Technologies, Palo Alto, USA) equipped with an electrochemical detector (DECADE II Antec, Leyden, The Netherlands) and an Agilent interface 35900E. A C-18 Phenomenex Luna column, 5 μ m particle size, 150 \times 4.5 mm, was used with a mobile phase of 99% water with 0.05% TFA (v/v) and 1% MeOH at a flow rate of 1 ml/min. The electrochemical detector was set at an oxidizing potential of 0.74 V. A calibration curve was created using standards

of GSH, GSSG (Sigma-Aldrich, Milan, Italy) injected at different concentrations. The sample (20 μ l) was injected into HPLC system by autosampler.

STATISTICAL ANALYSIS

MULTIVARIATE STATISTICAL ANALYSIS

Multivariate statistical data analysis was performed using SIMCA-P software (version 15.0, Umetrics, Sweden) (92). Raw data from both ¹H-NMR and GC-MS analysis were processed and organized in a matrix for the multivariate statistical analysis. Before multivariate statistical analysis, the data sets were normalized to the total area or cell number for plasma and PMN analysis respectively to minimize dilution factors. All imported data were scaled for the multivariate statistical analysis, using Pareto scaling for ¹H-NMR data and UV-scaling for GC-MS data. Pareto scaling was preferred for NMR data because it gives greater weight to the variables of the NMR data with less intensity. The initial data analyses were conducted using the Principal Component Analysis (PCA), The PCA allows the exploration of sample distributions without classification. To identify potential outliers, DmodX and Hotelling's T² tests were applied. Partial least squares discriminant analysis (PLS-DA) and orthogonal partial least squares discriminant analyses (OPLS-DA) were subsequently applied. PLS-DA and OPLS-DA maximize the discrimination between samples assigned to different classes. A PLS-DA was performed to investigate the metabolomics differences between the three classes: A and NA patients and healthy subjects. OPLS-DA was used to reduce model complexity and to better highlight sample discrimination, when the metabolomics profile of samples was compared in pairs. OPLS-DA a supervised classification technique and maximizes the covariance between the measured data of the X-variable (peak intensities) and the response of the Y-variable (class assignment) within the groups. The estimated predictive power of the models was expressed by R²_Y and Q²_Y, which represent the fraction of the variation of Y-variable and the predicted fraction of the variation of Y-variable, respectively. A good prediction

model is achieved when $Q^2 > 0.5$. (93). The quality of OPLS-DA models was evaluated on the corresponding PLS-DA models using a 7-fold cross-validation and permutation test ($n = 400$). The permutation test was calculated by randomizing the Y-matrix (class assignment or continuous variables) while the X-matrix (peak intensity) was kept constant. The permutation plot then displays the correlation coefficient between the original y-variable and the permuted y-variable on the x-axis versus the cumulative R^2 and Q^2 on the y-axis and draws the regression line. The intercept is a measure of the overfit, Q^2Y intercept value less than 0.05 is indicative of a valid model. To identify the metabolites playing a role in class separation, the S-plot was considered.

UNIVARIATE STATISTICAL ANALYSIS

GraphPad Prism software (version 7.01, GraphPad Software, Inc., San Diego, CA, USA) was used to perform the univariate statistical analysis of the data resulting from the multivariate analysis. The metabolite concentrations identified with NMR analysis were determined by using Chenomx NMR suite 7.1. Chenomx NMR Suite is an integrated set of tools for identifying and quantifying metabolites in NMR spectra. It is equipped with reference libraries that contain numerous pH-sensitive compound models that are identical to the spectra of pure compounds obtained under similar experimental conditions. Essentially, a Lorentzian peak shape model of each reference compound is generated from the database information and superimposed upon the actual spectrum. The linear combination of all modeled metabolites gives rise to the total spectral fit, which can be evaluated with a summation line. The statistical significance of the differences in metabolite concentrations for both analytical techniques (NMR and GC-MS), was calculated by using the Mann-Whitney U test and a p-value < 0.05 was considered statistically significant. The Benjamini-Hochberg adjustment was subsequently applied to the obtained p-values to acquire the level of significance for multiple testing.

IV. RESULTS

OPTIMISING PROTOCOLS FOR GC-MS and ¹H-NMR METABOLOMICS ANALYSES OF HUMAN NEUTROPHILS

One aim of this project was to optimise the protocol for GC-MS and H-NMR metabolomics analysis to study changes in neutrophils' metabolomics profiles. Working with human neutrophils in vitro generates some technical challenges meaning that the standard protocols for most assays must be optimized. In particular, it was necessary to establish protocols to optimise sample preparation, metabolite extraction, and analysis to reduce chemical and physical degradation of neutrophils' metabolites and the introduction of interfering compounds commonly used in isolation procedures.

COMPARISON OF TWO COMMERCIAL USED ISOLATION PROTOCOLS FOR PURITY OF ENRICHED GRANULOCYTES

PMNs were isolated from healthy volunteers' blood using in parallel two of the most common commercial method: Lympholyte-H and Lympholyte-poly. Analysis of the purities of granulocytes by FACS was performed using CD-14 FITC and CD-15 APC antibodies. CD14 is expressed at high levels on monocytes and macrophages, and lower levels on granulocytes, while CD15 is expressed on granulocytes and monocytes. The purity of isolated cells analysed by flow cytometry amounted to 92.6% (± 2 %) and 98.9% (± 1 %) for Lympholyte-poly and Lympholyte-H methods, respectively (Fig. 4, Tab. 1). Moreover, with lympholyte-H isolation method the higher recovery rates of PMNs after the isolation procedure were obtained (Tab. 1) Furthermore, May-Grünwald-Giemsa staining and light microscopy were used to ensure that a pure population of PMNs (>90 % purity) with typical morphology had been isolated. PMNs are among the shortest-lived cells in the body and due to this physiological characteristic, they are extremely fragile cells and are prone to apoptosis upon withdrawal from the blood. For this purpose, the cells were stained using the Trypan Blue dye exclusion method. Numbers of live and dead leukocytes for sample were assessed using a Burker

chamber. The viability was >95 % in all experiments. With a purity of 99% and the highest overall yield granulocyte enrichment, Lympholyte-H seems to be the optimal method when a high number of cells are required and, for this reason, Lympholyte-H method isolation protocol was used in all subsequent experiment.

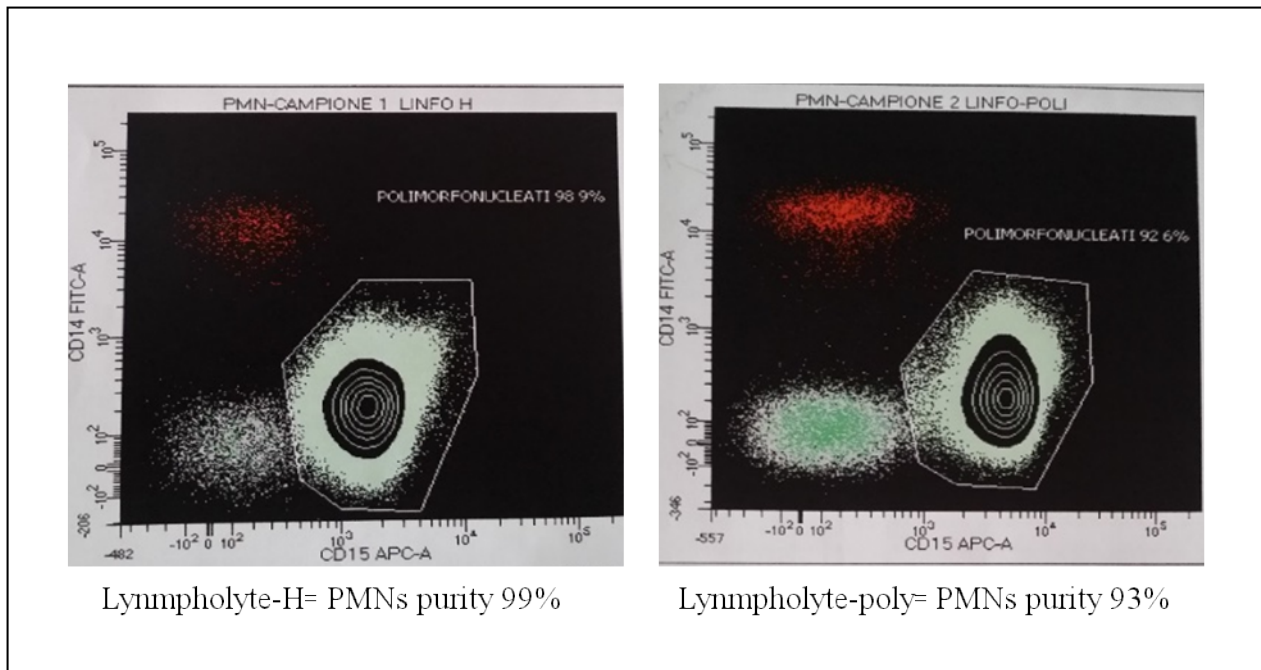


Figure 4. Purities of enriched granulocyte. Representative flow cytometry dot plots show the purity of the enriched granulocyte isolates obtained by either i) Lympholyte-H (left) and ii) lympholyte-poly (right) density centrifugation methods.

Method	Yield ^a	Purity ^a	Procedure Time (h)
Lympholyte-H	$15 \times 10^5 \pm 5.3 \times 10^5$	98.9% $\pm 2\%$	2
Lympholyte-poly	$13.8 \times 10^5 \pm 3.3 \times 10^5$	92.6% $\pm 2\%$	2

Table 3. Comparison of yields and purities of granulocytes, time consumption, of the two different isolation procedures evaluated in the study: (i) Lympholyte-H (ii) lympholyte-poly.

Means of 4 independent experiments. The purity is expressed as percentage of total nucleated cells.

METABOLITE EXTRACTION

The successful extraction of metabolites is a critical step in the metabolomic analysis. In order to optimize metabolite isolation, four different extraction mixtures were used: methanol/chloroform 2:1; methanol/chloroform 1:2; methanol/chloroform 1:1; cold methanol/water (80:20 V/V). The effect of these different extraction mixtures can be observed from their total ion chromatogram (TIC) obtained after GC-MS analysis of 5×10^6 cells (Fig. 5). After data analysis, 30 metabolites were detected and there were no significant differences in the number of metabolites found in the different extraction mixture. When the metabolites were extracted with methanol/chloroform 1:2, the intensity of the GS-MS signal seemed greater than the other extraction mixtures. However, the chromatogram also showed an increase in background noise (Fig.5b). In our preliminary experiment, cold methanol/water (80:20) extraction proved to be the best (Fig.5d). Also, optimisation for cells number was necessary. For the clinical sample (3-5ml) the total number of neutrophils that can be routinely obtained from the blood of patients and healthy donors was 2×10^6 cells. Therefore, it was critical to determine the minimum volume of peripheral blood to obtain a number of enough neutrophils required to acquire both GC-MS chromatograms and $^1\text{H-NMR}$ spectra with the optimal signal-to-noise ratio. For this purpose, three different total cell numbers of neutrophils (1.4×10^6 , 2.6×10^6 , 6.9×10^6), were analysed. A good data analysis was possible with at least 5×10^6 cells for the GC-MS method. At the same time, with the same number of cells, it was not possible to obtain appreciable spectra with H-NMR analysis. β -thalassemic patients have high variability in neutrophil counts, so about 20ml of blood sample was required to obtain a minimum number of 5 million cells per experiment. Due to its higher sensitivity, for the study of metabolites in granulocytes neutrophils of β -thalassemic patients GC-MS approach was chosen.

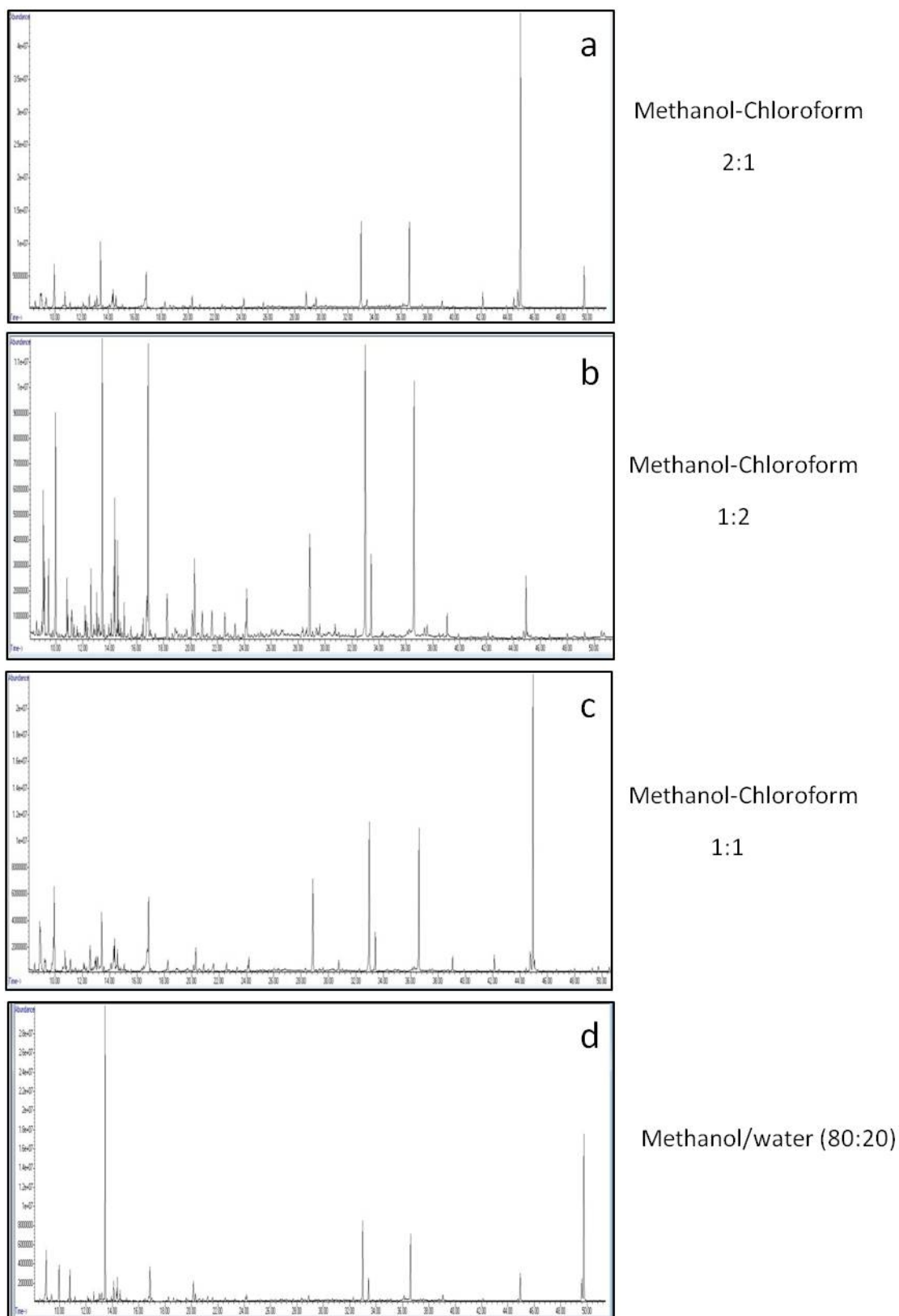


Figure 5. Comparison of different metabolite extraction mixtures. Representative TIC (total ion current) of four different mixtures of methanol/chloroform and methanol/water used for metabolite extraction. The figure shows the TIC representative by $> 5 \times 10^6$ cells analysed.

PMNs METABOLOMICS ANALYSIS

PMNs from peripheral blood of twenty-three β -Thalassemic patients (11 A and 12 NA) and 13 healthy subjects (C) were analysed with GC-MS. Peaks were identified and attributed endogenous metabolites including organic acids, amino acids, short fatty acids, and sugars. Multivariate statistical analysis (MVA) is crucial in metabolomics studies because all metabolites are considered at the same time, allowing trends to be detected between both samples and metabolites. First, a PCA model was applied to the entire dataset (Fig 6). Fig. 6 shows the projection of the samples on the plane formed by the first two PCs explaining 50.0% of the total variance. PCA scores plot showed no outliers, and the whole dataset was subjected to supervised analysis. So, a supervised analysis (PLS-DA) was applied to remove information unrelated to the disease of interest. The PLS-DA model (Fig. 7) was built by comparing the GC-MS metabolomics profile of the three different classes (control subjects, A and NA patients). Figure 7 showed good separation between A and NA subjects and controls indicating differences in the metabolomics profile between the three groups. The validity of the PLS-DA model was evaluated through a permutation test using 400 times. The test results are reported in Table 3 and indicate the statistical validity of the PLS-DA model. Moreover, one of the agranulocytosis (A) samples was distributed in an anomalous way so it was excluded from further statistical analysis. Interestingly, this patient showed a longer time to onset of the side effect compared to other members of the same group.

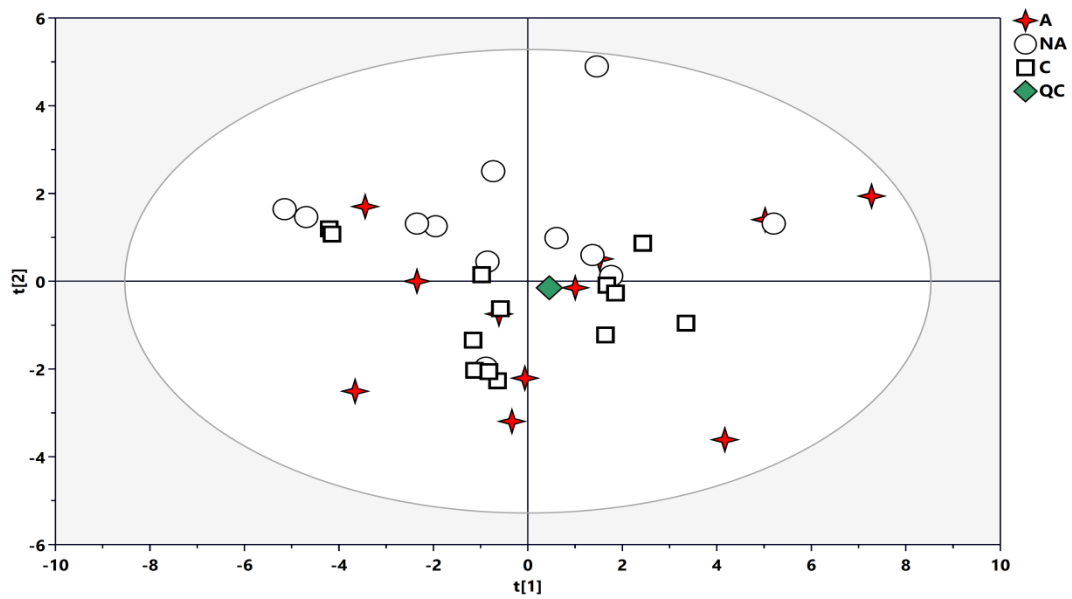


Figure 6. PCA scores plot of PMN samples from patients and control subjects. (A) β -thalassemic patients with agranulocytosis, (NA) β -thalassemic patients without agranulocytosis, (C) healthy controls, QC: quality control. Plots were obtained with GC-MS

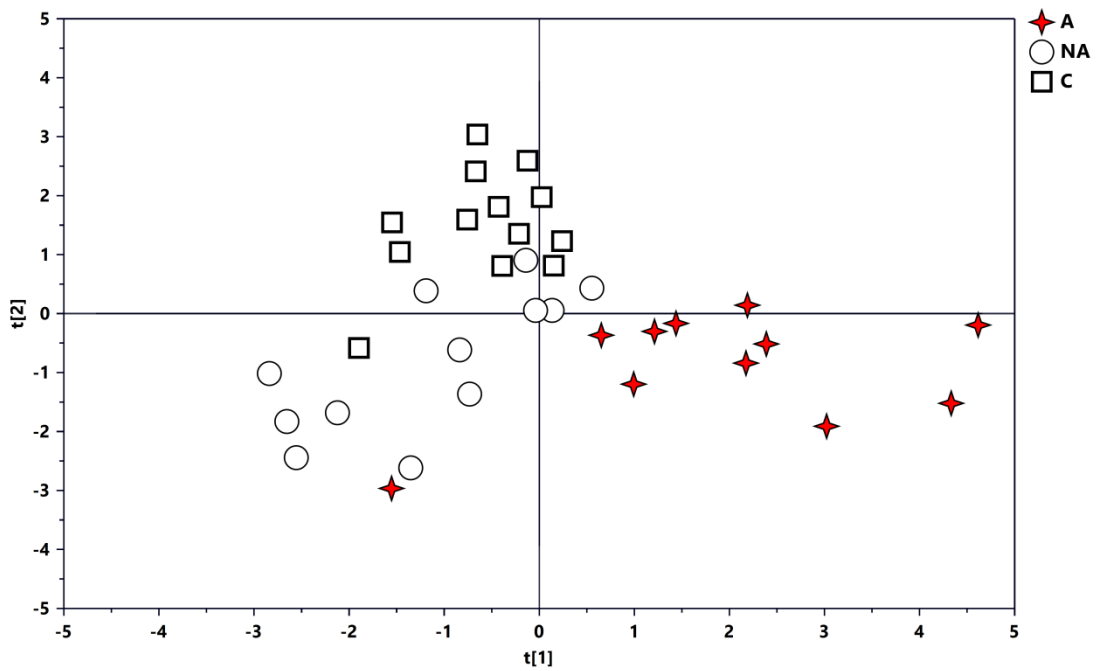
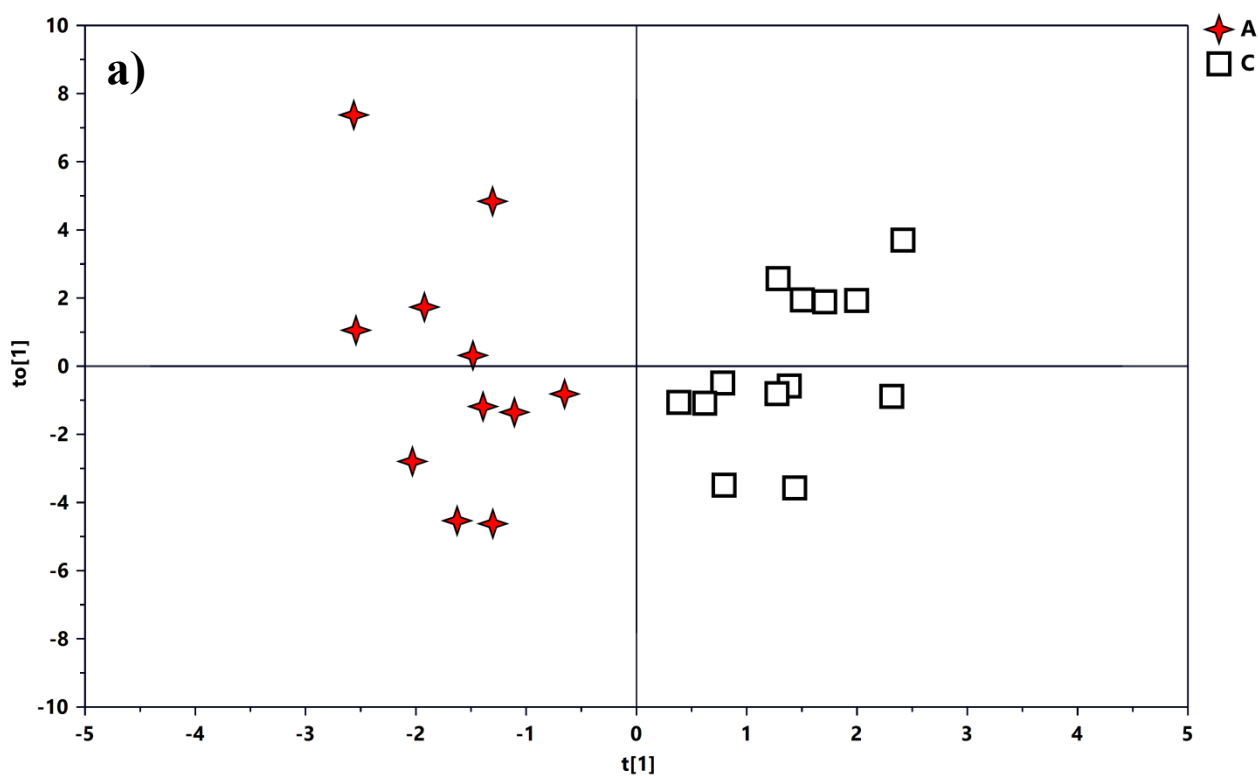


Figure 7. PLS-DA scores plot of PMN samples from patients and control subjects, (A) β -thalassemic patients with agranulocytosis, (NA) β -thalassemic patients without agranulocytosis, (C) healthy controls. Plots were obtained with GC-MS

Three separate OPLS-DA models were built using the same 3 groups of samples: agranulocytosis (A) vs controls (C), non-agranulocytosis (NA) vs controls (C) and agranulocytosis (A) vs non-agranulocytosis (NA) samples. The results of these pairwise comparisons enabled improved assessment and identification of the metabolites that were responsible for the separation between the distinct groups. A first OPLS-DA analysis (Fig.8a) was performed by comparing agranulocytosis (A) versus the healthy subjects (C). The OPLS-DA model was established with one predictive and one orthogonal component, and showed good values of R2 X, R2 Y and Q2 (Table 3). Samples showed a good separation into two distinct groups, indicating a different metabolomics profile between the two groups. The metabolites responsible for the separation between PMN cells from A patients and controls were identified in the corresponding S-plot (Fig. 8b).



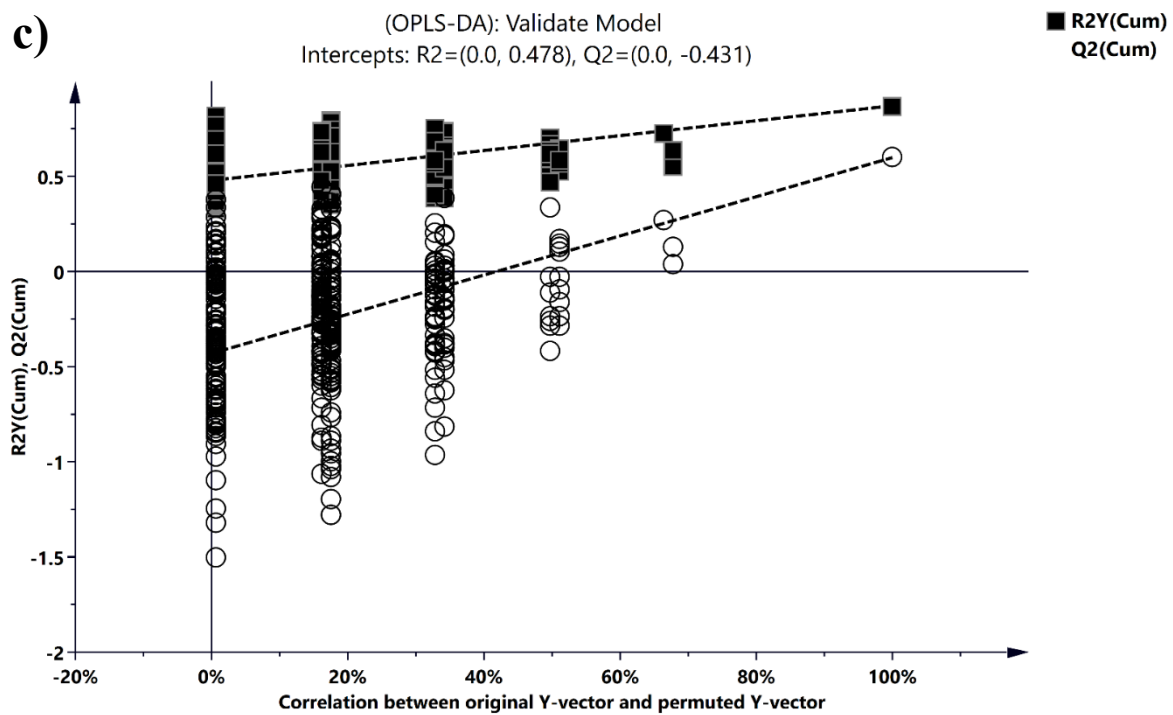
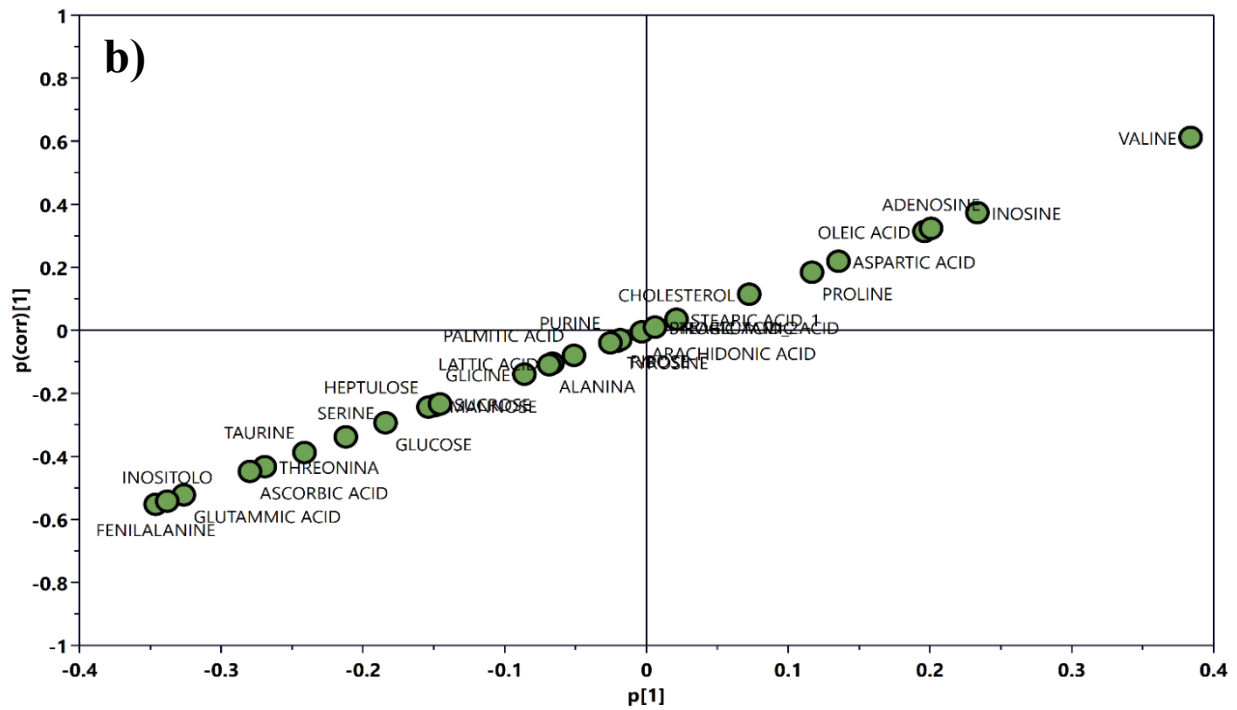
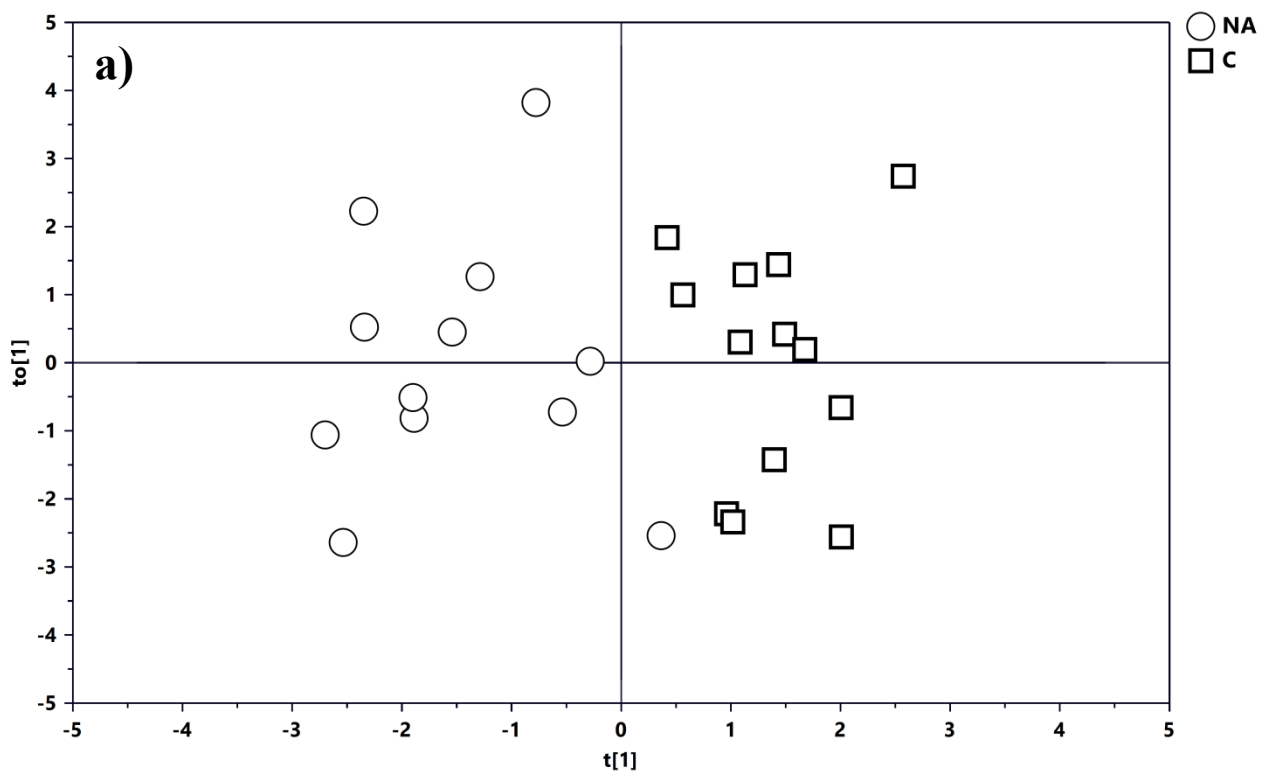


Figure 8. OPLS-DA analysis of PMN samples A vs C. (a) OPLS-DA scores plot of PMNs samples A (β-thalassemic patients with agranulocytosis) vs C (healthy controls). (b) S-Plot corresponding to the OPLS-DA model used to characterize the most significant variables associated with group A and C subjects. Arbitrarily cut-off values for the covariance of $|p| \geq 0.1$ and for the correlation $|p(\text{corr})| \geq 0.1$ were used. (c) The permutation test of OPLS-DA model. Plots were obtained with GC-MS

The validity of the OPLS-DA model was evaluated through a permutation test using 400 times (Fig.8c). The test results are reported in Table 3 and indicate the statistical validity of the OPLS-DA model. A second OPLS-DA analysis was conducted comparing the metabolomics profile of the no-agranulocytosis (NA) vs controls (C) subjects. The OPLS-DA scores plot showed (Fig.9a) a clear separation between groups, indicating a significant difference in the metabolic profile. The OPLS-DA model was established with one predictive and one orthogonal component and showed good values of R2 X, R2 Y and Q2 (Table 3). The metabolites responsible for the separation between PMN cells from NA patients and controls were identified in the corresponding S-plot (Fig. 9b). The validity of the OPLS-DA model was evaluated through a permutation test using 400 times (Fig. 9c). The test results are reported in Table 3 and indicate the statistical validity of the OPLS-DA model.



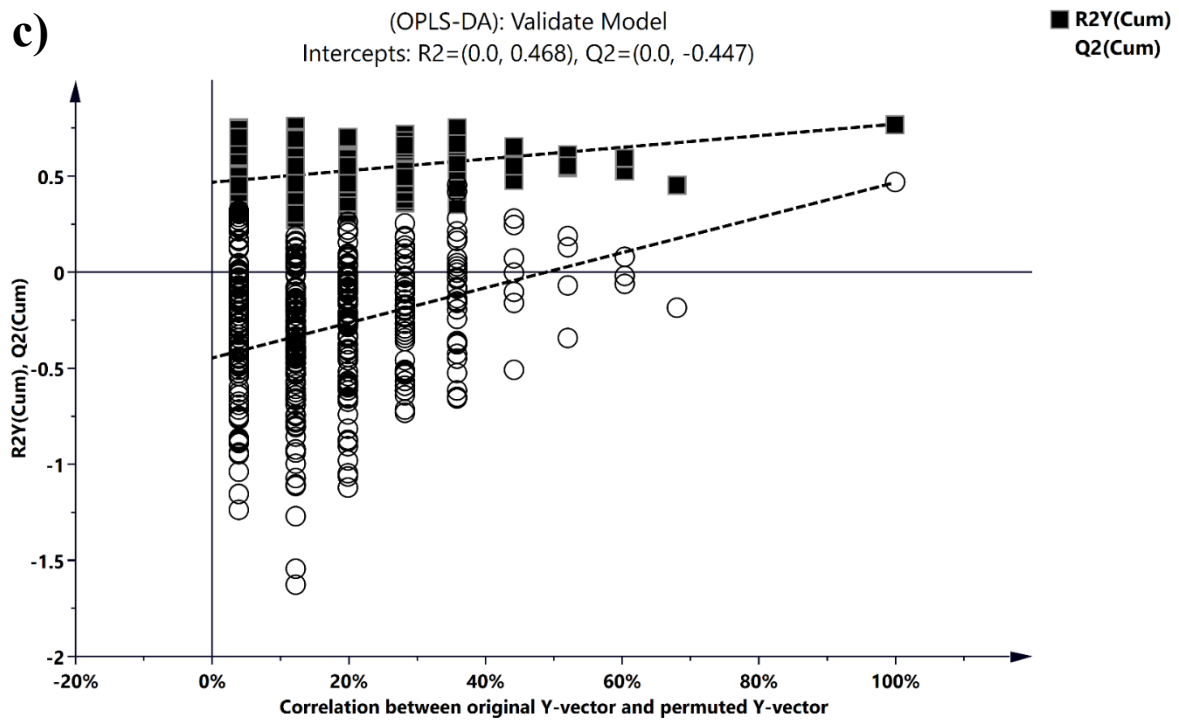
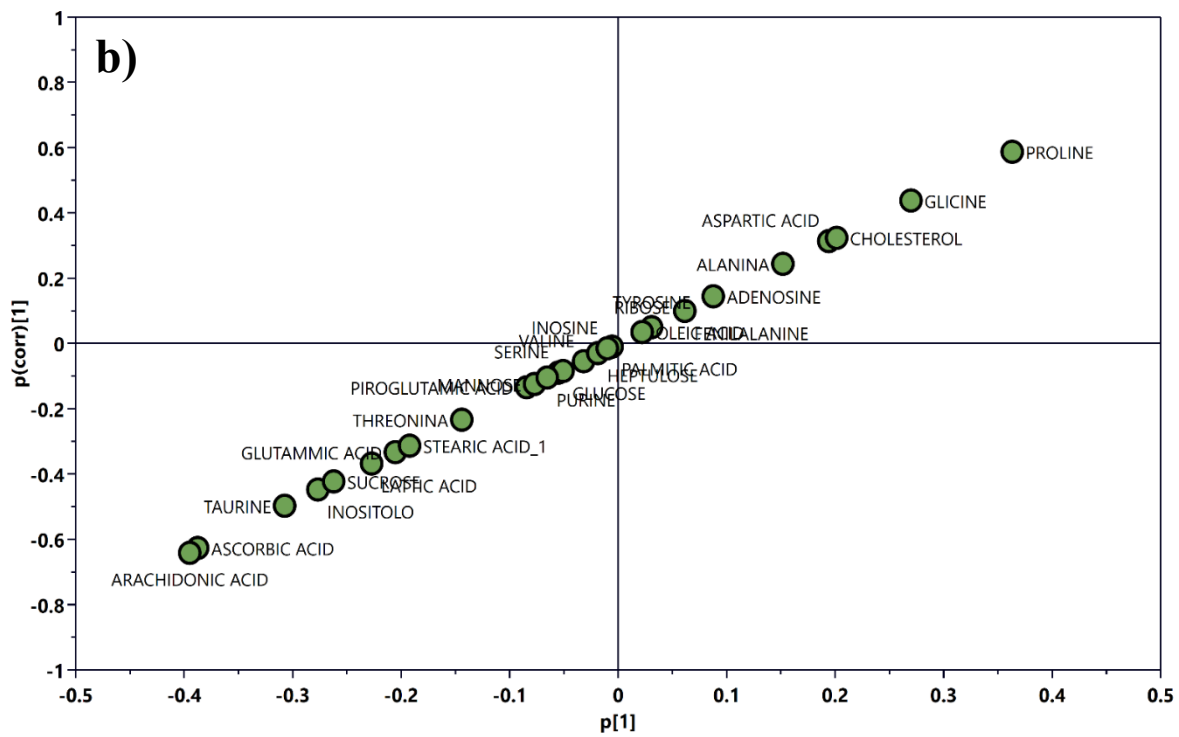
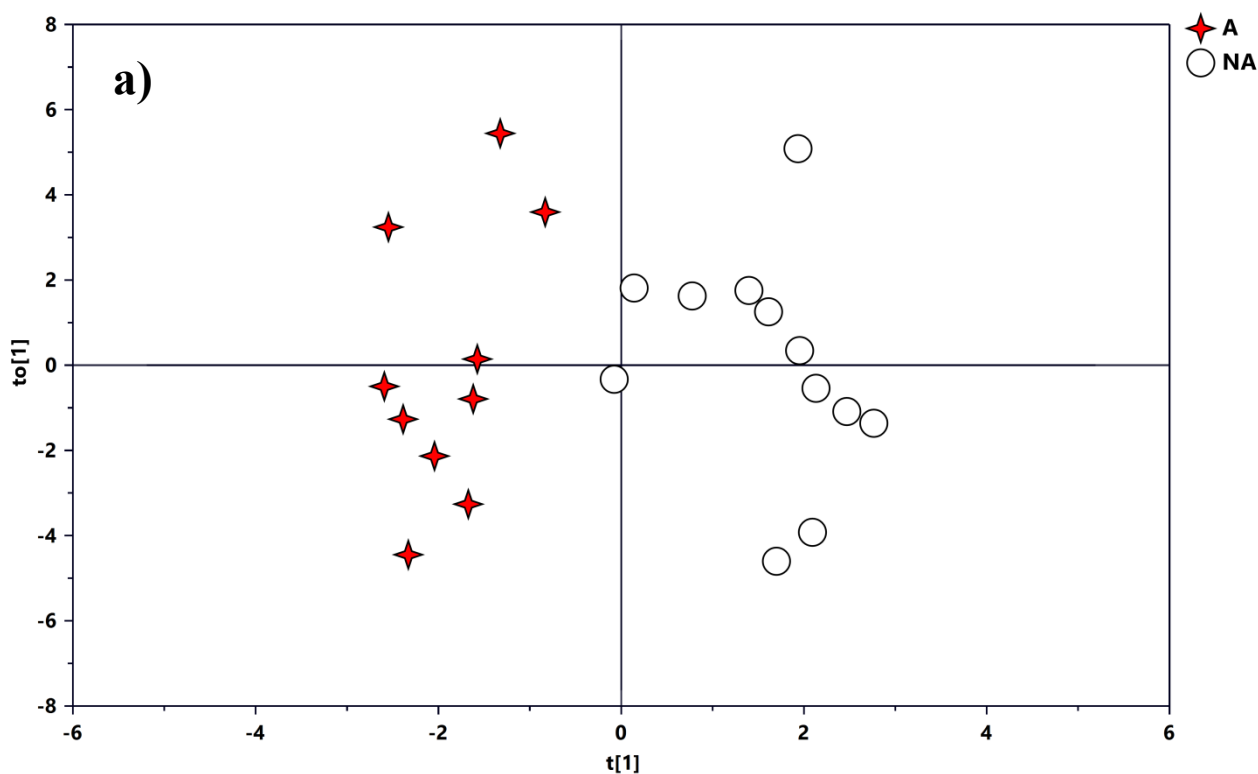


Fig. 9. OPLS-DA analysis of PMN samples NA vs C. (a) OPLS-DA scores plot of PMNs samples NA (β -thalassemic patients without agranulocytosis) vs C (healthy controls). (b) S-Plot corresponding to the OPLS-DA model used to characterize the most significant variables associated with group NA and C subjects. Arbitrary cut-off values for the covariance of $|p| \geq 0.1$ and for the correlation $|p(\text{corr})| \geq 0.1$ were used. (c) The permutation test of OPLS-DA model. Plots were obtained with GC-MS

Finally, the OPLS-DA analysis was conducted by comparing Agranulocytosis (A) versus No-agranulocytosis (NA) subjects. The OPLS-DA scores plot (Fig. 10a) showed good separation of the subjects into two distinct groups, indicating a difference in the metabolomics profile between the NA and A subjects. The OPLS-DA model was established with one predictive and one orthogonal component and showed good values of R^2_X , R^2_Y and Q^2 (Table 3). Metabolites responsible for the separation between PMN cells from NA patients and controls were identified in the corresponding S-plot (Fig. 10b). The validity of the OPLS-DA model was evaluated through a permutation test using 400 times (Fig. 10c). The test results are reported in Table 3 and indicate the statistical validity of the OPLS-DA model.



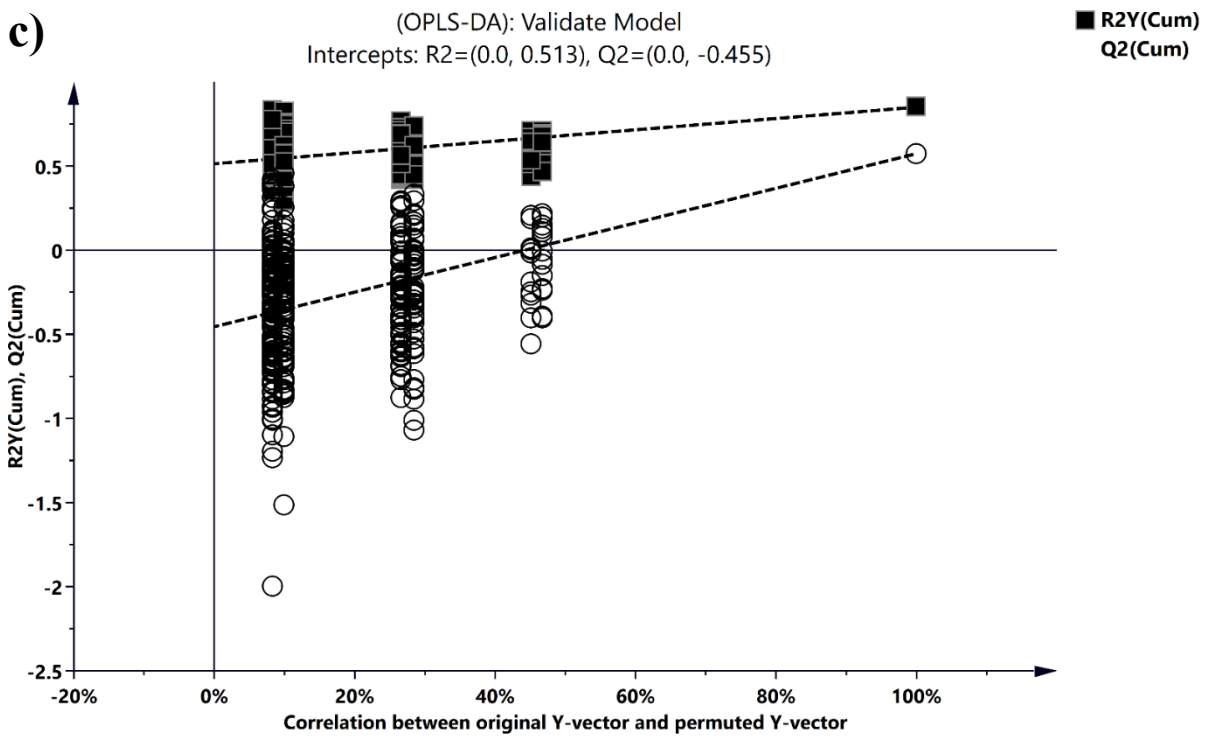
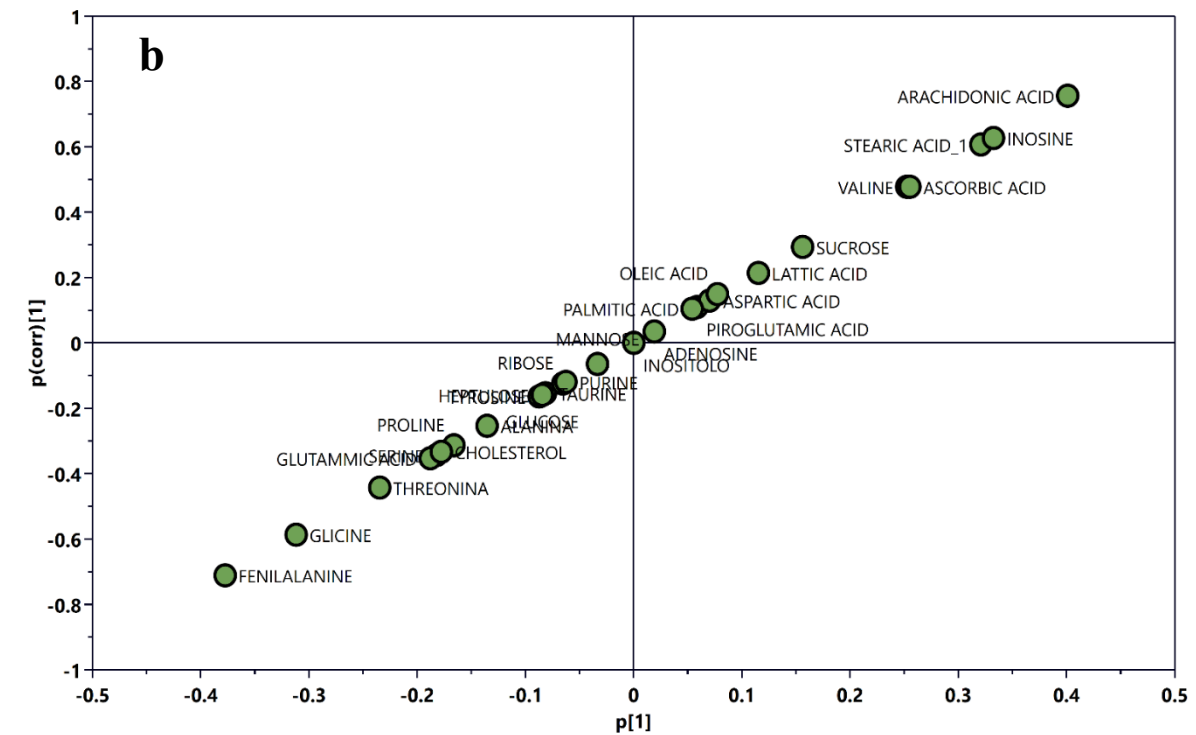


Figure 10. OPLS-DA analysis of PMN samples NA vs A. (a) OPLS-DA scores plot of PMNs samples NA (β -thalassemic patients without agranulocytosis) vs A (β -thalassemic patients with agranulocytosis). (b) S-Plot corresponding to the OPLS-DA model used to characterize the most significant variables associated with group NA and A subjects. Arbitrary cut-off values for the covariance of $|p| \geq 0.1$ and for the correlation $|p(\text{corr})| \geq 0.1$ were used. (c) The permutation test of OPLS-DA model. Plots were obtained with GC-MS

PLS-DA and OPLS-DA models					Permutation*	
GC-MS						
Groups	Componentets ^a	R ₂ Xcum ^b	R ₂ Ycum ^c	Q ₂ cum ^d	R ₂ intercept	Q ₂ intercept
C, A, NA	2	0.248	0.562	0.149	0.224	-0.171
Controls vs A	1P+1O	0.381	0.871	0.598	0.478	-0.431
Controls vs NA	1P+1O	0.206	0.771	0.500	0.468	-0.447
A vs NA	1P+1O	0.415	0.850	0.573	0.513	-0.455

Table 4. PMNs samples MVA parameters. The number of Predictive and Orthogonal components used to create the statistical models. ^b R₂X and R₂Y indicated the cumulative explained fraction of the variation of the X block and Y block for the extracted components. Q₂cum values indicated cumulative predicted fraction of the variation of the Y block for the extracted components. * R₂ and Q₂ intercept values are indicative of a valid model.

The most important metabolites were evaluated through analysis of the S-plot for all three comparisons. The metabolites were subjected to Mann-Whitney U test to identify significant variations of their concentration. Significantly, discriminant metabolites were characterized by VIP > 1 and p ≤ 0.05. The results of the univariate statistical analysis showed that only eighteen metabolites were responsible for the separation between A patients and the healthy control (Fig. 11). Of these, five were significantly increased in A patients, glutamic acid, inositol, phenylalanine, taurine, and threonine, while the inosine significantly decreased in A patients (Table 4).

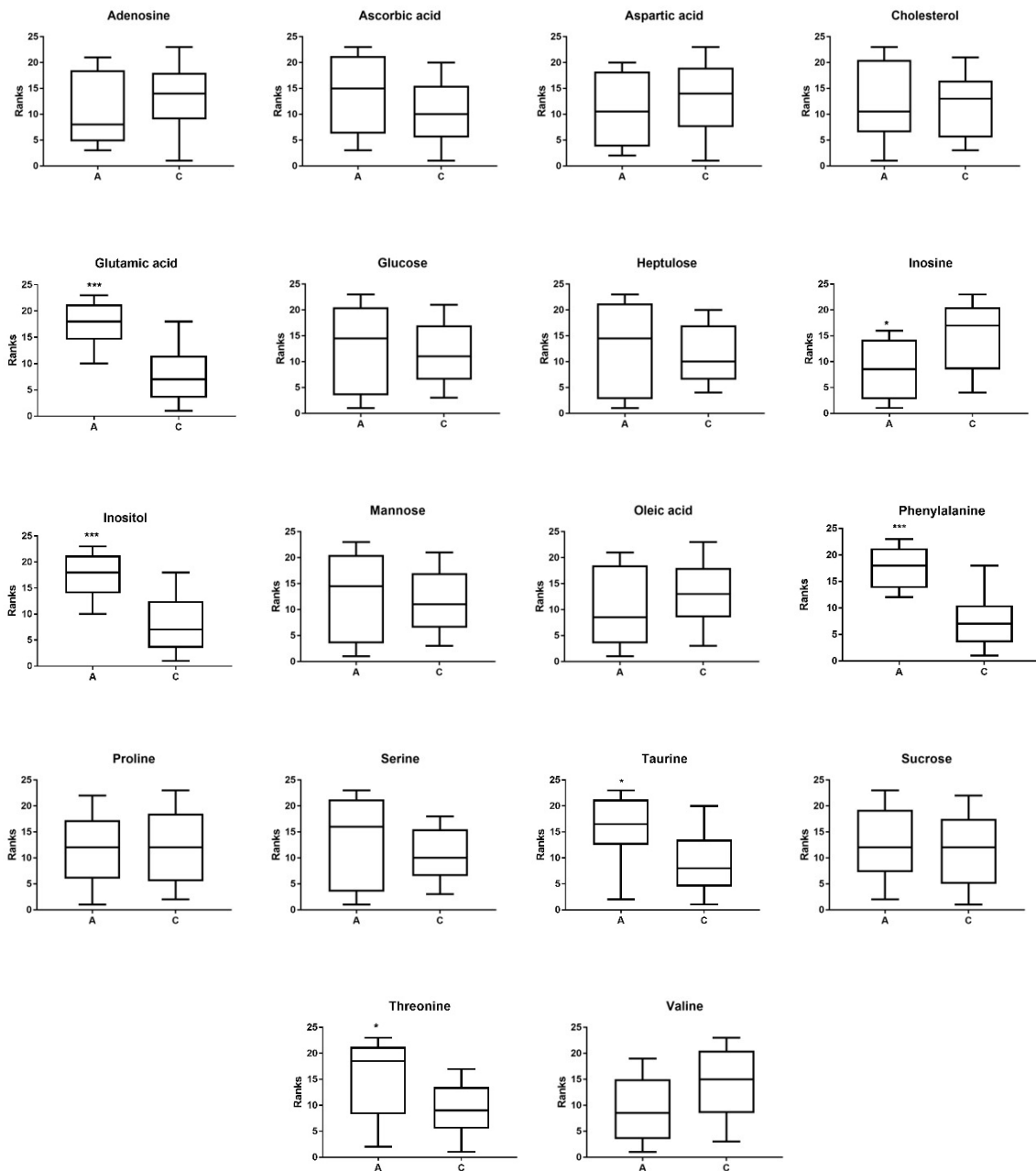


Figure. 11: Discriminant metabolites in A patients versus healthy subjects (C) obtained with the MVA are shown and expressed in the graphs y axis as ranks (data transformation in which numerical or ordinal values are replaced by their rank when the data are sorted). Discriminant metabolites obtained with the MVA, underwent a Mann-Whitney test to determine which metabolites were statistically significantly varied. * and *** indicates levels of significance with $p < 0.05$ and <0.001 respectively.

MEANS (SD) OF GROUP

METABOLITES	A	C	p VALUE
ADENOSINE	7.417±7.16	10.34±7.197	0.3758
ASCORBIC ACID	0.183±0.213	0.073±0.054	0.208
ASPARTIC ACID	0.315±0.209	0.548±0.546	0.3758
CHOLESTEROL	46.19±14.16	46.45±8.098	0.8315
GLUCOSE	0.567±0.539	0.325±0.298	0.3434
GLUTAMIC ACID	0.693±1.089	0.054±0.052	0.0002
HEPTULOSE	0.662±0.667	0.383±0.335	0.6049
INOSINE	0.175±0.129	1.337±1.641	0.0303
INOSITOL	0.403±0.305	0.088±0.093	0.0003
MANNOSE	1.92±2.018	1.195±1.049	0.6926
OLEIC ACID	1.152±0.419	1.346±0.311	0.3758
PHENILALANINE	0.174±0.116	0.047±0.034	0.0001
PROLINE	2.682±1.363	2.944±1.239	0.8793
SERINE	0.298±0.433	0.092±0.040	0.3128
SUCROSE	0.707±0.917	0.455±0.393	0.7381
TAURINE	0.550±1.23	0.046±0.040	0.0214
THREONINE	0.800±1.01	0.135±0.089	0.0358
VALINE	0.089±0.056	0.159±0.088	0.0769

Table 5. Statistical differences of metabolites characterized by Variable Importance for the Projection (VIP) > 1. Metabolites were selected on VIP > 1 based on Orthogonal Partial Least Squares Discriminant Analysis (OPLS-DA). a Relative concentrations were calculated by normalization of the molar concentration of each metabolite to the total molar concentration of all 18 metabolites for each sample. b A Mann–Whitney U test was performed and the p-value reported. The Holm-Bonferroni adjustment was applied.

Regarding the comparison between NA patients and healthy subjects (C) fourteen metabolites were able to discriminate significantly NA patients vs. healthy subjects (Fig. 12). In detail, arachidonic acid, sucrose, and taurine were significantly increased in NA patients, while the proline was significantly decreased in NA patients (Table 5).

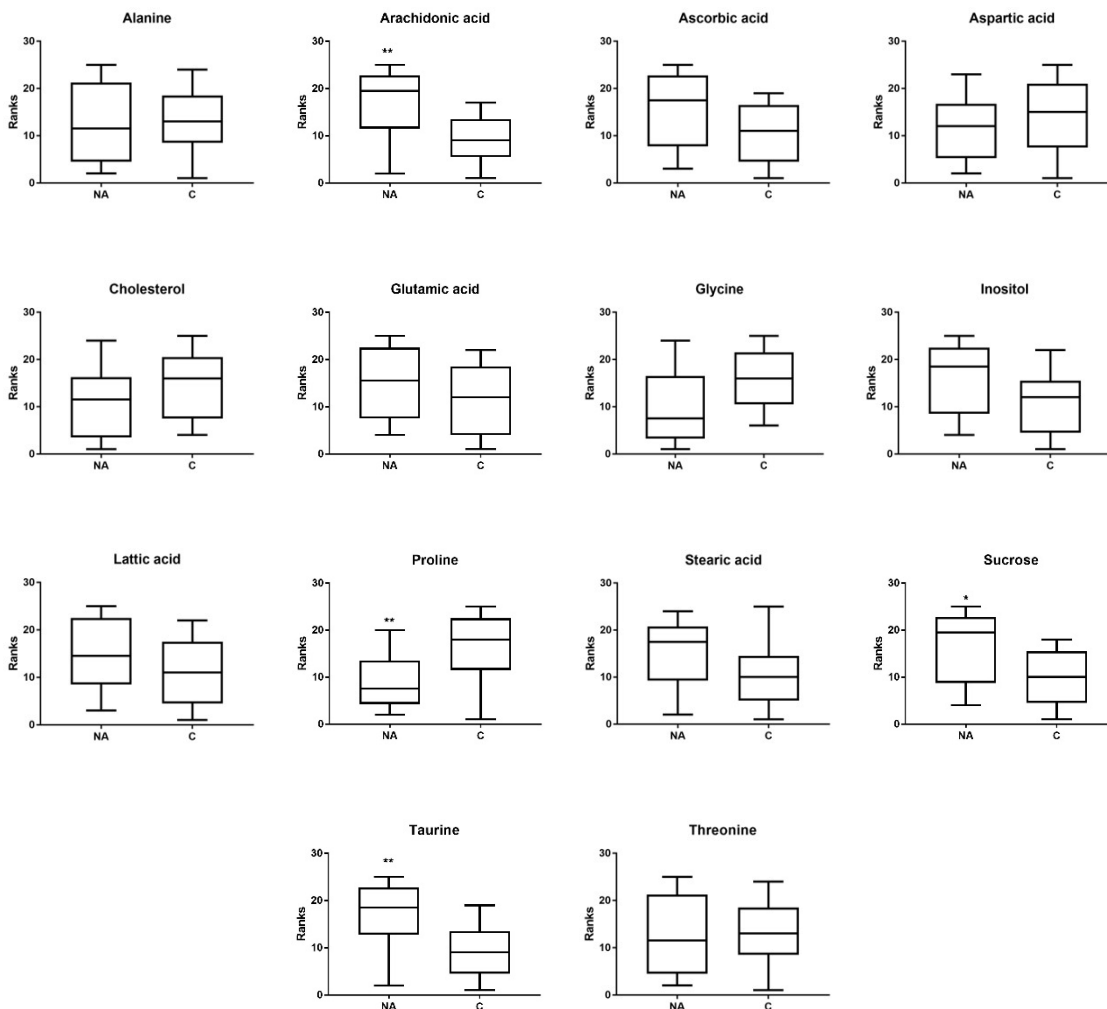


Figure 12. Discriminant metabolites in NA patients vs healthy subjects (C) obtained with the MVA are shown and expressed in the graphs y axis as ranks (data transformation in which numerical or ordinal values are replaced by their rank when the data are sorted). Discriminant metabolites obtained with the MVA, underwent a Mann-Whitney test to determine which metabolites were statistically significantly varied * and ** indicates levels of significance with $p < 0.05$ and <0.01 respectively.

MEANS (SD) OF GROUP

METABOLITES	C	NA	p VALUE
ALANINA	0.136±0.089	0.154±0.155	0.8938
ARACHIDONIC ACID	0.517±0.155	3.375±2.544	0.008
ASCORBIC ACID	0.073±0.054	0.355±0.332	0.0678
ASPARTIC ACID	0.548±0.546	0.354±0.224	0.4371
CHOLESTEROL	46.45±9.089	39.02±15.06	0.2471
GLUTAMIC ACID	0.054±0.052	0.168±0.319	0.2471
GLYCINE	0.159±0.131	0.099±0.075	0.0523
INOSITOL	0.088±0.093	0.289±0.414	0.0868
LATTIC ACID	13.75±5.214	17.92±7.196	0.1683
PROLINE	2.944±1.239	1.761±0.656	0.0066
STEARIC ACID	0.951±0.707	1.433±0.716	0.1095
SUCROSE	0.455±0.393	3.201±6.46	0.0289
TAURINE	0.046±0.040	0.217±0.258	0.0096
THREONINE	0.135±0.089	0.154±0.155	0.8938

Table 6. Statistical differences of metabolites characterized by Variable Importance for the Projection (VIP) > 1. Metabolites were selected on VIP > 1 based on Orthogonal Partial Least Squares Discriminant Analysis (OPLS-DA). a Relative concentrations were calculated by normalization of the molar concentration of each metabolite to the total molar concentration of all 14 metabolites for each sample. b A Mann–Whitney U test was performed, and the p-value reported. The Holm-Bonferroni adjustment was applied.

Finally, fourteen metabolites were responsible for the separation of the A patients from NA patients (Fig. 13). Four metabolites were significantly increased in A patients (glycine, glutamic acid, phenylalanine, proline) and three were significantly decreased in A patients (arachidonic acid, inosine, stearic acid). The relative concentrations of these metabolites in the two groups were compared using box-and-whisker plots as shown in Fig. 13.

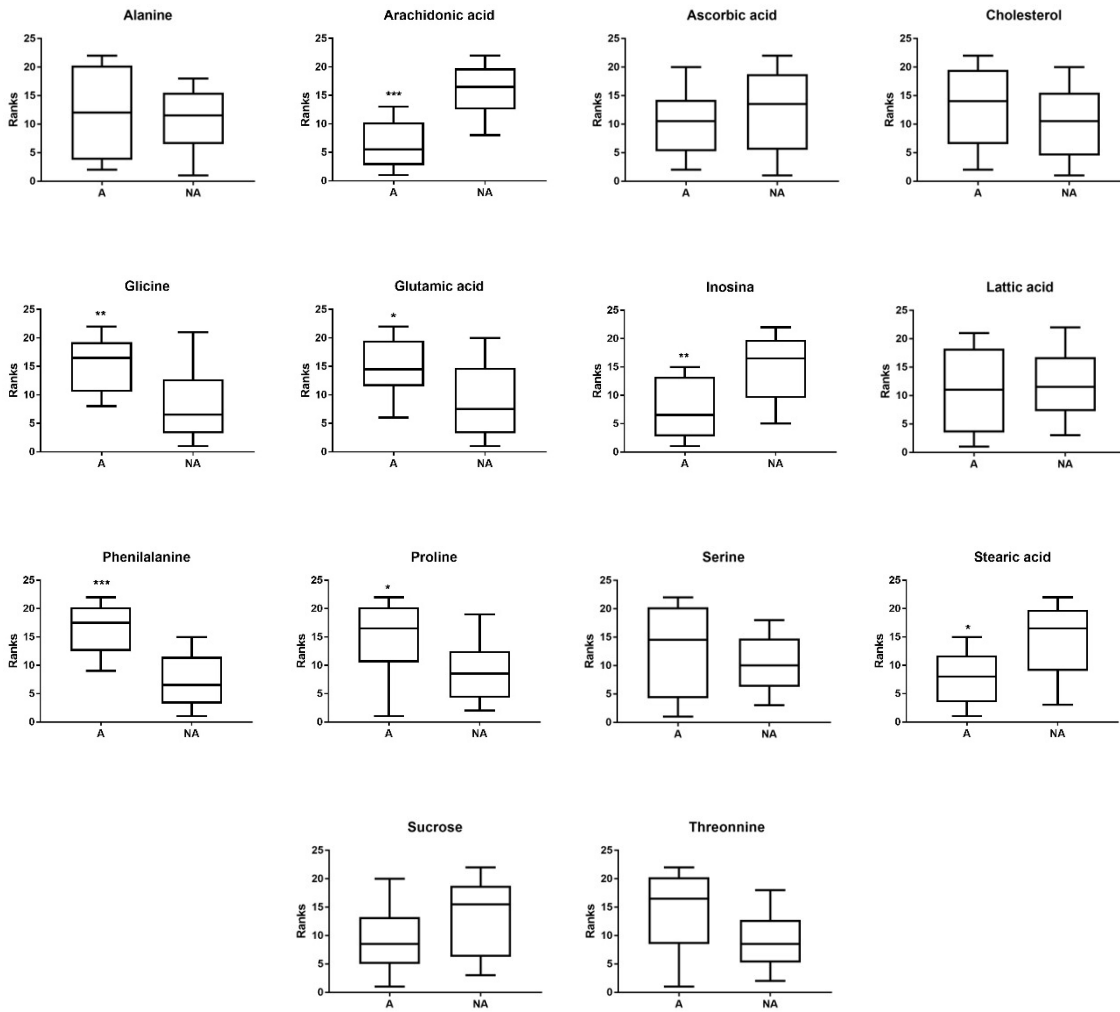


Figure 13. Discriminant metabolites in A patients vs NA patients obtained with the MVA are shown and expressed in the graphs y axis as ranks (data transformation in which numerical or ordinal values are replaced by their rank when the data are sorted). Discriminant metabolites obtained with the MVA, underwent a Mann-Whitney test to determine which metabolites were statistically significantly varied *, ** and*** indicates levels of significance with $p < 0.05$, <0.01 and <0.001 respectively.

MEANS (SD) OF GROUP

METABOLITES	A	NA	p VALUE
ALANINA	0.282±0.233	0.188±0.080	0.6744
ARACHIDONIC ACID	0.135±0.193	3.375±2.544	0.0001
ASCORBIC ACID	0.183±0.213	0.355±0.332	0.4176
CHOLESTEROL	46.19±14.16	39.02±15.06	0.381
GLYCINE	0.197±0.093	0.099±0.075	0.009
GLUTAMMIC ACID	0.693±1.089	0.168±0.319	0.0206
INOSINE	0.175±0.129	1.307±1.274	0.0071
LATTIC ACID	15.39±9.557	17.92±7.196	0.6277
PHENILALANINE	0.174±0.116	0.041±0.032	0.0003
PROLINE	2.682±1.363	1.761±0.656	0.0358
SERINE	0.298±0.433	0.101±0.052	0.381
STEARIC ACID	0.764±0.376	1.433±0.716	0.0169
SUCROSE	0.707±0.917	3.201±6.46	0.1229
THREONINE	0.800±1.01	0.154±0.155	0.0503

Table 7. Statistical differences of metabolites characterized by Variable Importance for the Projection (VIP) > 1. Metabolites were selected on VIP > 1 based on Orthogonal Partial Least Squares Discriminant Analysis (OPLS-DA). a Relative concentrations were calculated by normalization of the molar concentration of each metabolite to the total molar concentration of all 14 metabolites for each sample. b A Mann–Whitney U test was performed and the p-value reported. The Holm-Bonferroni adjustment was applied.

Table 8 shows the different trends in the concentrations of the statistically significant metabolites in the different comparisons (A versus C; NA versus C; A versus NA).

	GC-MS Analysis		
	A vs C	NA vs C	A vs NA
ARACHIDONIC ACID	—	↑	↓
GLUTAMIC ACID	↑	—	↑
GLYCINE	—	—	↑
INOSINE	↓	—	↓
INOSITOL	↑	—	—
PHENYLALANINE	↑	—	↑
PROLINE	—	↓	↑
STEARIC ACID	—	—	↓
SUCROSE	—	↑	—
TAURINE	↑	↑	—
THREONINE	↑	—	—

Table 8. Summary table of significantly increase and decrease metabolites with GC-MS Method in the three different groups. Increase (↑) or decrease (↓) metabolites were always referred to the pathological condition.

REDOX STATUS IN POLYMORPHONUCLEAR NEUTROPHIL

Oxidative stress is defined as the imbalance between reactive oxygen species (ROS) production and antioxidant defences in a biological system (94). ROS include superoxide anions (O_2^-), hydroxyl radicals ($OH\cdot$) and hydrogen peroxide (H_2O_2). The glutathione system consisting of glutathione reductase, glutathione oxidase and glutathione, maintains the concentration of O_2^- and H_2O_2 at physiological levels necessary for tissue repair and immune defence (95). Therefore, the ratio of oxidised and reduced glutathione indicates the redox state of a cell. It is known that oxidative stress, which plays a crucial role in the pathophysiology of β -thalassemia, leads to excessive production of ROS that by binding to cellular components such as DNA, proteins and membrane lipids can induce cytotoxicity suggesting a possible role of it also in the side effects in the presence of DFP. To elucidate possible alteration in the redox state of polymorphonuclear, neutrophils were treated in vitro with different doses of DFP and the intracellular ROS levels were investigated by exposing cells to 2', 7'- dichlorodihydrofluorescein diacetate H2-DCF-DA ($20\mu M$) for 30 minutes. The intracellular ROS levels expressed as a percentage of control (untreated cells) are presented in Fig 14. PMN cells obtained from healthy controls showed a slight increase in ROS production when treated with $100\mu m$ deferiprone compared to non-treated neutrophils. However, this difference was not statistically significant. The organic peroxide, tert-butyl hydroperoxide was used as a positive control. ROS generation was increased in DFP exposed neutrophils derived from A and NA patients, but also in these cases the differences were not statistically significant, due to large variability in the response.

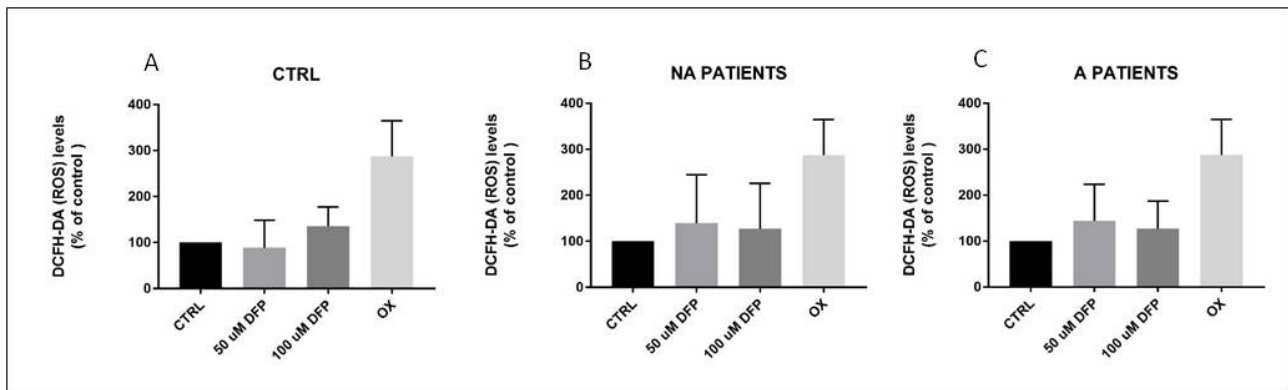


Figure 14. ROS production DFP induce in PMNs. ROS levels were measured in neutrophils from healthy controls (CTRL) (A), NA patients (B) and A patients (C) after DFP treatment (50uM and 100uM) or 5nM TBH (OX). Results are expressed as a percentage of untreated cells.

Unfortunately, due to the variability of the number of leucocyte PMNs that can be isolated from 6 ml of peripheral blood of the subjects enrolled in the study, the levels of reduced and oxidized glutathione were investigated only in four NA patients and two A patients. Reduced and oxidized glutathione was assessed by HPLC coupled with an electrochemical detector (ECD). GSH/GSSG ratio, a marker for oxidative stress, was decreased in a dose-dependent manner in DFP-treated neutrophils from healthy control (Fig. 15A). In neutrophils from NA patients the GSH/GSSG ratio was significantly decreased at all concentrations of DFP (Fig. 15B), even in A patients the decrease was observed with all the concentrations used but due to the low number of subjects (n=2) a statistical analysis of the difference could not be performed (Fig. 15C)

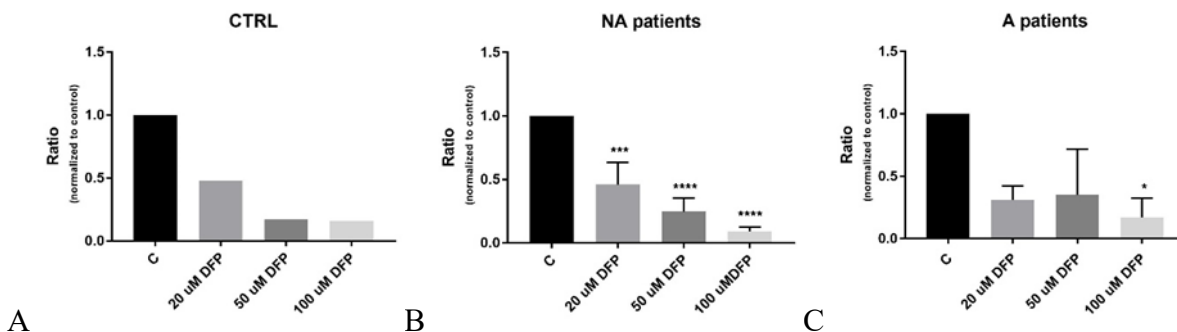


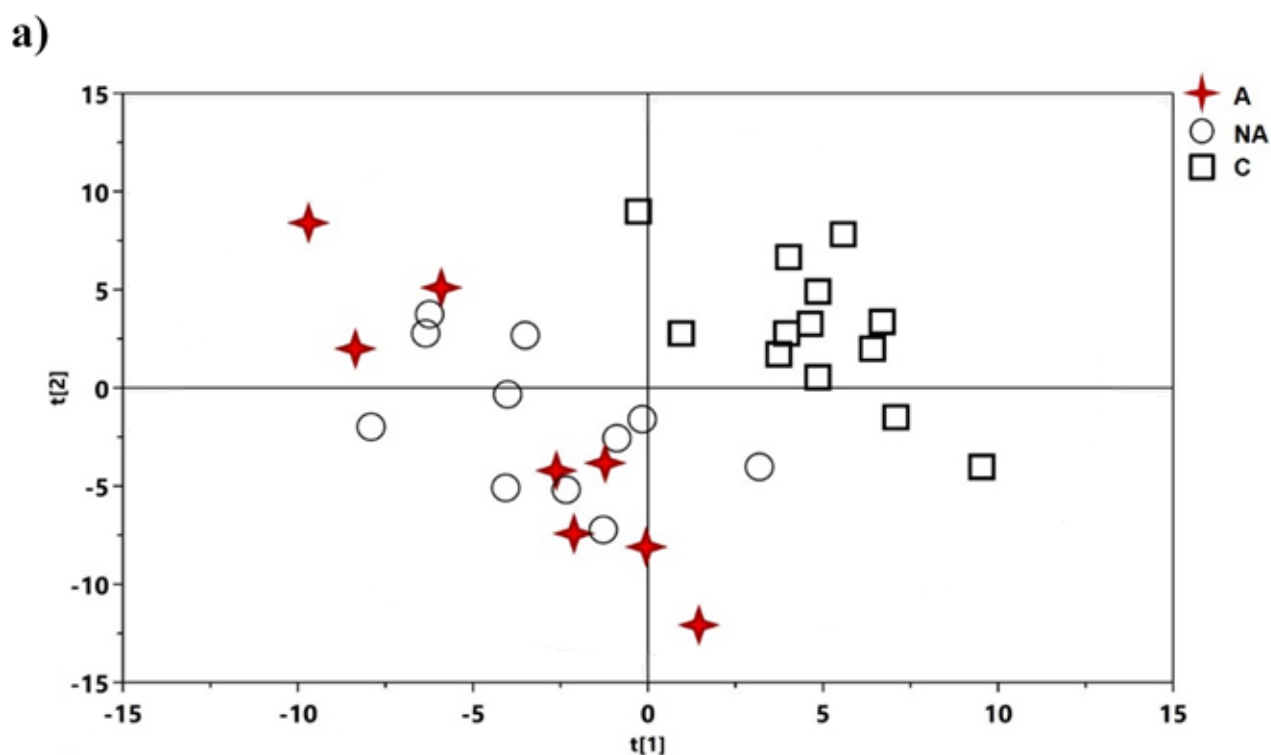
Figure 15. GSH/GSSG ratio in PMNs treated with different doses of DFP. Healthy controls (A), NA patients (B) and A patients (C). Peak areas were normalized to untreated cells (C) and express as a ratio of reduced and oxidized form.

PLASMA METABOLOMICS ANALYSIS

To have a better metabolomics view, the analysis of plasma samples from β -thalassemic patients with Deferiprone-induced agranulocytosis (A), β -Thalassemic patients without Deferiprone-induced-agranulocytosis (NA), and healthy subjects (C), was performed with $^1\text{H-NMR}$ and GC-MS methods.

$^1\text{H-NMR}$ METABOLOMICS ANALYSIS

A PLS-DA analysis was conducted comparing the plasma metabolomic profile of the agranulocytosis (A) patients and no-agranulocytosis (NA) patients versus healthy subjects. The model showed (Fig. 16 A) a good separation from β -Thalassemic patients and healthy subjects. The validity of the PLS-DA model was evaluated through a permutation test using 400 times. The test results are reported in Table 8 and indicate the statistical validity of the PLS-DA model (Fig. 16 B). Unlike the analysis conducted on PMNs, the plasma profile is not able to distinguish between A and NA patients, indicating a strong similarity between the two groups.



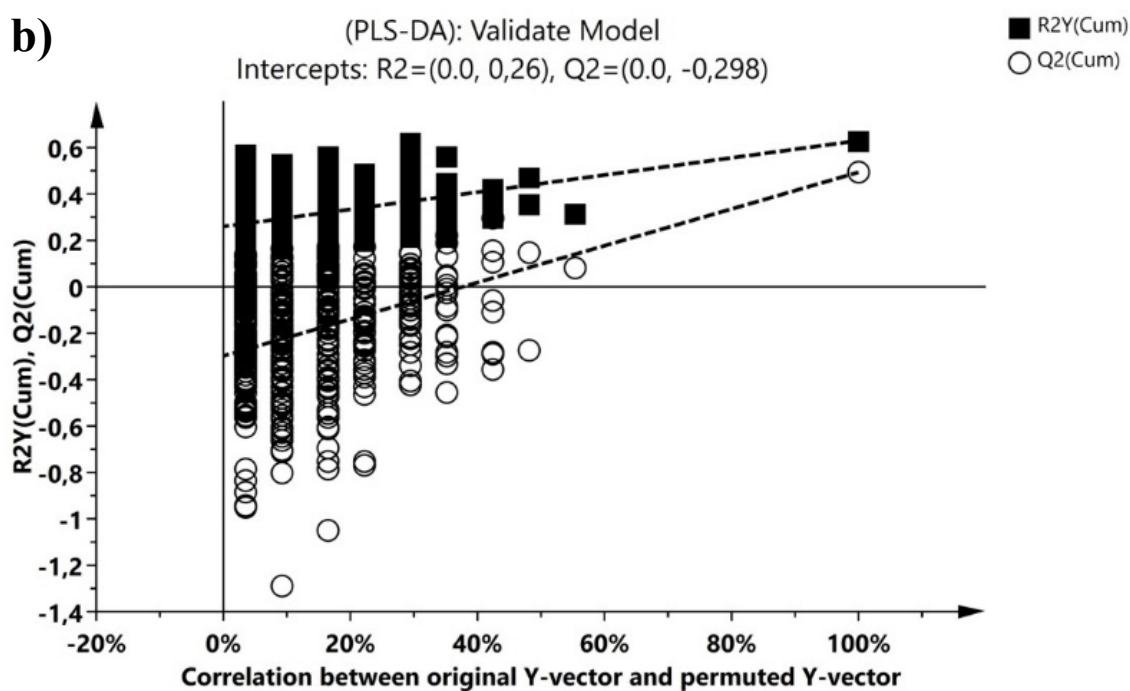
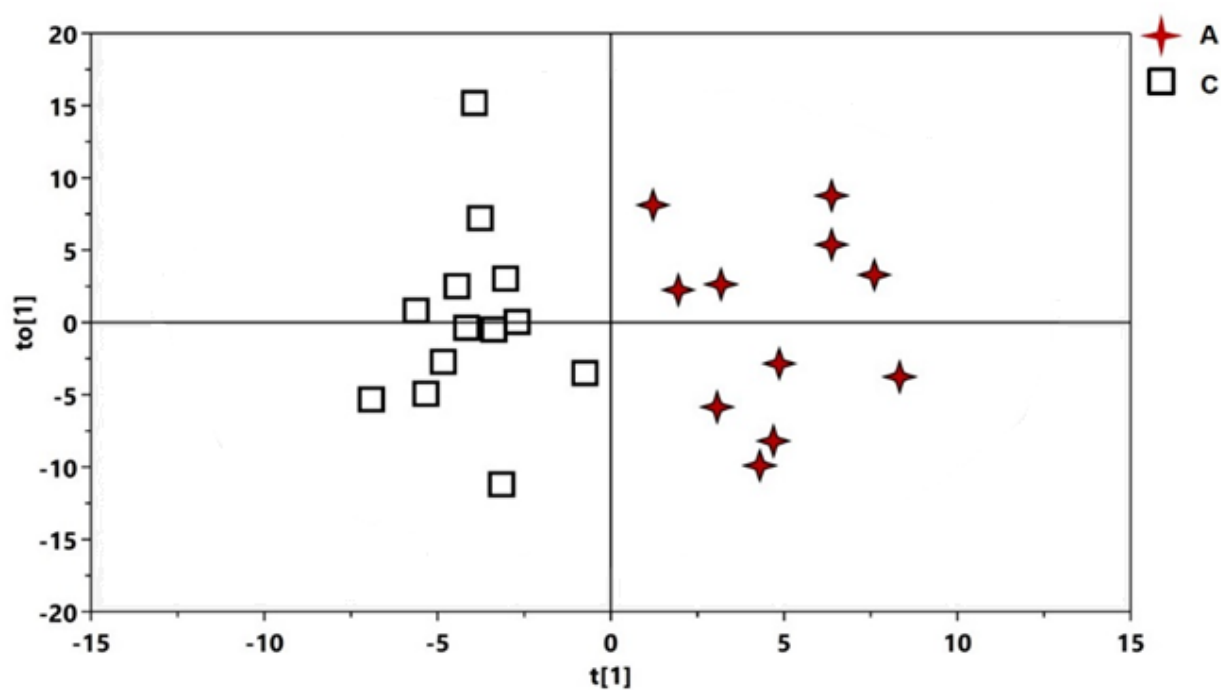


Figure 16. PLS-DA analysis of plasma samples. (a) PLS-DA scores plot of plasma samples agranulocytosis patients (A), no-agranulocytosis patients (NA) and healthy subjects (C). (b) The PLS-DA model was validated using the permutation test. Plots were obtained with $^1\text{H-NMR}$.

Two separate OPLS-DA models were built: agranulocytosis (A) vs controls (C) and non-agranulocytosis (NA) vs controls (C). The results of these pairwise comparisons enabled improved assessment and identification of the metabolites that were responsible for the separation between the distinct groups. A first OPLS-DA analysis (Fig.17a) was performed by comparing agranulocytosis (A) versus the healthy subjects (C). The OPLS-DA model was established with one predictive and one orthogonal component and showed good values of R^2X , R^2Y and Q^2 (Table 8). Samples showed a good separation into two distinct groups, indicating a different metabolomics profile between the two groups. The metabolites responsible for the separation between A patients and controls were identified in the corresponding S-plot (data not shown). The validity of the OPLS-DA model was evaluated through a permutation test using 400 times (Fig. 17 b). The test results are reported in Table 8 and indicate the statistical validity of the OPLS-DA model.

a)



b)

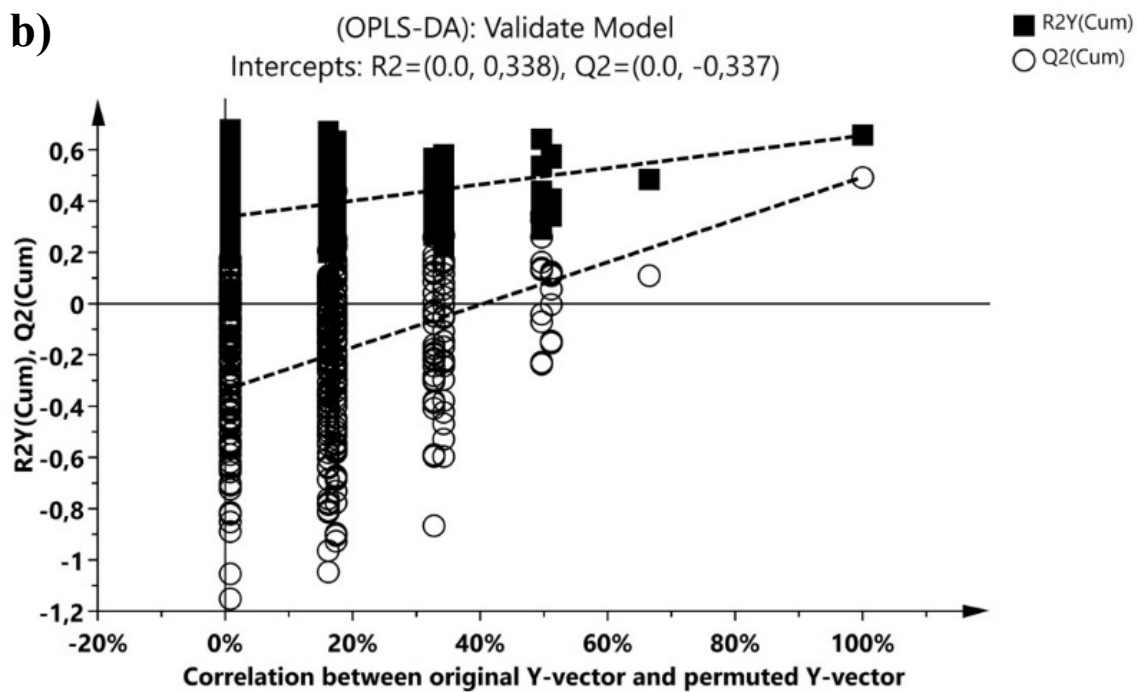
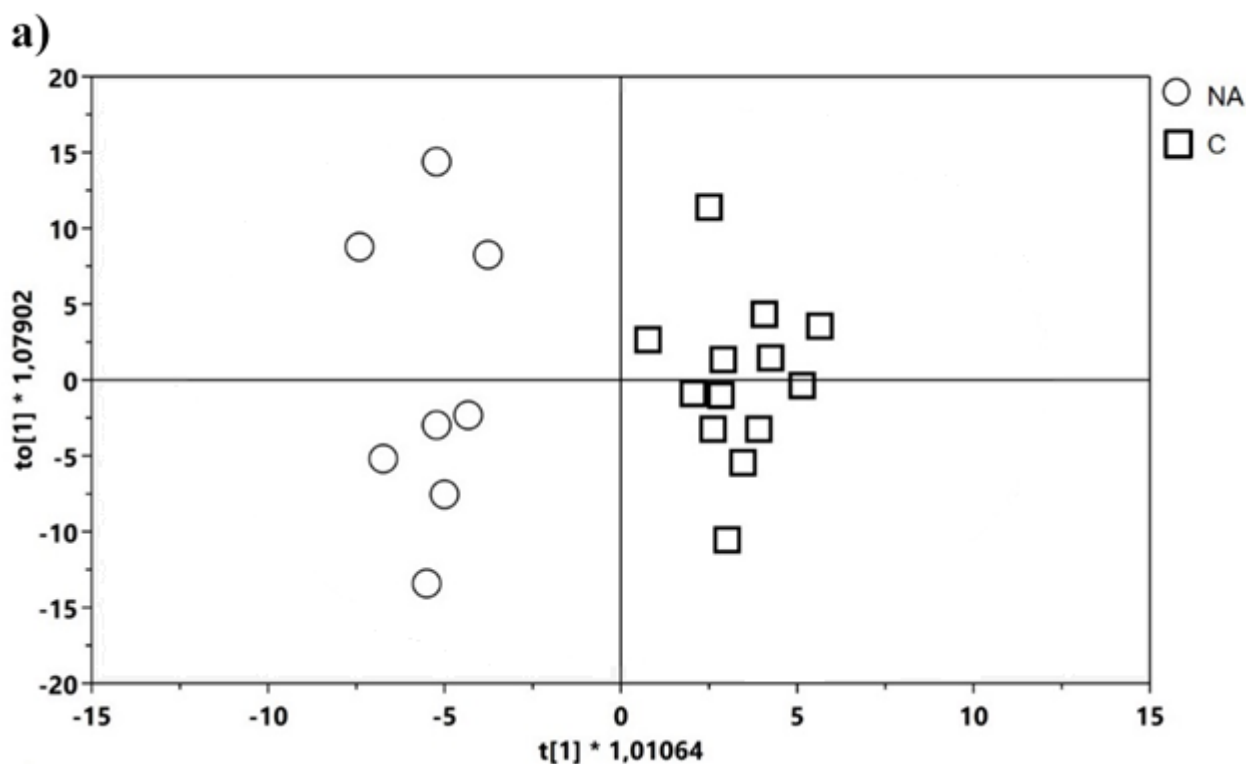


Figure 17. OPLS-DA analysis of plasma samples A vs C. a) OPLS-DA scores plot of plasma samples A (β -thalassemic patients with agranulocytosis) vs C (healthy controls). b) The OPLS-DA model was validated with the permutation test. Plots were obtained with 1H -NMR.

Finally, the OPLS-DA analysis was conducted by comparing No-agranulocytosis (NA) patients versus healthy subjects. The OPLS-DA scores plot (Fig. 18a) showed good separation of the subjects into two distinct groups, indicating a difference in the metabolomics profile between the NA and C subjects. The OPLS-DA model was established with one predictive and one orthogonal component and showed good values of R2 X, R2 Y and Q2 (Table 8). Metabolites responsible for the separation between NA patients and controls were identified in the corresponding S-plot (data not shown). The validity of the OPLS-DA model was evaluated through a permutation test using 400 times (Fig. 18b). The test results are reported in Table 8 and indicate the statistical validity of the OPLS-DA model.



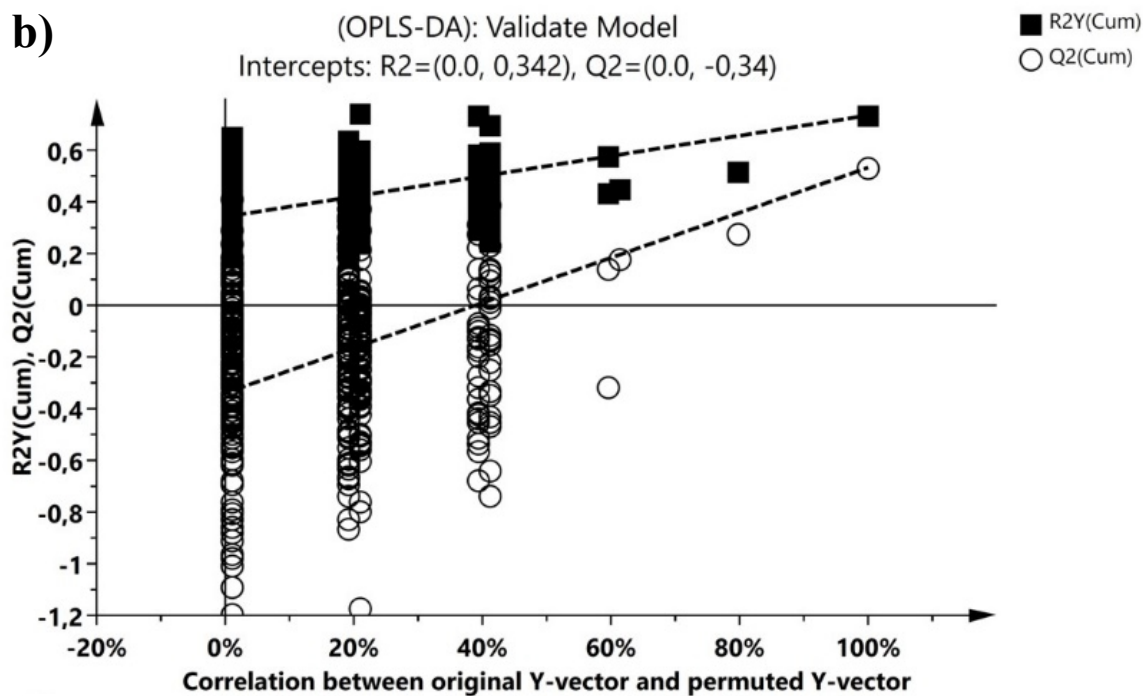


Figure 18. OPLS-DA analysis of plasma samples NA vs C. a) OPLS-DA scores plot plasma samples NA (β -thalassemic patients without agranulocytosis) vs C (healthy controls). b) The OPLS-DA model was validated with the permutation test. Plots were obtained with $^1\text{H-NMR}$.

PLS-DA and OPLS-DA models					Permutation*	
NMR						
Groups	Componenets ^a	R ₂ Xcum ^b	R ₂ Ycum ^c	Q ₂ cum ^d	R ₂ intercept	Q ₂ intercept
C vs NA vs A	2	0.399	0.867	0.759	0.26	-0.298
Controls vs A	1P+1O	0.210	0.734	0.532	0.338	-0.337
Controls vs NA	1P+1O	0.394	0.850	0.577	0.342	-0.34

Table 9. PMNs samples MVA parameters. The number of Predictive and Orthogonal components used to create the statistical models.^b R₂X and R₂Y indicated the cumulative explained fraction of the variation of the X block and Y block for the extracted components. Q₂cum values indicated cumulative predicted fraction of the variation of the Y block for the extracted components. * R₂ and Q₂ intercept values are indicative of a valid model.

The discriminant metabolites based on a $p(\text{corr})$ of <0.05 were quantified using Chenomx NMR suite 7.1 and subjects to univariate statistical analysis to determine their statistical significance. Statistical significance was determined using the Mann-Whitney U test. The metabolic plasma profile of the Agranulocytosis (A) patients, when compared to controls, was characterized by a significant increase of arginine and tyrosine and a decrease in lactate (Fig. 19).

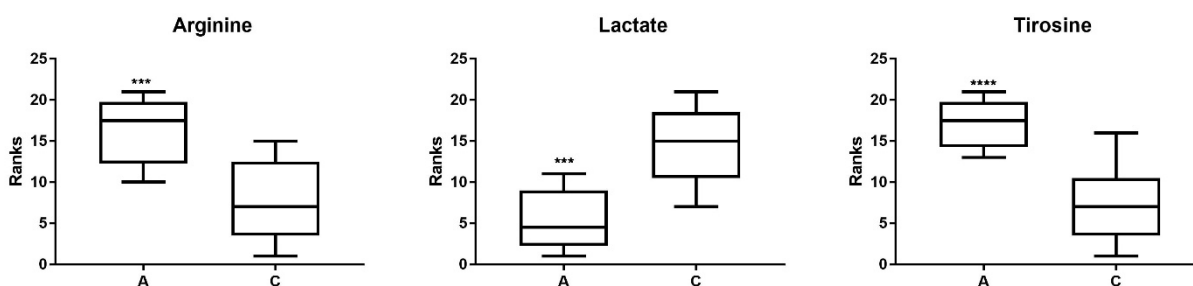


Figure 19. Discriminant metabolites in A patients vs healthy subjects (C) obtained with the MVA are shown and expressed in the graphs y axis as ranks (data transformation in which numerical or ordinal values are replaced by their rank when the data are sorted). Discriminant metabolites obtained with the MVA, underwent a Mann-Whitney test to determine which metabolites were statistically significantly varied. *** and **** indicates levels of significance with $p < 0.001$ and 0.0001 respectively.

The metabolites that were significantly increased in no-Agranulocytosis (NA) patients were Arginine, Tyrosine, Valine, while Lactate was decreased compared to controls (Fig. 20).

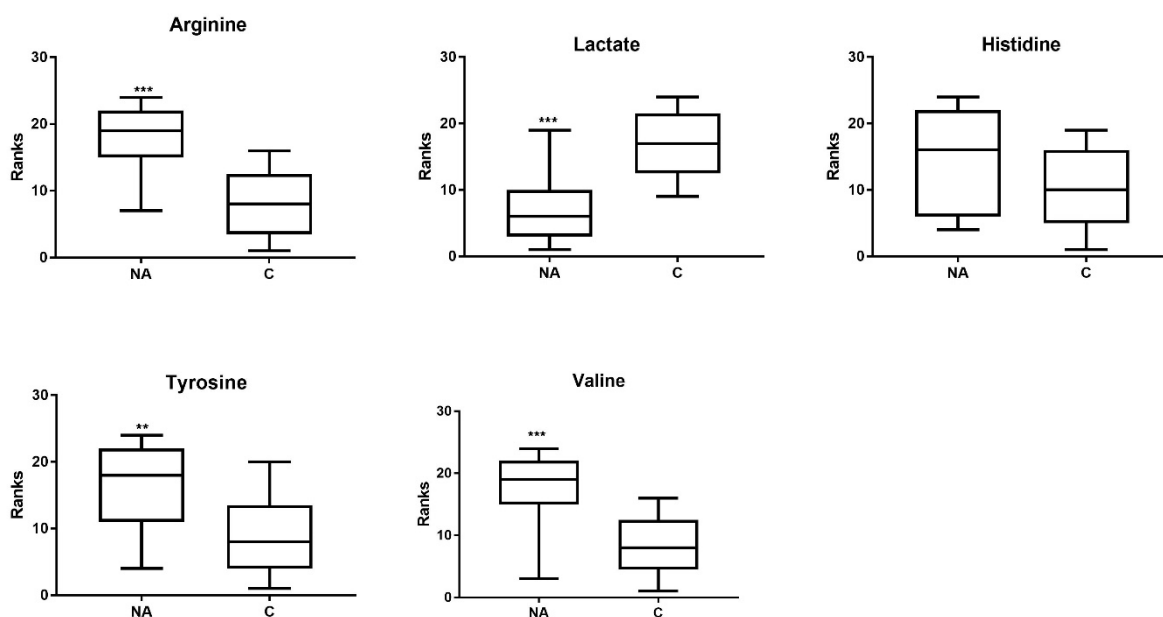


Figure 20. Discriminant metabolites in NA patients vs healthy subjects (C) obtained with the MVA are shown and expressed in the graphs y axis as ranks (data transformation in which numerical or ordinal values are replaced by their rank when the data are sorted). Discriminant metabolites obtained with the MVA, underwent a Mann-Whitney test to determine which metabolites were statistically significantly variated. ** and *** indicates levels of significance with $p < 0.05$ and 0.001 respectively.

GC-MS METABOLOMICS ANALYSIS

The metabolomic profile of the plasma of the same patients was also studied and analyzed with the GC-MS. As with NMR analysis, a PLS-DA analysis was conducted comparing the plasma metabolomic profile of the agranulocytosis patients and no-agranulocytosis patients versus healthy subjects. The model showed (Fig. 21a) a good separation from β -Thalassemic patients (A+NA) and healthy subjects. The validity of the PLS-DA model was evaluated through a permutation test using 400 times. The test results are reported in Table 9 and indicate the statistical validity of the PLS-DA model. Two samples (16 and 4) were located away from their classes. In this case, unlike the analysis conducted on PMNs, the plasma profile did not distinguish between A and NA patients, indicating a strong similarity between the two groups.

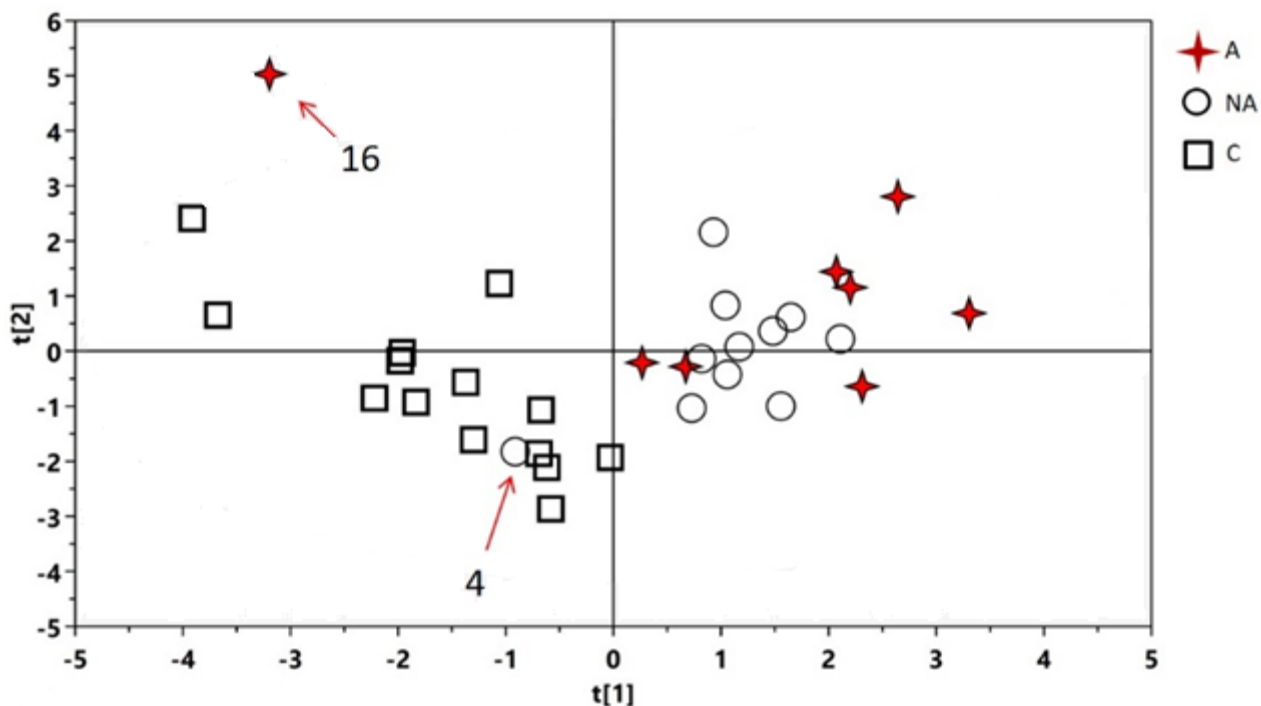
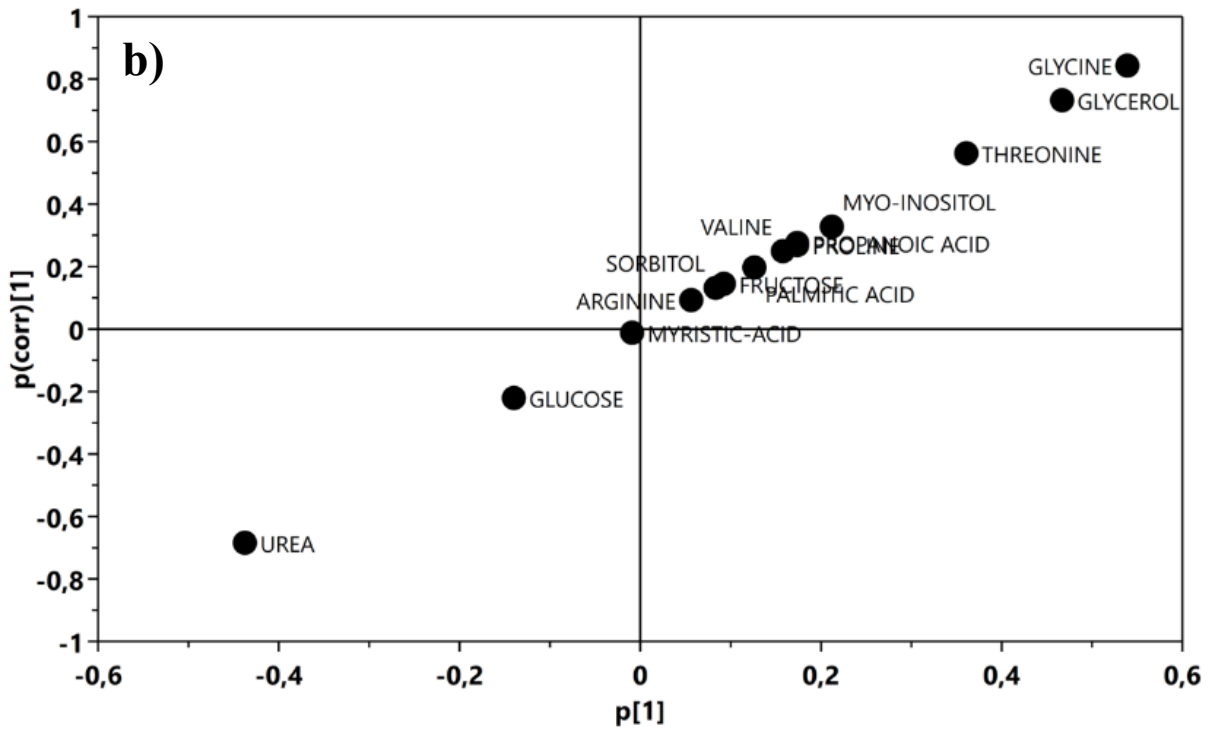
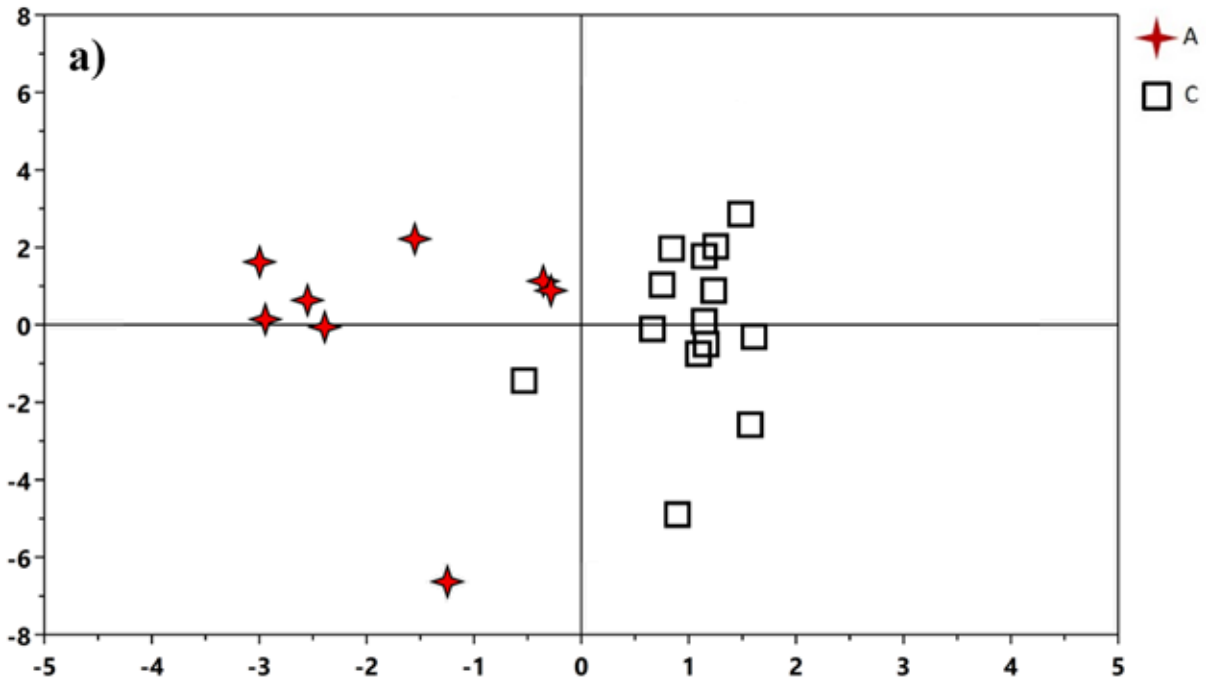


Figure 21. PLS-DA analysis of plasma samples of patients and healthy controls. (A) PLS-DA scores plot of plasma samples from agranulocytosis patients (A), no-agranulocytosis patients (B) and healthy subjects (C). (B) The PLS-DA model was validated using the permutation test. Plots were obtained with GC-MS

As for NMR analysis, two separate OPLS-DA models were built: agranulocytosis (A) vs controls (C) and non-agranulocytosis (NA) vs controls (C). The results of these pairwise comparisons enabled improved assessment and identification of the metabolites that were responsible for the separation between the distinct groups. A first OPLS-DA analysis (Fig. 22a) was performed by comparing agranulocytosis (A) versus the healthy subjects (C). The OPLS-DA model was established with one predictive and one orthogonal component and showed good values of R^2_X , R^2_Y and Q^2 (Table 9). Samples showed a good separation into two distinct groups, indicating a different metabolomics profile between them. The metabolites responsible for the separation between A patients and controls were identified in the corresponding S-plot (Fig. 22 b). The validity of the OPLS-DA model was evaluated through a permutation test using 400 times (Fig. 22 c). The test results are reported in Table 9 and indicate the statistical validity of the OPLS-DA model.



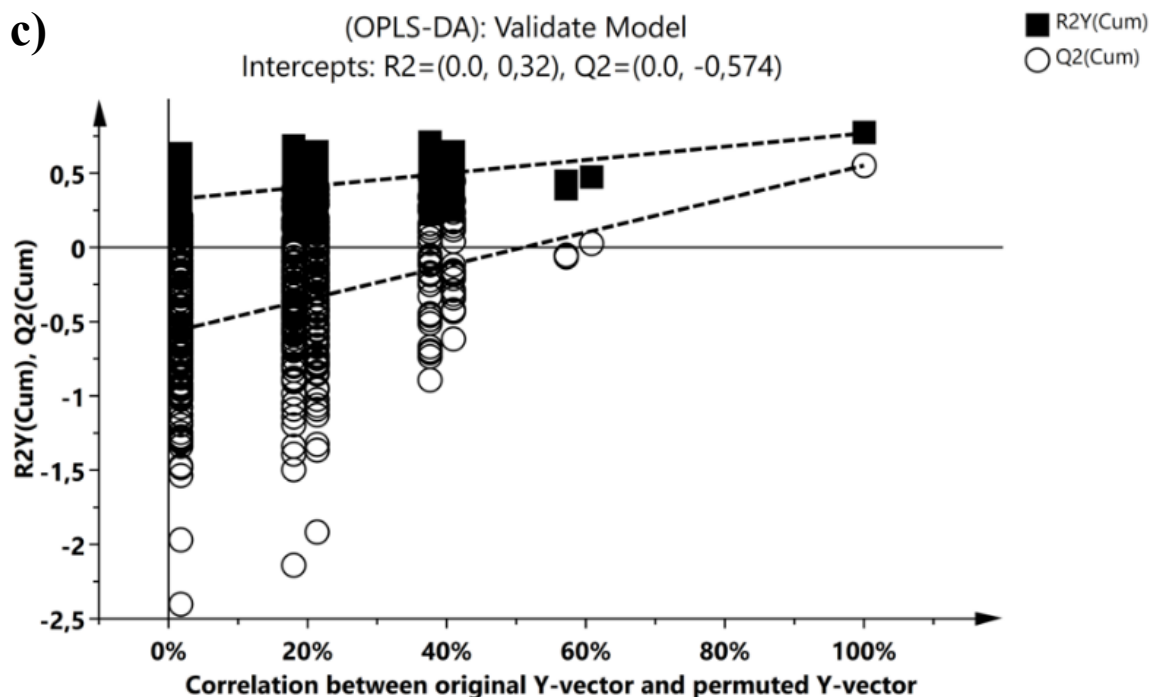
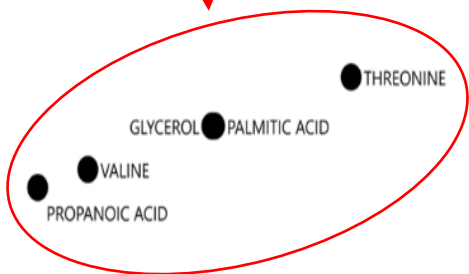
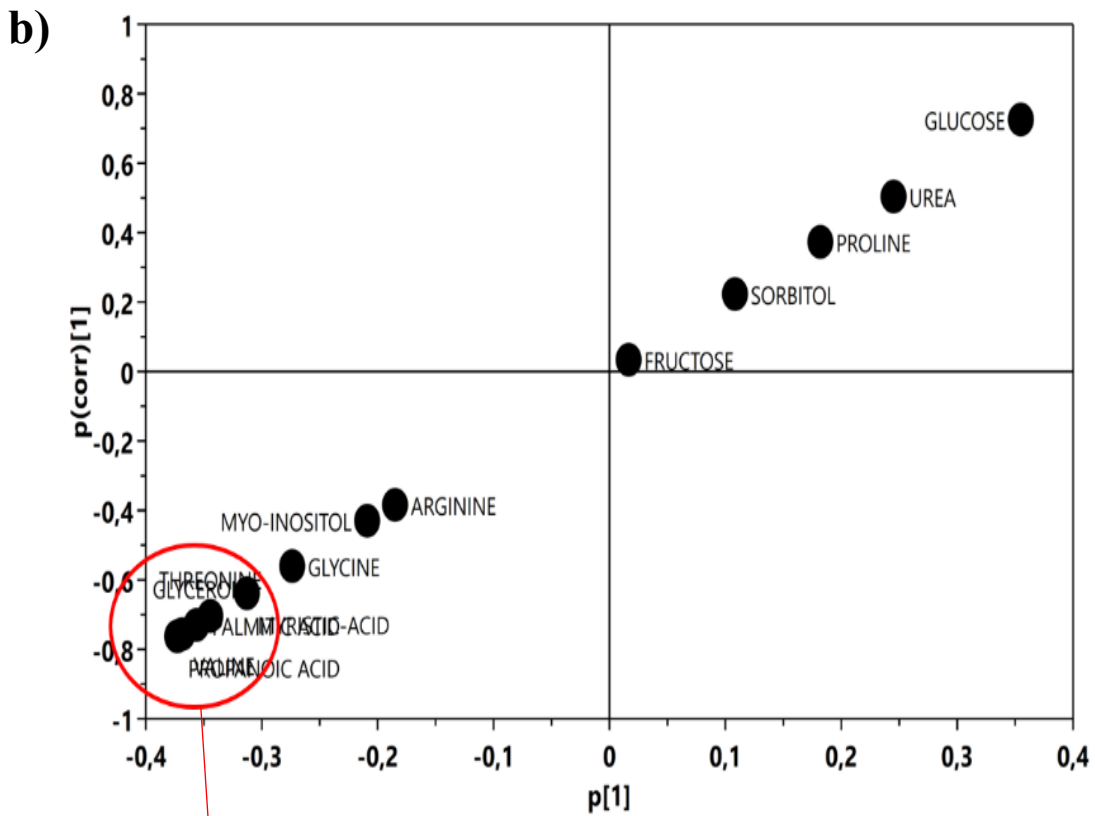
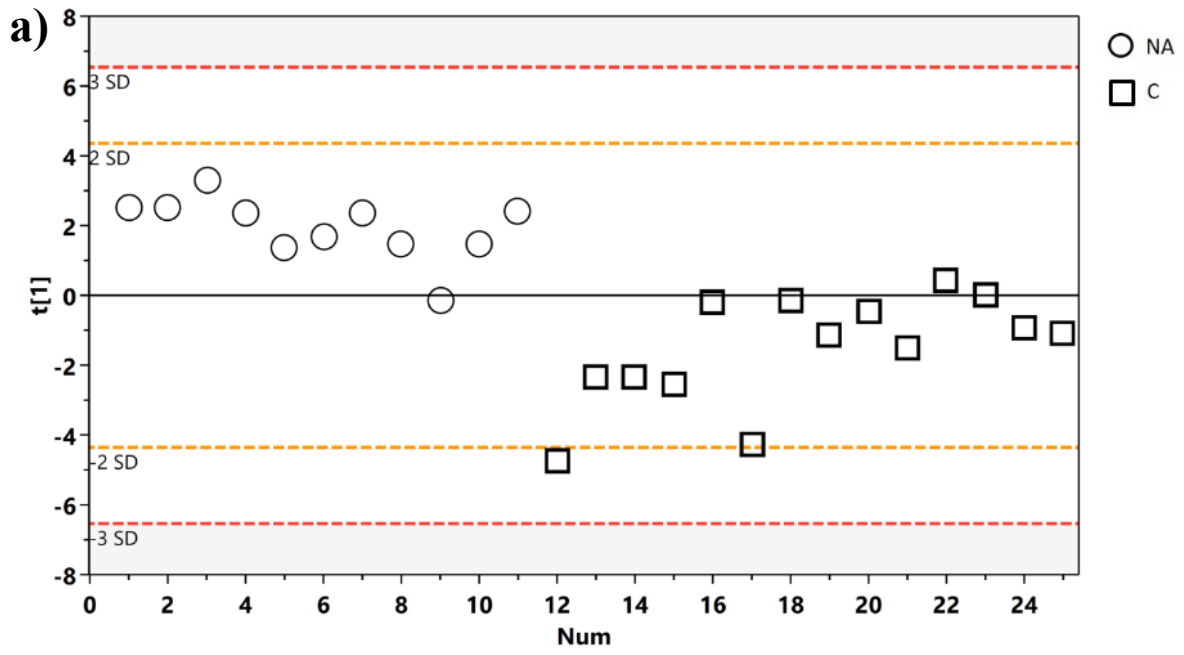


Figure 22. OPLS-DA analysis of plasma samples A vs C. (a) OPLS-DA scores plot of PMNs samples A (β -thalassemic patients with agranulocytosis) vs C (healthy controls). (b) S-Plot corresponding to the OPLS-DA model used to characterize the most significant variables associated with group A and C subjects. Cut-off values for the covariance of $|p| \geq 0.2$ and for the correlation $|p(\text{corr})| \geq 0.2$ were used. (c) The permutation test of OPLS-DA model. Plots were obtained with GC-MS

Finally, the OPLS-DA analysis was conducted to compare the No-agranulocytosis patients versus healthy subjects. The OPLS-DA scores plot (Fig. 23a) showed good separation of the subjects into two distinct groups, indicating a difference in the metabolomics profile between the NA and C subjects. The OPLS-DA model was established with one predictive component and showed good values of R2 X, R2 Y and Q2 (Table 9). Metabolites responsible for the separation between NA patients and controls were identified in the corresponding S-plot (Fig. 23b). The validity of the OPLS-DA model was evaluated through a permutation test using 400 times (Fig. 23c). The test results are reported in Table 9 and indicate the statistical validity of the OPLS-DA model.



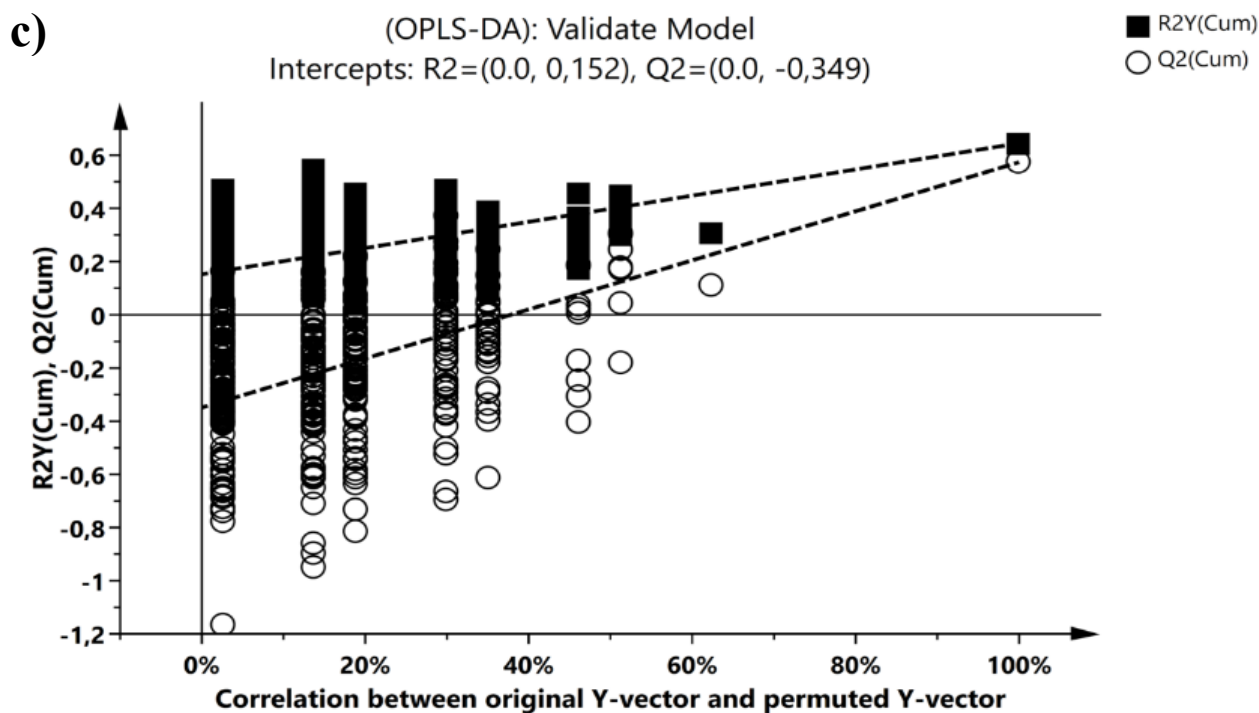


Figure 23. OPLS-DA analysis of plasma NA vs C. (a) OPLS-DA scores plot of PMNs samples NA (β -thalassemic patients without agranulocytosis) vs C (healthy controls). (b) S-Plot corresponding to the OPLS-DA model used to characterize the most significant variables associated with group A and C subjects. Cut-off values for the covariance of $|p| \geq 0.2$ and for the correlation $|p(\text{corr})| \geq 0.2$ were used. (c) The permutation test of OPLS-DA model. Plots were obtained with GC-MS

Groups	PLS-DA and OPLS-DA models				Permutation*	
	Componenets ^a	R ₂ Xcum ^b	R ₂ Ycum ^c	Q ₂ cum ^d	R ₂ intercept	Q ₂ intercept
C vs NA vs A	2	0.537	0.710	0.528	0.284	-0.531
Controls vs A	1P+1O	0.547	0.769	0.552	0.320	-0.574
Controls vs NA	1P	0.550	0.779	0.672	0.152	-0.349

Table 10. Plasma samples MVA parameters. The number of Predictive and Orthogonal components used to create the statistical models.^b R₂X and R₂Y indicated the cumulative explained fraction of the variation of the X block and Y block for the extracted components. Q₂cum values indicated cumulative predicted fraction of the variation of the Y block for the extracted components. * R₂ and Q₂ intercept values are indicative of a valid model.

The most important metabolites were evaluated through analysis of the S-plot for all two comparisons. The metabolites were subjected to Mann-Whitney U test to identify significant variations of their concentration. Significantly, discriminant metabolites were characterized by VIP > 1 and $p \leq 0.05$. The results of the univariate statistical analysis showed that only five metabolites were responsible for the separation between A patients and the healthy control (Fig. 24). The metabolomics profile of A patients showed an increase in levels of urea and decrease in levels of glycerol, glycine, and threonine compared to controls (Fig. 24.), while the NA patients showed an increase of urea and a decrease of glycerol, glycine, myo-inositol and threonine compared to controls (Fig. 25). Significant changes in plasma metabolites of A or NA vs C are summarised in table 10.

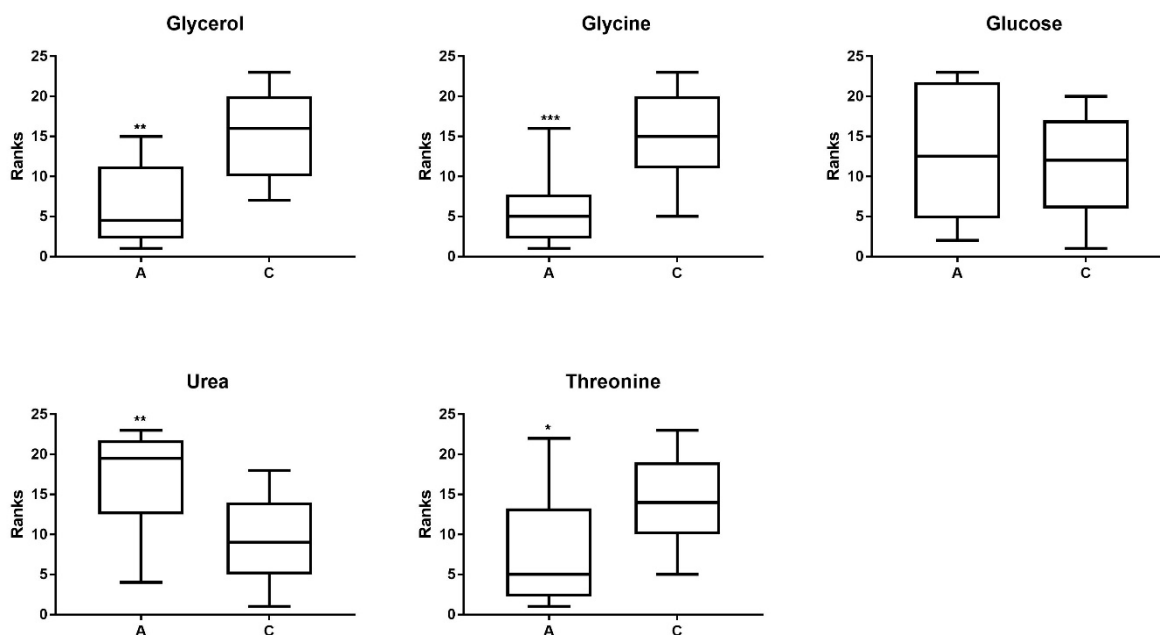


Figure 24. Discriminant metabolites in A patients vs healthy subjects (C) obtained with the MVA are shown and expressed in the graphs y axis as ranks (data transformation in which numerical or ordinal values are replaced by their rank when the data are sorted). Discriminant metabolites obtained with the MVA, underwent a Mann-Whitney test to determine which metabolites were statistically significantly varied. *, ** and *** indicates levels of significance with $p < 0.05$, 0.01 and 0.001 respectively.

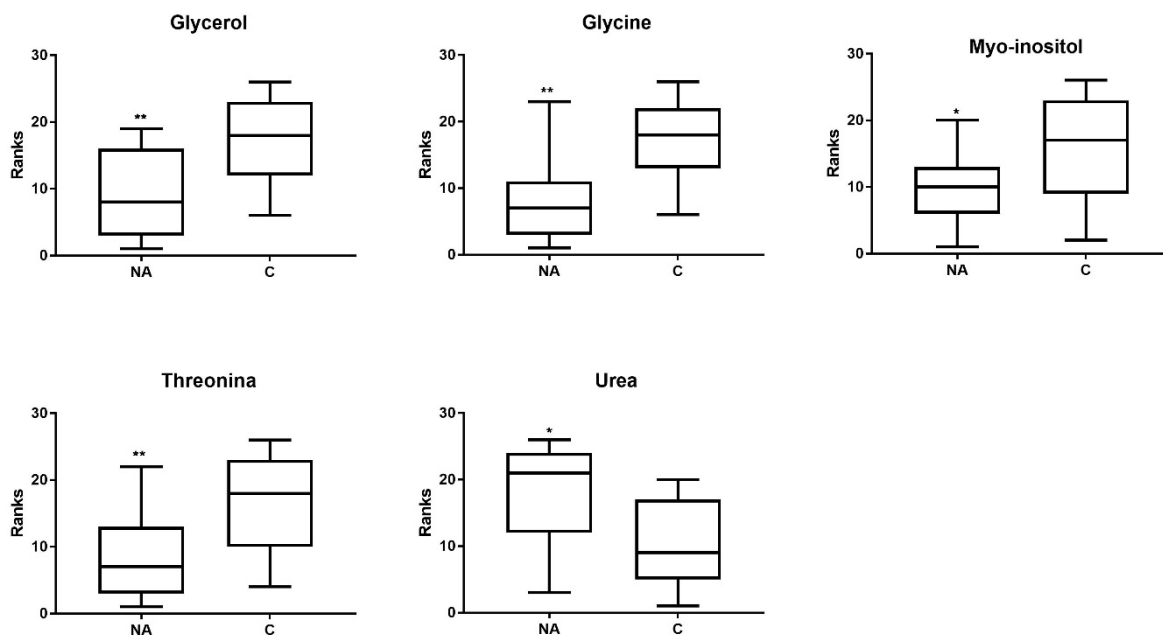


Figure 25. Discriminant metabolites in NA patients vs healthy subjects (C) obtained with the MVA are shown and expressed in the graphs y axis as ranks (data transformation in which numerical or ordinal values are replaced by their rank when the data are sorted). Discriminant metabolites obtained with the MVA, underwent a Mann-Whitney test to determine which metabolites were statistically significantly variated. * and ** indicates levels of significance with $p < 0.05$ and 0.01 respectively.

	H-NMR Analysis		GC-MS Analysis	
	A vs C	NA vs C	A vs C	NA vs C
ARGININE	↑	↑	—	—
GLYCEROL	—	—	↓	↓
GLYCINE	—	—	↓	↓
LACTATE	↓	↓	—	—
MYO-INOSITOL	—	—	—	↓
THREONINE	—	—	↓	↓
TYROSINE	↑	↑	—	—
VALINE	—	↑	—	—
UREA	—	—	↑	↑

Table 11. Summary table of significantly increase and decrease plasma metabolites in two different methods (H-NMR/GC-MS) and two different groups. Increase (↑) or decrease (↓) metabolites were always referred to the pathological condition.

V. DISCUSSION

Neutrophils are the most abundant of all white blood cells and are the first responder in cases of infection and inflammation. As such, they are highly sensitive to external cues and are easily activated. Besides, neutrophils have a very short half-life and a rapid turnover. Together, these characteristics raise several difficulties in working with neutrophils, such as unique experimental strategies are required. Our research aimed to develop protocols for the study of human neutrophils using two platforms for metabolomics analysis: Nuclear Magnetic Resonance spectroscopy and Gas-Chromatography-Mass Spectrometry. It has been shown that quantitative evaluation of certain metabolites was directly related to a physiological state. Therefore, its application in the field of clinical research is of potential interest. One of the core tasks of metabolomics in clinical applications is to identify novel and accurate biomarkers that can aid in better understanding the causes of disease and its pathological processes, but also in predicting the progression or monitoring the outcome of disease treatments. Since the level of metabolic activity in neutrophils relative to other primary human cells is unknown but assumed to be low and the total numbers of neutrophils that can be obtained from the blood of patients and healthy donors may be limited, the development of protocols to allow the measurement of metabolites in neutrophils required a significant amount of preliminary work. So, our protocols were developed to take into account the low levels of metabolites in human neutrophils and the number of neutrophils obtained after the isolation methods. Isolation is the first step to study neutrophil behaviour and requires an efficient, aseptic, and reproducible method to obtain pure, non-activated, and viable cells, and *ex vivo* handling should not influence neutrophil behaviour, in particular induction of inappropriate activation. For this purpose, PMNs were isolated from healthy volunteers' blood using in parallel two of the most common commercially used methods: Lympholyte-H and Lympholyte-poly. Although all two PMNs isolation procedures tested in

this study yielded viable cells, purity and recovery results were different for the two procedures. Granulocyte enrichment by lympholite-H protocol reaches a purity of 99% and the highest overall yield and, for our purpose, it was considered the optimal method for neutrophils isolation. On the contrary, granulocytes isolated with Lympholite-poly method showed a higher level of impurities, which can be problematic in the metabolomics experiment when a single cell population is required. Another considerable drawback in the use of Lympholyte-poly is the fact that relatively high purities can only be reached using EDTA as an anticoagulation agent, but this could determine some problematic signals in NMR analysis. After establishing the best method for the isolation of PMNs for our protocols, it was necessary optimizing the metabolite extraction methods for metabolomic analyses. The range of metabolites that can be detected and quantitated by H-NMR and GC-MS analysis depends on the metabolites that can be extracted from the biological sample. Metabolite extraction mixture can play a significant role in determining the detection and quantitation of metabolites. Therefore, it was critical to determine the minimum volume of peripheral blood to obtain the number of neutrophils required to detect a significant number of metabolites by GC-MS or ¹H-NMR analysis and generate an optimal signal-to-noise ratio. In this study, we have shown that for neutrophils metabolites, extraction with cold methanol/water (80:20 v/v) is satisfactory and that a good data analysis was possible with at least 5×10^6 cells for the GC-MS method. Unfortunately, with this number of cells, it was not possible to obtain appreciable spectra with ¹H-NMR analysis. NMR has an important role in metabolomics due to its easy and rapid sample preparation, non-destructiveness, no need for chromatographic separation and a high degree of reproducibility (96, 97). However, it has lower sensitivity and resolution compared to MS-based techniques. To confirm our data, a recent study by Richer and colleagues shows that at least 20 million of neutrophils were required for metabolite extraction and successful NMR analysis (98, 99). This is a very high number of cells that could not be routinely available in clinical studies. The second focus of

the present study was to investigate the metabolic profile in beta-thalassemic patients treated with the iron chelator deferiprone and to explore its potential relationship with the susceptibility to develop agranulocytosis. The untargeted metabolomics approach constitutes one of the most frequently applied methods in metabolomic studies. The main goal of the application of the untargeted approach in biomedical studies is to discover novel biological markers as well as to gain insights into mechanisms underlying the pathophysiology of human disease. In the present study, we have characterized for the first time the metabolic fingerprint of PMNs obtained from β -Thalassemic patients by a GC-MS approach. This study showed that analysis of the metabolomic profiles of PMNs leukocytes, from the subjects enrolled in the study, allowed the identification of different classes of compounds. When the multivariate statistical analysis was applied to the GC-MS data, and the analysis was carried out for controls vs agranulocytosis, controls vs non-agranulocytosis, agranulocytosis vs non-agranulocytosis samples, OPLS-DA reported excellent statistical parameters, indicating that the models are robust and with good prediction power. Furthermore, the analysis was focused on understanding which metabolites were responsible for this separation. The metabolites significantly responsible for the different metabolic profiles in the three groups were: saturated fatty acids (arachidonic acid, stearic acid), amino acids (glutamic acid, glycine, phenylalanine, proline, taurine, threonine), polyols (inositol), and nucleosides (inosine) (Tab.8). Particularly while we might have expected to be able to discriminate β -thalassemic patients from healthy controls, our attention has focused on the separation between patients with Deferiprone-induced agranulocytosis (A) vs patients without Deferiprone-induced agranulocytosis (NA). Fourteen metabolites were detected to be responsible for the separation of the A patients from NA patients (Fig. 13). Four were significantly increased in A patients (glycine, glutamic acid, phenylalanine, proline) and three were significantly decreased in A patients (arachidonic acid, inosine, stearic acid). Glycine is one of the most important amino acids in mammals and other animals. It is

synthesized from serine, threonine, choline, and hydroxyproline via inter-organ metabolism involving primarily the liver and kidneys. Glycine is utilized for the biosynthesis of glutathione, heme, creatine, nucleic acids, and uric acid, for this reason, glycine plays an important role in metabolic regulation and anti-oxidative reactions (100). Glutamine is an α -amino acid and is the most abundant free amino acid in the body. Glutamine can be used in all the cells as a substance for the production of nicotinamide, adenine phosphate, nucleotides, purines, pyrimidine, antioxidants, and numerous additional biosynthetic pathways concerned with the integrity of cells and their normal function (101). Neutrophils utilize more glutamine than other leukocytes such as lymphocytes and macrophages (102). In neutrophils, most of the glutamine is converted into aspartate, glutamate, and lactate through the Krebs cycle. For the proper function of leukocytes and the generation of vital compounds, including GSH and its metabolism, glutamine, glutamate, and carbon dioxide play an essential role. Both these amino acids are involved in the glutathione pathway, indeed GSH biosynthesis requires sufficient quantities of glutamate, cysteine, and glycine to maintain appropriate levels of the tripeptide. GSH is responsible for protection against ROS and RNS, and the detoxification of endogenous electrophilic toxins. GSH directly reacting with ROS, RNS, and other reactive species, particularly HO•, HOCl, RO•, RO₂•, O₂⁻, and ONOO⁻, often resulting in the formation of glutathione-thiyl radicals (GS•). The reduced and oxidized forms of glutathione (GSH and GSSG) act in concert with other redox-active compounds (NAD(P)H) to regulate and maintain cellular redox status (103). Under normal conditions, the processes that generate ROS are well counterbalanced by the antioxidant system. Proline is a non-essential amino acid that is synthesized from glutamic acid. Proline is utilized by different organisms to offset cellular imbalances caused by environmental stress. The wide use in nature of proline as a stress adaptor molecule indicates that proline has a fundamental biological role in stress response. The molecular mechanism of cell protection mediated by proline during stress conditions is not fully understood but appears

to involve the chemical properties and effects on redox systems of the GSH pool (104). It is known that oxidative stress is an important mechanism in the progression of β -thalassemia, and alterations in this pathway are not unexpected. Oxidative stress in patients with β -thalassemia is mainly caused by peroxidative injury due to secondary iron overload. For this reason, in the present study, we wanted to investigate whether *in vitro* there could be a correlation between the addition of DFP and changes in the redox state of the PMNs. To elucidate the redox state in PMNs treated with different concentrations of DFP, we measured intracellular ROS levels. In our study, PMNs from healthy subjects and β -thalassemia patients did not display a significant increase in the ROS level. These findings are in agreement with previous studies, indeed a high antioxidant potential of deferiprone has been shown in a larger number of *in vitro*, *in vivo* and clinical studies (105). On the other hand, a reduction of the GSH/GSSG ratio is observed after treatment of the PMNs with DFP and this effect appears to be stronger on PMNs from patients who underwent agranulocytosis. Our study suggests that the PMNs of patients with Deferiprone-induced agranulocytosis have a metabolic profile characterized by an increase in metabolites directly involved in the metabolic pathways of GSH synthesis. We hypothesized that agranulocytosis onset could not be directly correlated with a direct effect of the drug on the redox balance of PMNs but further experiments are needed to elucidate the molecular mechanism of deferiprone-induced agranulocytosis. The metabolomic profile of PMNs from Deferiprone-induced agranulocytosis patients was also characterized by a decrease of two saturated fatty acids: arachidonic acid and stearic acid. Arachidonic acid (AA) performs important functions in the body. The major action of AA metabolites is the promotion of acute inflammatory response, characterized by the production of proinflammatory mediators such as PGE₂ and PGI₂, followed by a second phase in which lipid mediators with pro-resolution activities may be generated. Moreover, AA is a fundamental component of cell membranes, conferring it with fluidity and flexibility, so necessary for the function of all

cells, especially in the nervous system, skeletal muscle, and immune system. Free AA modulates the function of ion channels, several receptors, and enzymes. AA control of membrane fluidity influences the function of specific membrane proteins involved in cell signalling (106, 107). Furthermore, AA plays a fundamental role in the maintenance of cell and organelle integrity and vascular permeability (107). Stearic acid (or octadecanoic acid) is a saturated fatty acid involved in mitochondrial beta-oxidation of long-chain saturated fatty acids and plasmalogen synthesis. These pathways mainly contribute to maintaining the dynamics of membrane and cell signalling, so low levels of stearic acid in the cells may contribute to decreasing the strength of RBCs membrane and alter the cell signalling (107). Moreover, fatty acids have also been found to modulate phagocytosis, reactive oxygen species production, cytokine production, and leukocyte migration, also interfering with antigen presentation by macrophages (106). The downregulation of fatty acid in PMNs of agranulocytosis patients could be related to mechanisms of immune-mediated toxicity. The purine nucleoside inosine is generated intracellularly and extracellularly by deamination of adenosine or intracellularly through the action of 5'-nucleotidase on inosine monophosphate. Inosine is a ubiquitous purine nucleoside that exerts an anti-inflammatory and immunomodulatory effect. Inosine and its metabolically stable analogue utilize adenosine receptors to modulate anti-inflammatory effects. Inosine is further metabolized to hypoxanthine, xanthine and ultimately uric acid. Like adenosine, the transport of inosine across the cell membrane is facilitated by nucleoside transporters. While the role of adenosine as a versatile signalling molecule is well documented, the biological actions of inosine continue to be uncovered. Considering the important physiological roles of these metabolites, the lower levels of arachidonic acid, stearic acid and inosine detected in PMNs of patients Deferiprone-induced agranulocytosis could contribute to define the complex relationship between Deferiprone and onset of agranulocytosis. Moreover, the decrease in stearic and arachidonic acid, which characterizes the metabolic profile of Deferiprone-

induced agranulocytosis patients, could be related to the result of a recent article in which it was shown that autophagy is essential for neutrophil differentiation in a cell-intrinsic manner, *in vitro* as well as *in vivo* (108). More in detail, the Authors observed extensive metabolic reprogramming during normal differentiation, limiting glycolytic activity while engaging mitochondrial respiration and mobilizing intracellular lipid stores. To study the role of autophagy in early granulopoiesis *in vivo*, they used mice with a conditional deletion of the essential autophagy machinery component Atg7. The autophagy-deficient neutrophil precursor was unable to shift toward mitochondrial respiration and displayed excessive glycolysis, droplet accumulations, and ATP depletion. Notably, inhibition of lysosomal lipolysis or fatty acid oxidation within mitochondria alone was sufficient to cause defective neutrophil differentiation. Importantly, the administration of free fatty acids or pyruvate for mitochondrial respiration rescued differentiation in autophagy-deficient neutrophil precursors and restore normal glucose metabolism. Since the suggested mechanism in deferiprone-induced agranulocytosis included maturation arrest of the granulocytic lineage at the stage of the CFU, the establishment of autophagy and energy-metabolic adaptation as a unique critical regulator of normal granulopoiesis and their interaction for an autophagy-FAO-OXPHOS (fatty acid oxidation- oxidative phosphorylation) pathway may also be relevant in the context of deferiprone-induced agranulocytosis. Finally, as a complementary analysis, to have a complete metabolic profile of the individuals enrolled in our study, the plasma samples were analyzed with both ¹H-NMR and GC-MS methods. The PLS-DA of the data obtained by ¹H-NMR and GC-MS analysis indicated that when the model was built by comparing controls subjects *vs.* patients, samples were clustered into two groups. Unlike what happened for PMNs, the model separated, with good statistical results, pathological subjects from healthy subjects, but not agranulocytosis (A) patients from no-agranulocytosis (NA) patients. Both OPLS-DA between agranulocytosis (A) patients *vs* healthy subjects and no-agranulocytosis (NA) patients *vs* healthy subjects, showed again good statistical

parameters. The comparison of the plasma metabolites between β -thalassemia patients and normal subjects revealed evident alterations of metabolites in the pathological class. This change in metabolite profile indicates that in β -Thalassemia patients metabolism is shifted from the normal state and it is disturbed in this genetic disease, as reported in the literature (109). In our study, the univariate analysis showed that in the plasma samples the altered metabolites were very similar in A and NA profile in comparison with healthy subjects. Univariate H-NMR analysis identified an increase of arginine, tyrosine, and a decrease of lactate both in A and NA plasma samples, while showed an increase of valine only in NA patients. Univariate GC-MS analysis highlighted an increase of urea and decrease of glycerol, glycine, threonine in both pathological patients' groups (A and NA) and a decrease of myo-inositol only in NA patients. Altogether, this data shows both similarities and differences in the plasma of the thalassemic patients with and without agranulocytosis.

VI. CONCLUSIONS

In summary, our result showed that GC-MS metabolomics has great potential to identify metabolomics change in neutrophils. The observed metabolomics changes correlate with different metabolomic profiles in patients with Deferiprone-induced agranulocytosis (A) vs patients without Deferiprone-induced agranulocytosis (NA). Metabolomics has the potential to provide novel insight into the onset of deferiprone-induced agranulocytosis and could offer new information on the molecular effects of this drug on neutrophil function *in vivo*. The metabolic changes observed in the neutrophils from agranulocytosis (A) patients required elucidation. Our study is a pilot study that has been only validated in a small independent cohort and, therefore, further confirmation in larger studies is required.

VII. BIBLIOGRAPHY

1. Nathan C. Neutrophils and immunity: challenges and opportunities. *Nat Rev Immunol*. 2006; 6:173–82.
2. Amulic B, Cazalet C, Hayes GL, Metzler KD, Zychlinsky A. Neutrophil function: from mechanisms to disease. *Annu Rev Immunol*. 2012; 30:459–89.
3. Edwards SW. The development and structure of mature neutrophils. In: Edwards SW, editor. *Biochemistry and Physiology of the Neutrophil*. Cambridge Univ. Press; New York: 2005.
4. Segal AW. How neutrophils kill microbes. *Annu Rev Immunol*. 2005; 23:197–223.
5. Brinkmann V, Reichard U, Goosmann C, Fauler B, Uhlemann Y, Weiss DS, et al. Neutrophil extracellular traps kill bacteria. *Science*. 2004; 303:1532–5.
6. Pattanaik S, Jain A, Ahluwalia J. Evolving Role of Pharmacogenetic Biomarkers to Predict Drug-Induced Hematological Disorders. *Ther Drug Monit*. 2021; 43(2):201-220.
7. O'Neill LA, Kishton RJ, Rathmell J. A guide to immunometabolism for immunologists. *Nature reviews Immunology*. 2016; 16(9):553–65.
8. Boccard J, Veuthey JL, Rudaz S. Knowledge discovery in metabolomics: an overview of MS data handling. *Journal of separation science*. 2010; 33, 290-304.
9. Soltow QA, Jones DP, Promislow DE. A network perspective on metabolism and aging. *Integrative and comparative biology*. 2010; 50, 844-854.
10. Thomas HB, Moots RJ, Edwards SW, Wright HL. Whose Gene Is It Anyway? The Effect of Preparation Purity on Neutrophil Transcriptome Studies. *PLoSOne*. 2015; 10(9).
11. Calzetti F, Tamassia N, Arruda-Silva F, Gasperini S, Cassatella MA. The importance of being "pure" neutrophils. *The Journal of allergy and clinical immunology*. 2017;139(1):352–5e6.

12. Payne CM, Glasser L, Tischler ME, Wyckoff D, Cromey D et al. Programmed cell death of the normal human neutrophil: An in vitro model of senescence. *Microscopy Research and Technique*. 1994; 28(4), 327-344.
13. Galanello R. Deferiprone in the treatment of transfusion-dependent thalassemia: a review and perspective. *Ther Clin Risk Manag*. 2003; 3:795-805.
14. Borgna-Pignatti C, Rugolotto S, De Stefano P, Zhao H, Cappellini MD, Del Vecchio GC, Romeo MA, Fomi GL, Gamberini MR, Ghilardi R, Piga A & Cnaan A. Survival and complications in patients with thalassemia major treated with transfusion and deferoxamine. *Haematologica*, 2004; 89 , 11 87-1193.
15. Griffiths WJ, et al., Targeted Metabolomics for Biomarker Discovery. *Angewandte Chemie International Edition*. 2010; 49(32): p. 5426-5445.
16. Nicholson JK, Lindon JC, Holmes E. 'Metabonomics': understanding the metabolic responses of living systems to pathophysiological stimuli via multivariate statistical analysis of biological NMR spectroscopic data. *Xenobiotica Fate Foreign Compd Biol Syst*. 1999; 29(11):1181-9.
17. Johnson CH, Ivanisevic J, Siuzdak G. Metabolomics: beyond biomarkers and towards mechanisms. *Nat Rev Mol Cell Biol*. 2016; 17(7):451-9.
18. Fiehn O. Metabolomics the link between genotypes and phenotypes. *Plant Mol Biol*. 2002; 48(1-2):155-71.
19. Nicholson JK, Lindon JC. Systems biology: Metabonomics. *Nature*. 2008; 23;455(7216):1054-6.
20. Nicholson JK. Global systems biology, personalized medicine and molecular epidemiology. *Mol Syst Biol*. 2006; 2:52.
21. Holmes E, Wilson ID, Nicholson JK. Metabolic phenotyping in health and disease. *Cell*. 2008; 134(5), 714-717.

22. Clish CB. Metabolomics: an emerging but powerful tool for precision medicine. *Cold Spring Harb Mol Case Stud.* 2015; 1(1).
23. Beger RD, Schmidt MA, Kaddurah-Daouk R. Current Concepts in Pharmacometabolomics, Biomarker Discovery, and Precision Medicine. *Metabolites.* 2020; 10(4):129.
24. Alvarez-Sanchez B, Priego-capote F, Luque de Castro MD. Metabolomics analysis II. Preparation of biological samples prior to detection. *TrAC Trends in Analytical Chemistry* Volume 29, Issue 2, 2010; 120-127
25. Vinayavekhin N, Saghatelian A. Untargeted metabolomics. *Curr Protoc Mol Biol.* 2010; 30.1.1-24.
26. Schrimpe-Rutledge AC, Codreanu SG, Sherrod SD, McLean JA. Untargeted Metabolomics Strategies-Challenges and Emerging Directions. *J Am Soc Mass Spectrom.* 2016; 27(12):1897-1905.
27. Beger RD, Dunn W, Schmidt MA, Gross SS, Kirwan JA, Cascante M, et al. Metabolomics enables precision medicine: 'A White Paper, Community Perspective'. *Metabolomics Off J Metabolomic Soc.* 2016; 12(10):149.
28. Armitage EG, Barbas C. Metabolomics in cancer biomarker discovery: current trends and future perspectives. *J Pharm Biomed Anal.* 2014; 87:1–11.
29. Emwas AH, Roy R, McKay RT, Tenori L, Saccenti E, Gowda GAN, Raftery D, Alahmari F, Jaremko L, Jaremko M, Wishart DS. NMR Spectroscopy for Metabolomics Research. *Metabolites.* 2019; 27;9(7):123.
30. Ramautar R, Berger R, van der Greef J, Hankemeier T. Human metabolomics: strategies to understand biology. *Curr Opin Chem Biol.* 2013; 17(5):841–6.
31. Gowda GA, Djukovic D. Overview of mass spectrometry-based metabolomics: opportunities and challenges. *Methods Mol Biol.* 2014; 1198:3-12.
32. Lei Z, Huhman DV, Sumner LW. Mass spectrometry strategies in metabolomics. *J Biol Chem.* 2011; 286(29):25435-42.

33. Kanani H, Chrysanthopoulos PK, Klapa MI. Standardizing GC-MS metabolomics. *J Chromatogr B. Analyt Technol Biomed Life Sci.* 2008; 871(2):191–201.
34. Koek M, Muilwijk B, van der Werf M, Hankemeier T. Microbial Metabolomics with Gas Chromatography/Mass Spectrometry. *Anal Chem.* 2006; 78: 1272–81.
35. Modell B, Darlison M. Global epidemiology of haemoglobin disorders and derived service indicators. *Bull World Health Organ.* 2008; 86:480–487.
36. Flint J, Harding RM, Boyce AJ, Clegg JB, Giardine B, van Baal S, Kaimakis P, Riemer C, Miller W, Samara M, Kollia P. The population genetics of the hemoglobinopathies. *Bailliere's Clinical Hematology.* 1998; 11:1-50
37. Anagnou NP, Chui DH, Wajcman H, Hardison RC, Patrinos GP. HbVar database of human hemoglobin variants and thalassemia mutations. *Hum Mutat.* 2007; 28:206.
38. Huisman THJ, Carver MFH, Baysal E. A Syllabus of Thalassemia Mutations. The Sickle Cell Anemia Foundation, *Augusta, GA* 1997.
39. Rund D. & Rachmilewitz E. Advances in the pathophysiology and treatment of thalassemia. *Crit Rev Oncol Hematol.* 1995; 20, 237-254.
40. Thalassemia International Federation: Guidelines for the clinical management of thalassemia 2nd edition. 2008
41. Borgna-Pignatti C, Galanello R, Lippincott Williams & Wilkins. Philadelphia. Thalassemias and related disorders: quantitative disorders of hemoglobin synthesis. In *Wintrobe's Clinical Hematology.* 2004; 1319-1365.
42. Aust SD, Morehous LA & Thomas CE. Role of metals in oxygen radical reactions. *J Free Radic Biol Med.* 1985; 1,3-25.
43. Britton RS, Leicester KL & Bacon BR. Iron toxicity and chelation therapy. *Int J Hematol.* 2002; 76, 219 -228.
44. Poggiali E, Cassinerio E, Zanaboni L, Cappellini MD. An update on iron chelation therapy. *Blood Transfus.* 2012; 10(4):411-22.

45. Anderson LJ, Wonke B, Prescott E, Holden S, Walker JM, Pennell DJ. Comparison of effects of oral deferiprone and subcutaneous desferrioxamine on myocardial iron concentrations and ventricular function in beta-thalassaemia. *Lancet*. 2002; 360:516-520.
46. Gabutti V, Piga A: Results of long-term iron-chelating therapy. *Acta Haematol*. 1996; 95:26-36.
47. Wonke B, Hoffbrand AV, Bouloux P, Jensen C, Telfer P. New approaches to the management of hepatitis and endocrine disorders in Cooley's anemia. *Ann NY Acad Sci*. 1998; 850:232-41.
48. Clarke ET, Martell AE. Stabilities of 1,2-dimethyl-3-hydroxy-4-pyridinone chelates of divalent and trivalent metal ions. *Inorg Chim Acta*. 1992; 191:57-63.
49. Stobie S, Tyberg J, Matsui D, et al. Comparison of the pharmacokinetics of 1,2-dimethyl-3-hydroxypyrid-4-one (L1) in healthy volunteers, with and without co-administration of ferrous sulfate, to thalassemia patients. *Int J Clin Pharmacol Ther Toxicol*. 1993; 31:602-5.
50. Galanello R, Campus S. Deferiprone chelation therapy for thalassemia major. *Acta Haematol*. 2009; 122(2-3):155-64..
51. Piga A, Gaglioti C, Fogliacco E, Tricta F. Comparative effects of deferiprone and deferoxamine on survival and cardiac disease in patients with thalassemia major: a retrospective analysis. *Haematologica*. 2003; 88:489-496.
52. Borgna-Pignatti C, Cappellini MD, De Stefano P, Del Vecchio GC, Forni GL, Gamberini MR, Ghilardi R, Piga A, Romeo MA, Zhao H, Cnaan A: Cardiac morbidity and mortality in deferoxamine-or deferiprone-treated patients with thalassemia major. *Blood*. 2006; 107:3733-3737
53. Ceci A, Baiardi P, Catapano M, Felisi M, Cianciulli P, De Sanctis V, Del Vecchio GC, Magnano C, Meo A, Maggio A. Risk factors for death in patients with beta-thalassemia major: results of a case-control study. *Haematologica*. 2006; 91:1420-1421.

54. Anderson LJ, Wonke B, Prescott E, Holden S, Walker JM, Pennell DJ. Comparison of effects of oral deferiprone and subcutaneous desferrioxamine on myocardial iron concentrations and ventricular function in beta-thalassaemia. *Lancet*. 2002; 360:516–20.
55. Piga A, Gaglioti C, Fogliacco E, Tricta F. Comparative effects of deferiprone and deferoxamine on survival and cardiac disease in patients with thalassemia major: a retrospective analysis. *Haematologica*. 2003; 88:489–96.
56. Wonke B, Wright C, Hoffbrand AV. Combined therapy with deferiprone and desferrioxamine. *Br J Haematol*. 1998; 103:361-364.
57. Origa R, Bina P, Agus A, Crobu G, Defraia E, Dessi C, Leoni GB, Muroli PP, Galanello R. Combined therapy with deferiprone and desferrioxamine in thalassemia major. *Haematologica*. 2005; 90:1309-1314.
58. Cappellini MD, Cohen A, Piga A, Bejaoui M, Perrotta S, Agaoglu L, Aydinok Y, Kattamis A, Kilinc Y, Porter J, Capra M, Galanello R, Fattoum S, Drelichman G, Magnano C, Verissimo M, Athanassiou-Metaxa M, Giardina P, Kourakli-Symeonidis A, Janka-Schaub G, Coates T, Vermynen C, Olivieri N, Thuret I, Opitz H, Ressayre-Djaffer C, Marks P, Alberti D. A phase 3 study of deferasirox (ICL670), a once-daily oral iron chelator, in patients with beta-thalassemia. *Blood*. 2006; 107:3455-3462.
59. Galanello R, Origa R. Once-daily oral deferasirox for the treatment of transfusional iron overload. *Ex Rev of Clin Pharma*. 2008; 1:231-240.
60. Porter JB, Elalfy MS, Taher AT, Aydinok Y, Chan LL, Lee SH, Sutcharitchan P, Habr D, Martin N, El-Beshlawy A. Efficacy and safety of deferasirox at low and high iron burdens: results from the EPIC magnetic resonance imaging substudy. *Ann Hematol*. 2013; 92(2):211-9.
61. Pennell DJ, Porter JB, Piga A, Lai Y, El-Beshlawy A, Belhoul KM, Elalfy M, Yesilipek A, Kilinç Y, Lawniczek T, Habr D, Weisskopf M, Zhang Y, Aydinok Y. A 1-year randomized

- controlled trial of deferasirox vs deferoxamine for myocardial iron removal in β -thalassemia major (CORDELIA). *Blood*. 2014; 123:1447–54.
62. Cohen AR, Galanello R, Piga A, Di Palma A, Vullo C, Tricta F. Safety profile of the oral iron chelator deferiprone: a multicenter study. *Br J Haematol*. 2000; 108: 305-12.
63. Galanello R, Agus A, Campus S, Danjou F, Giardina PJ, Grady RW. Combined iron chelation therapy. *Ann NY AcadSci*. 2010; 1202:79–86.
64. Tanner MA, Galanello R, Dessi C, et al. Combined chelation therapy in thalassemia major for the treatment of severe myocardial siderosis with left ventricular dysfunction. *J CardiovascMagnReson*. 2008; 10:12.
65. ApoPharma Inc. FerriproxVR (Deferiprone) Summary of Product Characteristics (SmPC).
66. Cohen AR, Galanello R, Piga A, et al. Safety profile of the oral iron chelator deferiprone: A multicenter study. *Br J Haematol*. 2000; 108:305– 312
67. Masera N, Tavecchia L, Longoni DV, et al. Agranulocytosis due to deferiprone: A case report with cytomorphological and functional bone marrow examination. *Blood Transfus*. 2011;4:1–4
68. Bertola U, Collell M, Piga A, et al. Neutropenia in homozygous b-thalassemic patients on desferrioxamine (DFO) treatment. In: *Proceedings of the 8th International Conference on Oral Chelation in the Treatment of Thalassemia and Other Diseases, Corfu, Greece; 1997*
69. Cohen AR, Galanello R, Piga A, et al. Safety and effectiveness of long-term therapy with the oral iron chelator deferiprone. *Blood*. 2003;102: 1583–1587.
70. El-Beshlawy AM, El-Alfy MS, Sari TT, et al. Continuation of deferiprone therapy in patients with mild neutropenia may not lead to a more severe drop in neutrophil count. *Eur J Haematol*. 2014; 92:337–340.

71. Elalfy M, Wali YA, Qari M, et al. Deviating from safety guidelines during deferiprone therapy in clinical practice may not be associated with higher risk of agranulocytosis. *Pediatr Blood Cancer*. 2014; 61:879–884.
72. Elalfy MS, Sari TT, Lee CL, et al. The safety, tolerability, and efficacy of a liquid formulation of deferiprone in young children with transfusional iron overload. *J Pediatr Hematol Oncol*. 2010; 32: 601–605.
73. Andes E, Maloisel F. Idiosyncratic drug induced agranulocytosis or acute neutropenia. *Curr Opin Hematol*. 2008; 15:15–21
74. Strom BL, Carson JLL, Schinnar R, et al. Descriptive epidemiology of agranulocytosis. *Arch Intern Med*. 1992; 152:1475–1480.
75. Ibanez L, Vidal X, Ballarin E, et al. Population based drug induced agranulocytosis. *Arch Intern Med*. 2005; 165:869–874
76. Tesfa D, Keisu M, Palmblad J. Idiosyncratic drug-induced agranulocytosis: Possible mechanisms and management. *Am J Hematol*. 2009; 84:428–434
77. Galanello R, Campus S. Deferiprone chelation therapy for thalassemia major. *Acta Haematol*. 2009; 122:155–164.
78. Hoffbrand AV, Bartlett AN, Veys PA, et al. Agranulocytosis and thrombocytopenia in patient with Blackfan-Diamond Anaemia during oral chelator trial [letter]. *Lancet*. 1989; 2:457– 458
79. Ceci A, Baiardi P, Felisi M, et al. The safety and effectiveness of deferiprone in a large-scale, 3- year study in Italian patients. *Br J Haematol*. 2002; 118:330–336
80. Hoffbrand AV. Oral iron chelation. *Semin Hematol*. 1996; 33:1–8
81. Atkin K, Kendall F, Gould D, et al. Neutropenia and agranulocytosis in patients receiving clozapine in the UK and Ireland. *Br J Psychiatry*. 1996; 169:483–488.

82. Peralta FG, Sanchez MB, Roiz MP, et al. Incidence of neutropenia during treatment of bone-related infections with piperacillin-tazobactam. *Clin Infect Dis*. 2003; 37:1568–1572. 1;
83. Tricta F, Uetrecht J, Galanello R, Connelly J, Rozova A, Spino M, Palmblad J. Deferiprone-induced agranulocytosis: 20 years of clinical observations. *Am J Hematol*. 2016; 91(10):1026-31.
84. Andres E, Noel E, Kurtz JE, et al. Life-threatening idiosyncratic drug-induced agranulocytosis in elderly patients. *Drugs Aging*. 2004; 21:427–435.
85. Monni G, Murgia F, Corda V, Peddes C, Iuculano A, Tronci L, Balsamo A and Atzori L. Metabolomic Investigation of β -Thalassemia in Chorionic Villi Samples. *J Clin Med*. 2019; 8 (6):798.
86. R Core Team. R: A language and environment for statistical computing. R Foundation for Statistical Computing. 2011.
87. Smith CA, Want EJ, O'Maille G, Abagyan R, Siuzda G. XCMS: Processing mass spectrometry data for metabolite profiling using nonlinear peak alignment, matching, and identification. *Anal. Chem*. 2006; 78, 779–787.
88. Liggi S, Hinz C, Hall Z, Santoru ML, Poddighe S, Fjeldsted J, Atzori L, Griffin JL. KniMet: A pipeline for the processing of chromatography-mass spectrometry metabolomics data. *Metabolomics*. 2018; 14, 52.
89. Piras C, Arisci N, Poddighe S, Liggi S, Mariotti S, Atzori L. Metabolomic profile in hyperthyroid patients before and after antithyroid drug treatment: Correlation with thyroid hormone and TSH concentration. *Int J Biochem Cell Biol*. 2017; 93:119-128

90. Fiehn O. Metabolomics the link between genotypes and phenotypes. *Plant Mol Biol.* 2002;48(1–2):155–71.
91. Khan A1, Khan MI, Iqbal Z, Shah Y, Ahmad L et al. A new HPLC method for the simultaneous determination of ascorbic acid and aminothiols in human plasma and erythrocytes using electrochemical detection. *Talanta.* 2011; 84(3):789-801
92. Eriksson L, Byrne T, Johansson E, Trygg J, Wikström C. *Multi- and Megavariate Data Analysis Basic Principles and Applications*, 3rd ed.; Umetrics Academy: Malmo, Sweden. 2013; pp. 1–501.
93. Bylesjö M, Rantalainen M, Cloarec O, Nicholson JK, Holmes E, Trygg J. OPLS discriminant analysis: combining the strengths of PLS-DA and SIMCA classification. *J Chemom.* 2006; 20:341–351
94. Dickinson DA, Forman HJ. Glutathione in defense and signaling: lessons from a small thiol. *Ann NY Acad Sci.* 2002; 973:488-504.
95. Vairetti M, Di Pasqua LG, Cagna M, Richelmi P, Ferrigno A, Berardo C. Changes in Glutathione Content in Liver Diseases: An Update. *Antioxidants (Basel).* 2021; 10(3):364.
96. Raftery D. *Mass Spectrometry in Metabolomics: Methods and Protocols.* Springer New York. 2014
97. Richer BC, Salei N, Laskay T, Seeger K. Changes in Neutrophil Metabolism upon Activation and Aging. *Inflammation.* 2018; 41(2):710–21.
98. Beckonert O et al. Metabolic profiling, metabolomic and metabonomic procedures for NMR spectroscopy of urine, plasma, serum and tissue extracts. *Nat Protoc.* 2007; 2(11)
99. Wang W, Wu Z, Dai Z, Yang Y, Wang J, Wu G. Glycine metabolism in animals and humans: implications for nutrition and health. *Amino Acids.* 2013;45(3):463-77.

100. Cruzat VF, Pantaleão LC, Donato J, De Bittencourt PIH, Tirapegui J. Oral supplementations with free and dipeptide forms of L-glutamine in endotoxemic mice: Effects on muscle glutamine-glutathione axis and heat shock proteins. *J. Nutr. Biochem.* 2014; 25, 345–352.
101. Pithon-Curi TC, De Melo MP, Curi R. Glucose and glutamine utilization by rat lymphocytes, monocytes and neutrophils in culture: A comparative study. *Cell Biochem. Funct.* 2004; 22, 321–326.
102. Meredith MJ, Reed DJ. Status of the mitochondrial pool of glutathione in the isolated hepatocyte. *J. Biol. Chem.* 1982; 257, 3747–3753.
103. Delauney AJ and Verma DPS. Proline biosynthesis and osmoregulation in plants. *Plant J.* 1993; 215–223,.
104. Kontoghiorghes GJ, Efstathiou A, Kleanthous M, Michaelides Y and Kolnagou A. Risk/benefit assessment, advantages over other drugs and targeting methods in the use of deferiprone as a pharmaceutical antioxidant in iron loading and non iron loading conditions. *Hemoglobin.* 2009; 33(5):386–397.
105. Pompéia C, Lopes LR, Miyasaka CK, Procópio J, Sannomiya P, Curi R. Effect of fatty acids on leukocyte function. *Braz J Med Biol Res.* 2000; 33(11):1255–68.
106. Brash AR. Arachidonic acid as a bioactive molecule. *J Clin Invest.* 2001; 107(11):1339–45
107. Beck R, Bertolino S, Abbot SE, Aaronson PI, Smirnov SV. Modulation of arachidonic acid release and membrane fluidity by albumin in vascular smooth muscle and endothelial cells. *Circ Res.* 1998; 83(9):923–31.
108. Riffelmacher T, Clarke A, Richter FC, Stranks A, Pandey S, Danielli S, Hublitz P, Yu Z, Johnson E, Schwerd T, McCullagh J, Uhlig H, Jacobsen SEW and Simon AK. Autophagy-Dependent Generation of Free Fatty Acids Is Critical for Normal Neutrophil Differentiation. *Immunity.* 2017; 47, 466–480

109. Musharraf SG, Iqbal A, Ansari SH, Parveen S, Khan IA & Siddiqui AJ. β -Thalassemia Patients Revealed a Significant Change of Untargeted Metabolites in Comparison to Healthy Individuals. *Scientific reports*. 2017; 7:42249